STUDIES OF SOUND PROPAGATION IN THE ACOUSTIC TRACHEA: AN EXPERIMENTAL, ANATOMICAL AND NUMERICAL APPROACH

UNIVERSITY OF LINCOLN

A thesis submitted for the award of a MSc Zoology by Research by the University of Lincoln, 2020, supervised by Prof Fernando Montealegre-Z and Dr Carl Soulsbury.

DANIEL JOHN ALEXANDER VEITCH

VEI15589756

Abstract

Bush-crickets (Ensifera: Tettigoniidae) rely on the perception of sound to detect and localise predators and potential mates, and this has led to the development of complex ears. This is not confined to bush-crickets, and a variety of sound detection and localisation mechanisms have arisen in other ensiferans and tetrapods. This thesis aims to summarise the literature across these two groups to provide an overview of auditory anatomy and directional hearing. Bush-crickets possess ears in their forelegs to detect and localise sound predators and potential mates. Each ear consists of two tympanic membranes which are exposed to sound both externally, where sound transmits to the ear through the environment, and internally, via an ear canal derived from the respiratory system. As sound propagates through the ear canal it reduces in velocity, causing a time delay between the arrival of the internal and external input. The delay was suspected to arise as sound propagation changes from adiabatic to isothermal, caused by the ear canal geometry. If true, then the reduction in sound velocity should persist independently of the gas composition in the ear canal. This method was first simulated on a simplified plastic model of the ear canal, formed by a linear tube with an opening at one end for sound input, and a balloon membrane at the other for sound reception. A probe-loudspeaker was used to project a signal into the linear tube, and laser Doppler vibrometer recorded the arrival time of the signal at the membrane. A reduction in sound propagation velocity was observed in the linear tube. The sound propagation velocity through air and carbon dioxide was also quantified. Experiments were then conducted on specimens of *Copiphora gorgonensis*. By integrating laser Doppler vibrometry, micro-CT scanning, and numerical analysis on 3D geometries of each experimental animal ear, we demonstrate that the narrowing radius of the ear canal is the main factor reducing sound velocity. The numerical simulations of the sound propagation use the precise 3D geometry of the ear canal and take into account the viscous and thermal boundary layers formed near the wall of the ear canal; whose thickness also depend on the tube radius. Likewise, the ear canal is asymmetrically bifurcated at the tympana organ

location (one branch for each tympanic membrane) creating two additional internal sound paths and imposing different sound velocities for each tympanic membrane. Therefore, external and internal inputs add up to four auditory paths for each ear (to compare, only one for humans). Implication of findings in avian directional hearing and potential applications in acoustic triangulation devices are discussed.

Acknowledgements

First and foremost, I would like to thank Prof Fernando Montealegre-Z and Dr Carl Soulsbury for their amazing support throughout this project. Your guidance and encouragement have been essential, and I could not have asked for a better team.

Thank you to Christian Pulver, Dr Emine Celiker, Dr Thorin Jonsson, Dr Darron Cullen, Charlie Woodrow, Jacob Duncan and Dr Eleftherios Siamantouras for helping me grow both as a scientist and as a person. I already miss discussing new ideas over a morning coffee.

Thank you also to the Minster House Technician Team: Paul, Baylee and Kelly. Whether it was finding bits and bobs, pointing out cool insects or the occasional cup of tea, you made long days in the lab so much better.

Last but definitely not least, I'd like to thank my family and friends for their constant support over the past two years, especially Rhiannon Samuel who has been my lifeline. Mum, Pete, Dad, Ellie, Aidan, Tom, Christian, Valerie (and many others!) I am forever grateful to you all. You've made the times outside of the lab some of the best in my life. I hope I make you all proud.

Table of Contents

Chapter One:

Tympanal Ears in the Animal Kingdom

Bush-crickets (Orthoptera; Ensifera; Tettigoniidae), also known as katydids, possess an ear comparable to mammals. Their hearing system features three main components: 1) an outer ear for sound capture, 2) a middle ear for impedance conversion, and 3) an inner ear for frequency analysis. Recent developments on the function of the bush-cricket outer ear has led to further research described in Chapter Two and Chapter Three of this thesis. To provide a background in auditory anatomy and function, this chapter will revise auditory structures in Tetrapoda and Ensifera, touching on the localisation of airborne sounds where applicable.

Ears in Tetrapoda

The development of the tetrapod ear begins in the jaws of early vertebrates (Manley, 2010). Similar to extant cartilaginous fishes, early vertebrates possessed highly mobile lower jaws which were attached to the upper component via a supporting structure derived from the hyoid gill arch – known as the hyomandibula (Carroll, 1988 in Manley, 2010; Rodríguez-Vázquez, 2005). Over time the hyomandibula became unnecessary as the upper and lower jaw formed a solid association, the gill opening forming a spiracle which connects the outer environment to the mouth cavity (Clack, 2002). After the transition from water to land, the ancestors of modern-day amphibians diverged from the stem amniotes. There is evidence that the Temnospondyls (primitive amphibians) possessed a tympanic middle ear around 300 million years ago, yet it is unconfirmed if these are the crown group (direct descendants) or stem group (diverged before the amphibian common ancestor) of amphibians (Manley, 2010; Ruta and Coates, 2007). At this stage the amniote common ancestor did not possess a tympanic ear, as the hyomandibula formed a new role in supporting the outer and inner

skull (dermal and endochondral bone, respectively) during biting motion (Hopson, 1966; Manley, 2010). This condition remained throughout the divergence of the modern lineages, including; the synapsids (basal mammals), lepidosaurs (snakes and lizards), and archosaurs (birds and crocodilians; Clack, 2002; Manley and Clack, 2004; Hopson, 1987). The skull components within each lineage developed more solid connections, in turn enabling the hyomandibula to take on the new function of transmitting loud low frequencies to the ancestral basilar papilla of the inner ear (Manley, 2010; Manley, 2000).

Tympanic ears were present in all modern amniotes by the early Triassic (Clack, 2002). For lepidosaurs and archosaurs, the tympanic membrane (TM) likely formed as a skin layer over the spiracle; the extracolumella-columella unit developing as the hyomandibula reduced in width and mass (Manley, 2010). Over time, a recess formed in the skull to house the TM, causing an increase in frequency response of the TM, which in turn selected for a larger basilar papilla. In synapsids, the TM would arise from deeper within the head, enabling a more complex ossicular chain to form (Maier, 1989; Manley, 2010). Instead of a single ossicle, the hyomandibula is transformed along with the quadrate and articular. The two latter bones were formerly the articulation for the upper and lower jaw, respectively. The hyomandibula becomes the extrastapes-stapes unit (homologous to the extracolumella-columella) the quadrate becomes the malleus, and the articular becomes the incus (Maier, 1989). The positioning of the ossicles formed a primary lever, reducing the energy lost during sound propagation through the middle ear. This permitted the high frequencies to pass through, kickstarting the evolution towards ultrasonic hearing (Puria and Steele, 2010)

This section will cover acoustic communication, auditory anatomy and the process of directional hearing (the ability to localise the source of a sound) throughout terrestrial tetrapods.

Anuran ear

Anura (frogs and toads) produce sound for two main reasons, advertising for potential mates and strength demonstration in aggressive encounters (Kelly, 2004). Males of the common tree frog, *Polypedates leucomysta*x (Rhaphoridae), produce a single call to attract females but use a diverse set of vocalisations to assert dominance over male competitors (Christensen-Dalsgaard et al., 2002). Conversely, male natterjack toads, *Epidalia calamita* (Bufonidae), form choruses of their singular call to establish domination over territory. Frequency is used in male-male assessment of body size, and individuals with low frequency calls are more likely to be avoided by others (Arak, 1983). Females, on the other hand, ignore frequency and seem to be attracted to the loudest call. Sound localisation is clearly important for sexual selection in Anura, and this is reflected by the specialisation of the hearing anatomy for both airborne and vibratory sound signals.

The anuran ear is situated on the lateral side of the head (Fig. 1A, B). It typically possesses a tympanic membrane (TM) for sound capture (Jaslow et al., 1988), an ossicular chain for signal transduction (Jørgensen and Kanneworff, 1998; Mason and Narins, 2002a), and an amphibian and basal papilla – for low and high frequency discrimination, respectively (Feng et al., 1975). The TM is held inside a bony ring and backed by an air-filled middle ear cavity that runs through the head to meet the other TM (Fig. 1B). Each TM is also connected to an ossicular chain, formed by the extracolumella and the columella (Fig. 1C; Jørgensen and Kanneworff, 1998). The former is cartilaginous and connected to both the TM and columella. The columella is partly ossified and extends from the extracolumella, suspended in the middle ear cavity, into the connective and muscle tissue of the head where the columellar footplate joins the oval window of the inner ear (Fig. 1C; Jaslow et al., 1998; Jørgensen and Kanneworff, 1998). This is the pathway for airborne sound transmission (Fig. 1C).

Anurans also possess an operculum, a bony structure unique to their hearing system. The operculum is coupled to the proximal columella and also connects to the oval window (Fig. 1C). The role of this structure in hearing has been debated but it likely has two functions: 1) the detection of substrate vibrations (Hetherington, 1988), 2) protecting the

inner ear from high amplitude soundwaves (Mason and Narins, 2002b). Low frequency substrate vibrations can transmit into the forearm, up to the shoulder girdle, and pass along the opercularis muscle to stimulate the operculum (Fig. 1C). The operculum distributes these vibrations to the inner ear via the oval window (Fig. 1C; Hetherington, 1988). The opercularis muscle can also contract, forcing the operculum and columella together. This is proposed to prevent the connection between the columella and the oval window, blocking the inner ear from stimulation caused by unwanted pressure changes on the tympanum (Mason and Narins, 2002b). Such pressure changes can occur from the motion of calling and breathing.

The inner ear consists of two entangled compartments: the perilymphatic and endolymphatic labyrinths (Fig. 1C; Schoffelen et al., 2008). The former is filled with perilymphatic fluid and connects the oval window to the round window, where sound energy is released from the ear (Purgue and Narins, 2002). The endolymphatic labyrinth is filled with endolymphatic fluid and contains the frequency discriminating papillae. The amphibian papilla detects low frequency stimuli and the basilar papilla detects high frequency stimuli (Fig. 1C; Feng et al., 1975).

The only frog known to possess an outer ear is the concave-eared torrent frog, *Odorrana tormota* (Ranidae; Fig. 2A). Males of this species have developed recessed tympana, positioned within a cavity akin to an ear canal (EC) (Fig. 2B; Feng and Narins, 2008). *Odorrana tormota* lives in an environment saturated in the low frequency sounds of rushing water and uses ultrasonic components in its call to aid the localisation of conspecifics. Thin tympana provide an advantage to hearing ultrasound but are more vulnerable to damage. The EC likely evolved to protect the delicate tympanic membrane from mechanical injury (Feng and Narins, 2008). Interestingly, the EC resonates at the carrier frequency of the song (4.3 kHz), increasing the hearing sensitivity at this frequency.

Directional hearing in Anura likely arises from a pressure-difference receiver system, formed from the internal connection between the two TM, via the mouth cavity (Fig. 1B Christensen-Dalsgaard, 2011; Feng et al., 1976). In frogs, differences in sound pressure at

247 the ipsilateral and contralateral ears can range from 6 to 10 dB (Christensen-Dalsgaard,
248 2005; Jørgensen et al., 1991).
249
250 **Lacertilian ear**
251 In Lacertilia (lizards), airborne sound is received in a similar manner to that in Anura.
252 The tympanic membranes are situated on the side of the head and the sound vibrations that
253 are received here are passed onto the extracolumella and columella (Fig. 3A, B; Young,
254 2016). The anterior and posterior tympanic processes maintain tight contact between the
255 extracolumella and the TM (in some species up to four processes are present). To facilitate
256 the joining of these segments, the distal extracolumella forms two appendages known as the
257 *pars inferior* and *pars superior* (Fig. 3C; Saunders et al., 2000). Sound passes from the
258 columella to the inner ear via the oval window (Manley, 1990 in Saunders et al., 2000;
259 Young, 2016). The inner ear consists of a basilar papilla with tonotopically arranged
260 mechanosensory hairs (Manley, 2002).
261 Similar to Anura, the internal surface of the lacertilian TM are connected by the
262 mouth cavity (Fig. 3B; Carr et al., 2016). This means the ears are coupled, where sound can
263 transmit from one TM to the other, through the internal airspace. This enables the animal to
264 discriminate sound pressure differences, from the same signal, between the two ears.
265 Christensen-Dalsgaard and Manley (2005) studied four species of lizard to find that the
266 ipsilateral ear received a sound stimulus at a consistently larger signal amplitude than the
267 contralateral ear – at a maximum 28 dB difference. The larger species of lizard were more
268 sensitive to lower frequencies (1.8 kHz than the smaller lizards (3 kHz; Christensen-
269 Dalsgaard and Manley, 2005). Sound can also travel to both ears externally, producing small
270 differences in amplitude between the two. A 2 dB interaural amplitude difference is seen in
271 large lizards at 1 kHz, and 2 kHz in small lizards (Christensen-Dalsgaard and Manley, 2005).
272 A shallow EC can exist in both larger and smaller species of lizard, but its presence has not
273 been explored in terms of hearing sensitivity (Christensen-Dalsgaard and Manley, 2005).

Lacertilians are not renowned for vocalising, yet geckos (Gekkonidae) are well documented in their ability to produce sound (Marcellini, 1977). These calls can be used in predator deterrence, male-male combat and claim territory to reduce aggressive interactions. These are more common in nocturnal species due to the lack of visual information for detecting predators and mates (Marcellini, 1977). Detecting and localising these sounds would be beneficial for an individual's survival and mating success; demonstrated by the fear response to conspecific distress calls in *Liolaemus chiliensis* (Iguanidae; Ruiz-Monachesi and Labra, 2020). The vocalisations of other animals can be of significance as well. The brown anole (*Anolis sagrei*) is able to detect and discriminate recordings of predatory and harmless birds, adopting increased awareness as appropriate (Cantwell and Forrest, 2013). Mediterranean house geckos (*Hemidactylus tursicus*) use their directional hearing to locate food (Sakaluk and Belwood, 1984). First, they locate male crickets, calling from their protective underground burrow, and then predate on the females that come to mate (Sakaluk and Belwood, 1984).

Crocodilian ear

Crocodilians are the most vocal of all non-avian reptiles (Burghardt, 1977). The ability to produce sound begins in the young, who start to communication before they are born, and continues through into adulthood (Vergne and Mathevon, 2009). Juvenile American alligators (*Alligator mississippiensis*) are known to emit low frequency 'contact calls' when approached by a human (Burghardt, 1977; Vergne and Mathevon, 2009). These contain frequencies from 200 to 2000 Hz and are thought to alert conspecifics to items of interest, such as potential food or perhaps even predators (Burghardt, 1977; Campbell, 1973 in Vergne et al., 2009). When physically touched, simulating capture by a predator, juveniles produce high frequency components (up to 5 kHz) as part of a distress call (Burghardt, 1977). The function of this call is to attract the presence of an adult for protection (Britton, 2001 in Vergne et al., 2009). Adult crocodilians can also produce a variety of calls (Garrick et

al., 1978). Bellows are low frequency sounds that transmit through air and water. In the American alligator, these calls have a frequency range of 20 to 400 Hz in air, and 20 to 250 Hz in water, propagating up to 165 and 1500 m, respectively (Todd, 2007). Both males and females can bellow, and these sounds may convey information about the quality of the sender during sexual communication (Garrick et al., 1978; Vergne and Mathevon, 2009). Deep grunts are used by females in response to the juvenile contact call, in turn recalling the young to the adult's location (Vergne and Mathevon, 2009; Hunt and Watanabe, 1982). In *A. mississippiensis* the main frequencies are 50 to 100 Hz and in spectacled caiman (*Caiman crocodilus*) this range is increased to 1 kHz (Garrick et al., 1978; Vergne and Mathevon, 2009). Hisses are low intensity, broad frequency calls below 1 kHz (Garrick et al., 1978). They are associated with territory defence: in nest protection and male-male aggressive encounters (Neil, 1971 in Garrick et al., 1978; Vergne and Mathevon, 2009).

Crocodilian ears are situated on the dorso-lateral part of the head behind the eye (Fig. 4A, B). The entrance to the EC is a slite-like aperture, which can be closed by a dorsal ear flap before diving (Saunders et al., 2000; Shute and Bellairs, 1955). This traps an air bubble within the EC and protects the TM. Hearing is still functional underwater, and the air bubble does not reduce or increase the sensitivity of the ear (Higgs et al., 2002). The TM is connected the columella via the tympanic, stylohyal, and suprastapedial processes (Fig. 4C; Vergne and Mathevon, 2009). The tympanic process is stabilised on the TM by the stylohyal process, and the suprastapedial process is linked to the ventral TM by the extracolumellar muscle (Vergne and Mathevon, 2009). Sound vibrations transmit through these structures to reach the inner ear (Carr et al., 2016), where the basilar papilla discriminates the frequencies present (Fig. 4C; Baird, 1974).

As in lacertilians, the spaces behind the tympanic membranes are connected, although in crocodilians this is formed by two channels running above and below the braincase (Fig. 4B). The dorsal channel is known as the intertympanic recess and the lower channel consists of the quadrate sinuses, pharyngotympanic recesses and the median pharyngeal recess (Fig. 4B; Bierman et al., 2014). These channels are thought to form a

pressure-difference receiver, resulting in increased interaural time and amplitude differences (Bierman et al., 2014; Carr et al., 2016). In *A. mississippiensis*, the ipsilateral ear receives a 1 kHz signal at a sound pressure 10 dB greater than at the contralateral ear (Bierman et al., 2014). This signal also arrives at the contralateral ear up to 300 μs later depending on the angle of the sound source (Bierman et al., 2014). These interaural differences enable the crocodilian to localise the position of the sound source.

Avian ear

Birdsong is perhaps the most recognised sound in nature. As with crocodilians, birds produce sound throughout their lives, beginning before they hatch (Evans, 1992; Saino and Fasola, 1996). Throughout the nesting period, young birds will beg to their parents signalling their and hunger or at the very least their individual presence (Kilner and Johnstone, 1997). Species with low sibling relatedness have evolved louder begging calls than other species (Briskie et al., 1994), suggesting that parents can favour offspring with the louder call. In adult birds, singing is used as a part of mate advertisement, social living, and predator deterrence. The complexity of a male call appears to be a significantly reliable indicator on their ability as a parent, along with expressing the conditions in which they were raised (Buchanan and Catchpole, 2000; Spencer et al., 2003). Zebra finches (*Taeniopygia guttata*) raised with low food availability or high stress produce fewer complex vocalisations, including shorter song components, difficulty producing higher frequencies and less variation in song syllables (Spencer et al., 2003). The song complexity of the male sedge warbler (*Acrocephalus schoenobaenus*) correlates with parental care effort, although fledgling success rate was not significantly greater than for males will low-complexity songs (Buchanan and Catchpole, 2000). None-the-less, females of this genus appear to select for mates with high parental care (Catchpole et al., 1984; Leisler and Catchpole, 1996).

Adaptation for acoustic communication is beneficial for living in social groups. Zebra finches can identify individuals by recognising small differences within their syllables (Elie and Thompson, 2018). In order to reduce their energetic costs of fighting, territorial pairs of skylarks (*Alauda arvensis*) reduce aggressive encounters with their known neighbours, which will share similarities in calling song (Briefer et al., 2008). Differences in syllable sequence are used to determine individuals that originate from distant territories, who will pose as more of a threat to the defending pair (Briefer et al., 2008). Warning calls are also useful for reducing the predation of conspecifics. The Siberian jay (*Perisoreus infaustus*) produces different alarm vocalisations depending on the behaviour of the predator (Griesser, 2008). Warning calls reduced the reaction time of conspecifics by 46 %, leading to a greater chance of survival (Griesser, 2013).

Bird ears are situated on the lateral side of their head, covered by feathers (Fig. 5A; Larsen et al., 2016). They possess a short EC (2-7 mm) that, much like in lizards, functions in protecting the TM. This enables the TM to be thinner and more sensitive to stimulation (Saunders et al., 2000). The TM is surrounded by the squamosol, exoccipital and basisphenoid bones, pulled taut against them by a series of ligaments (Saunders et al., 2000). The extracolumella is joined to the TM by three tympanic processes; the extrastapedial, superiorstapedial and inferiorstapedial processes. As it extends away from the TM, the extracolumella becomes the columella, an elongated shaft that expands into a footplate before reaching the round window of the inner ear (Fig. 5B). The morphology of the columella can differ significantly, depending on the species of bird (Krause, 1901 in Saunders et al., 2000). The inner ear consists of a basilar papilla for frequency discrimination. This ranges in length from 1.6 mm in the *T. guttata* to 11.5 mm in the barn owl (*Tyto alba*; Fischer et al., 1988; Gleich et al., 1994).

Similar to the other vertebrates discussed so far, the TMs in avian ears are connected via an interaural canal (Fig. 5C; Schwartzkopff, 1952, in Larsen et al., 2016; Wada, 1924 in Larsen et al., 2016). Sound can transmit through this canal at low frequencies (800 to 6300 Hz in the quail; *Coturnix japonica*), forming a pressure-difference receiver

system (Hill et al., 1980). Below 5 kHz, an attenuation of 5 dB occurs at the contralateral ear, yet this increases to 20 dB at higher frequencies. This suggests that higher frequency sounds provide the best directional cues (Hill et al., 1980). The time difference between sound arrival at the ipsilateral and contralateral TM is greater via the internal route than through the air externally (Calford and Piddington, 1988). The delay also increases for lower frequency sounds (Calford and Piddington, 1988). At around 1 kHz, sound takes 200 μs to pass through the interaural canal of *C. japonica* and the chicken, *Gallus gallus* (Calford and Piddington, 1988; Hyson et al., 1994). For *C. japonica* this is a delay of 40 μs when compared to the externally travelling signal (Larsen and Popov, 1995, in Larsen et al., 2016).

Birds have a complex cranial anatomy and the interaural canal is not the only internal route for sound to pass through. The zebra finch possesses a complex network of tubes that may function in the interaural time delay (Larsen et al., 2016). The interaural canal and inter-bullae passage are two large airspaces that directly connect each TM (Fig. 5C). Two different arching pathways run from the lateral interaural canal, connecting it to the superoantero-orbital sinus, which is positioned at the forehead (Fig. 5C). The first of these pathways is the interaural arc which connects to the sinus via the medio-orbital canal, the second being formed by the superolateral orbital canals which join directly to the sinus (Fig. 5C). The hypomedial orbital tube also link the interaural canal and the sinus through the medial plane (Fig. 5C). This anatomy is discussed further in the third chapter.

Mammalian ear

Mammal vocalisations span the widest range of frequencies out of all terrestrial vertebrates, ranging from 14 Hz (infrasound) in the African elephant (*Loxodonta africana*), up to 212 kHz in a species of bat (*Cloeotis percivali*; Ladich and Winkler, 2017; Poole et al., 1988; Fenton and Bell, 1981). Some mammals are capable of vocal learning, the ability to learn and control vocalisations based of context, and to comprehend such vocalisations from conspecifics (Janik and Slater, 1997). Mammals that are capable of learning the context of

their vocalisations include rats (Lal, 1967), pinnipeds (Schusterman, 2008), dogs (Salzinger and Waller, 1962), cats (Molliver, 1963) and primates (Myers et al., 1965). As a consequence, vocalisations are varied within and between social groups and populations and detecting such differences can have potential fitness consequences for an individual (Newman and Symmes, 1982, in Maestripieri and Call, 1996; Semple and McComb, 2000).

Most terrestrial mammals possess and elaborate outer ear, known as the pinna (Fig. 6A; Webster, 1966). These structures are composed of skin covered fibrocartilage, reside on the lateral side of the head, and vary in morphology across the taxa (Alvord and Farmer, 1997; Ekdale 2016). The main auditory functions of the pinnae are to capture, filter and amplify sound from the external environment and guide it into the EC to stimulate the middle ear (Tollin and Koka, 2009; Webster, 1966). Upon reaching the TM, sound passes into ossicular chain; formed by the malleus, incus and stapes in such an order (Fig. 6A; Hellström et al., 1982). In Sprague-Dawley rats (*Rattus norvegicus*) the malleus connects to the TM through two processes, and also articulates with the incus (Fig. 6A; Hellström et al., 1982; Henson, 1974). The incus attaches to the stapes which sits in contact with the oval window of the inner ear (Hellström et al., 1982; Henson, 1974). The mammalian inner ear consists of an ossified casing called the bony labyrinth, the lumen of which is known as the cochlea. The organ of Corti (homologous to the basilar membrane) is where the frequency discrimination of sound occurs (Hudspeth, 1989).

Unlike non-mammalian tetrapods, mammalian ears are acoustically isolated from each other (Fig. 6B; Manley, 2010). Although the ears are connected by the eustachian tubes (Fig. 6B), sound cannot transmit through these canals. This forms a pressure receiver system where sound can only act on the external surface of the TM. Similar to the avian and crocodilian ear, interaural time differences can be utilised in orienting sound (Heffner and Heffner, 1992). It should be noted here that the time delay of a signal, between the two ears, can be measured in two different modes – interaural time differences and interaural phase differences. Interaural time differences are the measurement of the time passing between the reception of particular landmarks in the signal, a useful method for localising complex

438 signals or noise (Volman and Konishi, 1989). Interaural phase differences are a
439 measurement of the shift in the waveform of a signal between the two ears, and hearing
440 systems compute this to localise pure tones (Volman and Konishi, 1989). Due to the
441 limitations on the ability of the auditory nerve compute the phase of high frequency
442 oscillations, using interaural time differences at frequencies above 2 to 5 kHz becomes
443 ineffective at providing directional cues (Rose et al., 1967). Analysing interaural spectral
444 differences may be an alternative when localisation of multi-frequency signals (Heffner and
445 Heffner, 1992). High frequency sounds attenuate quicker and are more likely to reflect off the
446 head than low frequency sounds. This means that the ear that is ipsilateral to the stimulus
447 will have greater intensity of the high-frequency sounds (Heffner and Heffner, 1992). Larger
448 heads will produce increased reflection and attenuation; so, for interaural spectral
449 differences, high and low frequencies are relative to the size of the mammal's head (Heffner
450 and Heffner, 1982).
451 Monoaural directional hearing can be made possible by the presence of the pinnae
452 (Heffner and Heffner, 1992). A pinna can passively amplify sounds that enter from the
453 direction in which it faces, whilst attenuating high frequency sounds that originate from
454 different directions (Calford and Pettigrew, 1984; Phillips et al., 1982). The passive
455 amplification of sound measured in several mammalian taxa (Coles and Guppy, 1985;
456 Rosowski et al., 1988); including humans (Voss and Allen, 1994). This is caused by the
457 geometry of the outer ear; together, the pinna and EC form an exponential horn that leads
458 directly to the TM (Coles and Guppy, 1985; Rosowski et al., 1988; Voss and Allen, 1994).
459 Low frequency sounds are less affected by the presence of a pinna, meaning that high
460 frequencies are needed for monaural localisation (Flynn and Elliott, 1965). The human ear
461 can utilise pinna cues when frequencies greater than 4 kHz are present in a sound (Butler,
462 1986; Musicant and Butler, 1984). Some mammals have the ability to manipulate the
463 orientation of their pinna (Tollin et al., 2009). Here, the vestibulo-auricular reflex can respond
464 to sound by orienting the pinna towards the source (Tollin et al., 2009). With the directional

position of the sound source stabilised, the effects of head rotation on auditory input are reduced (Tollin et al., 2009).

Summary of the tetrapod ear

The similarities and differences between the tympanal ears of terrestrial vertebrates is clear to see. Underlying features that are present across all groups are: 1) a lever system formed by the middle ear for transducing airborne vibrations into travelling waves, 2) a high ratio between the surface area of the TM and that of the contact point between the middle ear and inner ear (columella or stapes), 3) a slightly concave membrane (formed by the connections of the ossicular chain to the TM; Helmholtz, 1868 in Tonndorf and Khanna, 1971; Tonndorf and Khanna, 1971), 4) a series of mechanoreceptors for analysing frequencies within a signal. The underlying mechanisms of sound localisation rely in the formation of a pressure-difference or pressure receiver. Within the pressure-difference receiver systems discussed here, the more relict condition involves an interaural connection via the mouth cavity (anurans and lacertilians). More advanced pressure-difference receiver systems (as seen in crocodilians and birds) possess a separate interaural canal for sound transmission. Some features of Tetrapod sound receivers have evolved convergently in bush-crickets (Orthoptera; Ensifera).

Ears in Ensifera

Ensifera is one of two suborders within the order Orthoptera. The taxonomy has long been debated and is not fully resolved (Desutter-Grandcolas, 2003; Gorochov, 2001; 2003; Gwynne, 1995; Song et al., 2015, Zhou et al., 2017) but for the purposes of this chapter the phylogeny proposed by Song et al. (2015), and the taxa therein, will be used (Fig. 7). Nine families, seven superfamilies and two infraorders are represented here (Fig. 7; Song et al., 2015). Mogoplistidae (Gryllotalpoidea) and Myrmecophilidae (Gryllotalpoidea) have been excluded from this review, due to the lack of literature detailing their tracheal anatomy, but

Gryllotalpidae (Gryllotalpoidea) and Gryllidae (Grylloidea) are used representatives of the infraorder Gryllidea. All members of the infraorder Tettigoniidea are accounted for (Fig. 7). In this section, a summary of each family and their auditory (or homologous) anatomy will be detailed.

Gryllotalpoidea: Gryllotalpidae

Gryllotalpids, also known as mole-crickets, spend much of their time in underground burrows (Fig. 8A). As their common name suggests, they are specially adapted to digging; utilising robust forelegs to shift the earth and form tunnels (Fig. 8B; Baker, 2016). The burrows are a system of tunnels and chambers, used for locating food (plant roots) and housing their eggs, respectively. Males construct a special burrow entrance which amplify their calling song, aiding in mate attraction (Fig. 8A; Bennet-Clark, 1970). The male positions himself facing away from the entrance, which is shaped like an exponential horn, before scraping a file (*pars stridens*) on the right tegmen against a scraper (*plectrum*) on the left tegmen (some species are ambidextrous and possess a file and scraper on both wings; Kavanaugh and Young, 1989). The song of *Gryllotalpa vineae* has a carrier frequency of 3.5 kHz and, when singing at the entrance of the burrow, a sound pressure level of up to 115 dB (Bennet-Clark, 1970). The females are quite proficient at flying and will do so to locate the males at their burrow.

Gryllotalpids do possess ears to capture and process sound signals, although the author of this thesis could not locate or access a detailed description of the internal auditory anatomy. Otte and Alexander (1983) describe species with no TMs, exposed TMs and covered TMs; when present they are situated on the foretibia (Fig 8B; C). This characteristic has been present in Gryllotalpidae since the mid-Cretaceous, with a TM discovered on the foreleg of *Tresdigitus rectanguli*, a well-preserved specimen in Burmese amber (Xu et al., 2020). Desutter-Grandcolas (2003) states that the gryllotalpid EC exhibits an auditory bulla, a tracheal chamber situated between the trachea that emerges from the prothoracic spiracle

519 and the trachea that runs into the foreleg (see Fig. 9B; 15C; 16B for examples in other
520 Ensifera). Observation of an unidentified *Gryllotalpa* sp male reveals the TM is situated
521 inside a recess on the anterior fore-tibia (Fig. 8C). Setae are present around the entrance
522 perhaps to prevent loose earth from blocking the entrance whilst they dig (Fig. 8C).
523 The hearing range of gryllotalpids can extend considerably higher than their calling
524 song frequencies (Howard et al., 2008; Mason et al., 1998). Both *Gryllotalpa major* and
525 *Scapteriscus borellii* are most sensitive to their respective calling song carrier frequencies of
526 2 and 3 kHz yet shows a clear sensitivity peak around 25 kHz. This can be explained by their
527 ability to fly and subsequent need to detect echolocating bats (Howard et al., 2008; Mason et
528 al., 1998). This is supported by the fact that *S. borellii* has an aversion to high frequency
529 stimuli, and that *Scapteriscus abbreviatus*, a non-flying species, is limited to only low
530 frequency hearing Mason et al., 1998.
531
532 **Grylloidea: Gryllidae**
533 Gryllids, also known as true crickets, are a diverse group of insects with an almost
534 global distribution (Cigliano et al., 2020). They have the ability to produce sound via tegminal
535 stridulation, and these are typically at low frequencies (2 to 8 kHz; Fig. 9A; Bennet-Clark,
536 1999; Hoy et al., 1982), although some species in the subfamily Eneopterinae can generate
537 frequencies up to 15 kHz (Desutter-Grandcolas, 1997a in Robillard and Desutter-
538 Grandcolas, 2004; Robillard and Desutter-Grandcolas, 2004). Stridulation is used in mate-
539 attraction and the majority of species can detect these signals via a tympanal organ in the
540 foreleg. Some lineages have lost these the ability to sing and hear (Otte, 1992; Otte and
541 Alexander, 1983), and this process is driven by sound localising parasitoids (Pascoal et al.,
542 2014; Rayner et al., 2019; Zuk et al., 2006), and silent dominant predators (Otte, 1990).
543 In the genus *Gryllus*, the prothoracic tracheal system has adapted for airborne sound
544 transmission, and will therefore be referred to as the EC. The EC of Gryllidae begins at the
545 prothoracic spiracle (Fig. 9A; B; Schmitz et al., 1983). From here, the it emerges into the

prothorax, joining a chamber known as the auditory bulla (Schmidt and Römer, 2013). The auditory bulla of gryllids is joined to the contralateral auditory system by a thin layer of trachea known as the septum (Fig. B; Schmidt and Römer, 2013; Wendler et al., 1993). This enables a crosstalk of sound with the opposite EC, a process that can provide useful directional cues for sound localisation (Michelsen, Popov and Lewis, 1994). A trachea branches off the auditory bulla to continue the EC into the foreleg, through the femur (Fig. 9A; B; Schmidt and Römer, 2013). Once the EC passes the femoro-tibial joint it expands as it enters the tibia. Before reaching the posterior tympanic membrane (PTM; Fig. 9C), the EC begins to divide into two branches – one leading to the anterior tympanic membrane (ATM) and another to the PTM (Young and Ball, 1975). At the point of the ATM, the anterior and posterior branches are separated (Fig. 9C). The ATM is separated from its tracheal branch by a thick layer of epithelial tissue, known as the core (Nishino et al., 2019; Young and Ball, 1975). The core functions as a class 1 lever, similar to the tympanal plate in Tettigoniidae, playing a role in impedance conversion (Montealegre-Z and Robert, 2015; Nishino et al., 2019). The tympanal nerve runs dorsally to the EC, supplying the subgenual organ and the tympanal organ (Strauß et al., 2014). The subgenual organ is positioned proximally to tibial trachea bifurcation and the tympanal organ is situated on the anterior tracheal branch (Fig. 9C; Eibl, 1978; Young and Ball, 1975).

For *Gryllus bimaculatus*, it has been suggested that each ear on the foreleg has at least three inputs: the posterior TM, the ipsilateral prothoracic spiracle, and the contralateral prothoracic spiracle via the septum (Michelsen, Popov and Lewis, 1994). It has been predicted that directional cues are provided by an interaural phase-shift, produced internally as a signal passes through the septum (Fletcher and Thwaites, 1979). This would enable females and competing males to localise a calling individual (Seagraves and Hedwig, 2014). A time delay has also been reported for sound travelling through the EC of *G. bimaculatus* (Michelsen, Popov and Lewis, 1994) and *Teleogryllus oceanicus* (Larsen, 1981). This also occurs in Tettigoniidae and is discussed further in Chapter Two and Chapter Three.

Schizodactyloidea: Schizodactylidae

Schizodactylids, also known as dune crickets or splay-footed crickets, are a basal group of Tettigonioidea – named after their sandy habitats and tarsal adaptations to walking on such a substrate (Fig. 10A; Song et al., 2015). These predatory insects live in deep burrows and, unlike gryllotalpids, they use their enlarged mandibles to dig (Aydin and Khomutov, 2008). These insects are a relict group with only two remaining genera, *Comicus* and *Schizodactylus*, and fossil evidence suggests that their ecological niche has remained constant for over 100 million years (Heads and Leuzinger, 2011). Both the nymphs and adults of Schizodactylids are capable of producing sound by scraping a cuticular ridge on their inner femora against the files on their second, third fourth and fifth abdominal tergites (Mason, 1961). This is mechanism of sound production is known as femoro-abdominal stridulation.

Schizodactylidae are atympanate and have previously been described as possessing no auditory organs (Desutter-Grandcolas, 2003). Strauß and Lakes-Harlan (2009; 2010), however, demonstrate that *Comicus calcaris* not only possesses a subgenual and intermediate organ, in the foreleg, but also a series of neurones that are homologous to the *crista acustica*. The tibial organ is suggested to only receive vibrations via the substrate, and the *crista acustica* homolog has evolved from a deaf condition and is not a reduced form of that seen throughout most of Tettigonioidea (Strauß and Lakes-Harlan, 2010). This is supported by the fact that the prothoracic spiracle and tracheal system are adapted for reducing water loss and not for sound reception (Leubner et al., 2017; Strauß and Lakes-Harlan, 2010). Although a secondary reduction in prothoracic spiracle and trachea size has been suggested for other members of Ensifera (see section on Tettigoniidae), it is suspected that the *crista acustica* homolog is a precursor to the evolution of tympanal hearing.

The tracheal system of Schizodactylidae is not adapted for sound reception. The prothoracic spiracle is small in size and controlled by three valves. Two tracheae are formed from the spiracle opening, the narrow *trachea supraventralis* immediately enters the leg,

whilst the *trachea cephalia* runs into the thorax (connecting to the opposite tracheal system via the *transverse connective trachea*) before meandering anterolaterally and branching into the *trachea pedalis* (Fig. 10B; Strauß and Lakes-Harlan, 2010). The *trachea pedalis* enters the foreleg and runs alongside the *trachea supraventralis* before they join together at the femoro-tibial joint (Fig. 10C; Strauß and Lakes-Harlan, 2010). This coincides with the position of the tibial organs (Fig. 10C). After the tibial organ, the tracheae split into an anterior and posterior branch, which remerge after around 1.7 mm to form the distal tracheal chamber, which runs through the tibia (Fig. 10C).

Rhapidophoroidea: Rhaphidophoridae

Members of the family Rhaphiphoridae, known as cave crickets, are named after their typical habitat (Fig. 11A). They are not limited to caves, however, and *Macropathus filifer* is known to colonise a variety of places, from man-made cellars to unused seabird burrows; the key requirements are a high humidity and low light level – but never complete darkness (Richards, 1954). These insects can exist in both high and low densities, perhaps depending on the space available in their habitat. Both vegetation and animal proteins are important parts of the diet, and this varies between species (Richards, 1954; Di Russo et al., 2014). Evidence suggests that niche partitioning occurs throughout different stages of the lifecycle (Di Russo et al., 2014).

Rhaphidophorids do not possess any sound producing structures but have been observed using short-range vibratory tremulations as a part of courtship (Jeram et al., 1995; Stritih and Čokl, 2012). Pre-copulatory abdominal tremulations (below 120 Hz) were recorded in *Troglophilus neglectus*, and postcopulatory body shakes were seen in *T. neglectus* and *Troglophilus cavicola* (Stritih and Čokl, 2012). This type of communication is suspected to have evolved outside of caves for two reasons: first, both species prefer to tremulate on tree bark, and secondly the abdominal tremulations of *T. neglectus* are below

627 the threshold of hearing on rock (Stritih and Čokl, 2012). This form of signalling is suspected
628 to represent the primitive condition in Ensifera.
629 Members of Rhaphidophoridae do not possess a *crista acustica* (or homologous
630 organ) and are the only Family in Tettigonioidea to lack one (Fig. 11B; Jeram et al., 1995).
631 They are also atympanate, and the combination of these factors means that they are not
632 equipped for detecting airborne or high frequency sounds (Jeram et al., 1995). As previously
633 discussed, Rhaphidophorids can produce and perceive substrate vibrations. Perception is
634 achieved by the a subgenual organ and intermediate organ, which are situated at the
635 proximal tibia to form the subgenual organ complex (Fig. 11B). The intermediate organ is
636 believed to be similar to the ancestral ensiferan condition since the anterior and posterior
637 sensilla are supplied by the same innervation in one long line (Stritih and Strauß, 2015).
638 Jeram et al (1995) provides a detailed, unlabelled illustration of the tracheal system
639 which will be described with the tracheal anatomy used for Shizodactylidae (Fig. 10B; C;
640 Strauß and Lakes-Harlan, 2010). Similar to Shizodactylidae, the prothoracic spiracle and
641 tracheal system show no adaptation to sound capture and transmission (Jeram et al., 1995).
642 The entrance to the prothoracic spiracle is closed by three valves, and three tracheae
643 emerge from the spiracle into the prothorax. The smallest of the tracheae runs across the
644 midline of the prothorax to join the opposite tracheal system (Fig. 11B), another one
645 (suspected to be *trachea supraventralis*) splits twice before entering the foreleg (Fig. 11B),
646 and the widest (suspected to be *trachea cephalia*; Fig. 11B) extends the furthest before
647 branching into the foreleg (suspected to be *trachea pedalis*; Fig. 11B). Once in the foreleg,
648 the two tracheae extend through two-thirds of the femur, before fusing together to form a
649 single larger canal (Fig. 11C). The trachea continues past the femoro-tibial joint before
650 splitting into the anterior and posterior branch (Fig. 11C). The anterior branch is narrower
651 than the posterior, and supports the subgenual organ complex (Fig. 11C)
652
653 **Stenopelmatoidea: Stenopelmatidae**

Stenopelmatids, also known as Jerusalem crickets, are present in North and Central America, southern Africa, and Asia (Fig. 12A; Cigliano et al., 2020). These insects are omnivorous and have been known to feed on vegetable matter and other arthropods (Baker, 1971 in Weissman, 2005; Rathvon, 1877 in Weissman, 2005). They typically inhabit coastal dunes, the underside of rocks, and in forested areas (Weissman and Bazelet, 2013)

Stenopelmatidae are able to detect substrate vibrations, and possess a subgenual organ, intermediate organ and *crista acustica* homolog, all typical of the tibial organ in Tettigonioidea (Fig. 12B; Strauß and Lakes-Harlan, 2008a). Both New and Old-World species can perform femoro-abdominal stridulation (Gorochov, 2001; Weissman, 2001 in Vandergast et al., 2017), but they lack tympana for detection of airborne sound (Strauß and Lakes-Harlan, 2008a). The tracheal system of the prothorax and forelegs has not been fully described (at least in accessible literature) but Strauß and Lakes-Harlan (2008a) describe the spiracle and tibial trachea. The prothoracic spiracle is guarded by three valves, and two separate tracheae are seen entering the tibia – promptly forming a connection (Fig. 12B; Strauß and Lakes-Harlan, 2008a). The connection is brief, and the tracheae remain separated at the level of the subgenual and intermediate organ, but they fuse to form an anteriorly protruding chamber (Fig. 12B). The length of the *crista acustica* homolog makes contact with this tracheal chamber (Fig. 12B). Once contact with the tibial organ ceases, the tracheae split into an anterior and posterior branch – narrow and wide, respectively. The two branches extend two-thirds of the tibia reforming into the distal tracheal chamber (Fig. 12B; Strauß and Lakes-Harlan, 2008a).

Stenopelmatoidea: Anostostomatidae

Anostostomatidae are widely distributed in the southern hemisphere and are commonly known as wetas or king crickets (Field, 2001). Wetas are endemic to New Zealand and have been the focus of many studies on auditory anatomy and function (Ball and Field, 1981; Lomas et al., 2011; Nishino and Field, 2003; Strauß et al., 2017). Some

species possess TMs and others are atympanate (Strauß et al., 2017), and the former will be the focus of this section. Wetas are typically omnivorous but species appear to be more herbivorous or predatory (Cary, 1983; Griffin et al., 2011). Tree wetas (*Hemideina* spp) are large insects that form male dominated social galleries in tree cavities (Fig. 14A; Kelly, 2005). They do not possess tegmina but can produce sound by femoro-abdominal stridulation, which functions in aggression and mating (Field and Rind, 1992). *Hemideina* spp are equipped for detecting non-ultrasonic airborne sounds, with a maximum sensitivity at 2 to 3 kHz in some species (Field at al., 1980 in Lomas et al., 2011; Lomas et al., 2011).

Three tracheae emerge from the prothoracic spiracle into the thorax. One of these is the *trachea supraventralis*, which immediately divides in two (Fig. 14B). One of these divisions passes into the foreleg and will be referred to as posterior trachea. The other branch is the transversal connective trachea, which extends across the midline of the insect to connect with the auditory system of the opposite spiracle (Ball and Field, 1981). It is unknown if the left and right auditory systems of anostostomatids are acoustically connected, as in Gryllidae, or acoustically isolated, as in Tettigoniidae (Ball and Field, 1981). The other two tracheae that emerge from the spiracle do not enter the foreleg. Another trachea enters the foreleg, but it does not originate at the prothoracic spiracle; this is referred to as the anterior trachea (Fig. 14B). Throughout the femur, the anterior trachea is of greater diameter than the posterior, but this reverses when they enter the tibia. Here, the posterior trachea expands to form the proximal tracheal chamber whereas the anterior trachea remains separate (Fig. 14C). At the level of the TM, the anterior and posterior tracheae form the anterior and posterior tympanal chambers, which are comparable to the anterior and posterior tracheal branches demonstrated by other ensiferans in this review (Fig. 14C). The tympanal chambers are briefly connected by a foramen. Distally to the TM, both tympanal chambers connect to the distal tracheal chamber, which runs to the tarsus. The tympanal chambers each form two narrow canals that run ventrally to the distal tracheal chamber until they join at the distal tibia (Fig. 14C).

The complex tibial organ situated in the proximal fore-tibia, and similar to that of Tettigoniidae (Fig. 14D; Strauß, 2019) and Prophalangopsidae (Mason, 1991). It is comprised of a subgenual organ, an intermediate organ and a *crista acustica*. The subgenual organ is connected to the distal posterior tracheal chamber and the proximal anterior branch, and the intermediate organ and *crista acustic*a both associate with the anterior branch (Fig. 14C; Nishino and Field, 2003). The distal *crista acustica* also runs against the ATM.

Stenopelmatoidea: Gryllacrididae

Gryllacridids are known as leaf-rolling crickets or raspy crickets, names representing their nesting sites and tendencies to producing a 'raspy' broadband sound, respectively. Modification of the environment appears essential to a gryllacridids biology, and these insects can produce silk to reinforce debris and construct a shelter (Hale, 2000). Not all shelters are constructed from leaves, and some insects will dig burrows that are equipped with a silk trapdoor (Morton and Rentz, 1983). The name 'leaf-rolling crickets' has declined in popularity due to the lack of representation of the family (Young, 1983). The term 'raspy crickets' is given in response to the sound produced when they rub their hind femur on a series of cuticular pegs situated on the abdomen (Fig. 13A). Femoro-abdominal stridulation produces sounds with a carrier frequency around 4 to 5 kHz, with most of the energy below 10 kHz (Field and Bailey, 1997). Such signals are used as a defence mechanism, and not as a part of intraspecific communication (Field and Bailey, 1997; Rentz, 1996). Substrate vibrations, however, are used during courtship, and these vibrations are produced by drumming the hind legs against the substrate (Field and Bailey, 1997). Many species within Gryllacrididae do not possess tegmina (Fig. 13A), and those that do are not adapted for tegminal stridulation. Correspondingly, gryllacridids are not equipped to hear airborne as they possess no TMs (Strauß and Lakes-Harlan, 2008b).

734 The prothoracic tracheal system is not adapted for sound propagation. The
735 prothoracic spiracle is occluded by three valves and resembles a standard respiratory
736 spiracle (Strauß and Lakes-Harlan, 2008b). Two tracheae emerge from the spiracle (Fig.
737 13B). The first is the *trachea cephalica*, which advances anteriorly to the head (Fig. 13B).
738 For purposes of continuity, it should be noted that Strauß and Lakes-Harlan (2010) describe
739 the *trachea cephalia* in Schizodactylidae (Fig. 10B), and that *trachea cephalica* is possibly a
740 synonym of a homologous structure. The second trachea loops posteriorly before splitting
741 into four separate tracheae. Of these four branches, only the *trachea supraventralis* enters
742 the foreleg, and the transversal connective trachea links this tracheal system to that of the
743 opposite prothoracic spiracle (Strauß and Lakes-Harlan, 2008b). The *trachea pedalis* also
744 enters the leg, although the origin of this branch is not described (Strauß and Lakes-Harlan,
745 2008b). It is possible that the *trachea pedalis* is connected to the *trachea cephalica* (Fig.
746 13B; see Fig. 10B for Schizodactylidae). Strauß and Lakes-Harlan (2008b) state that only
747 the *trachea supraventralis* enters the tibia, implying that the *trachea pedalis* either ends in
748 the femur or merges with the *trachea supraventralis*.
749 Once in the tibia, the *trachea supraventralis* expands into a proximal tracheal
750 chamber before constricting and slitting into an anterior and posterior branch (Fig. 13C).
751 These two branches re-merge after approximately 500 µm to form the wide distal tracheal
752 chamber (Fig. 13C). The complex tibial organ is comprised of a subgenual organ,
753 intermediate organ and *crista acustica* homolog. The subgenual organ and intermediate
754 organ is situated proximally relative to the bifurcation of the anterior and posterior tracheal
755 branches (Strauß and Lakes-Harlan, 2008b). The *crista acustica* homolog begins at the level
756 of the bifurcation and distally associates with the anterior branch (Fig. 13C; Strauß and
757 Lakes-Harlan, 2008b). The complex tibial organ is adapted for detecting substrate vibrations
758 and the *crista acustica* homolog provides no acoustic function (Strauß and Lakes-Harlan,
759 2008).
760
761 **Hagloidea: Prophalangopsidae**

762 Prophalangopsidae contains eight species, known as grigs, which are the last
763 remaining members within Hagloidea. *Prophalangopsis obscura* provides a particularly
764 interesting case. Firstly, it bears a notable resemblance to many of the known fossil species,
765 which inhabited the earth from the Jurassic period onwards (Gorochov, 2003; Gu et al.,
766 2001; Wang et al., 2017). Secondly, it is extremely uncommon and has only been recorded
767 on two occasions. The male of *P. obscura* was described from 'British India' in 1869 and has
768 never been recorded since (Cigliano et al., 2020). In 2009, however two suspected females
769 were described from Tibet, giving hope for future studies on this living fossil (Liu et al.,
770 2009).
771 The North American genus *Cyphoderris* is the most studied of these insects.
772 *Cyphoderris monstrosa* inhabits montane forests, feeding on the pollen of conifers during the
773 summer months (Fig. 15A; Morris and Gwynne, 1978). During the winter, individuals remain
774 in burrows underneath layers of leaf litter and snow, but they also possess anti-freeze
775 agents in their haemolymph to help survive temperatures as low as -6 °C, for extended
776 periods of time (Morris and Gwynne, 1978; Toxopeus et al., 2016). *Cyphoderris* are able to
777 produce sound through two methods; tegminal stridulation and the use of the Ander's organ
778 (Ander, 1938; Morris and Gwynne, 1978; Spooner, 1973). Calling with their tegmina, *C.*
779 *monstrosa* produces a song with a 12 kHz carrier frequency (Chivers et al., 2017; Morris and
780 Gwynne, 1978). All *Cyphoderris* species are ambidextrous in their wing use, utilising the
781 presence of functional files and plectra on each wing throughout calling (Morris and Gwynne,
782 1978; Spooner, 1973). The Ander's organ is only functional in females and nymphs, which
783 both lack sound producing tegmina (Ander, 1938, Woodrow et al., in press). The organ
784 consists of a series of dorsoventrally oriented ridges on the first abdominal tergite, and a
785 series of teeth (up to 14) on the metanotum (Ander, 1938; Morris and Gwynne, 1978). When
786 the insect contracts and extends its abdomen, the teeth strike the ridges to generate sound
787 (Ander, 1938; Morris and Gwynne, 1978).
788 In order to receive the airborne acoustic signals produced by conspecifics, *C.*
789 *monstrosa* has two TMs situated on the proximal fore-tibia (Fig. 15A). This is a shared

feature throughout all of the remaining Prophalangopsidae but, unless specified, all further anatomy have only been investigated in *C. monstrosa* (Liu et al., 2009). The complex tibial organ is closely related to Tettigoniidae, and consists of a subgenual organ, intermediate organ, and *crista acustica* (Fig. 15B; Mason, 1991; Yack, 2004). The subgenual organ is positioned within a groove situated between the femoro-tibial joint and the TM (Mason, 1991). The intermediate organ and the *crista acustica* are arranged linearly, extending distally (Mason, 1991). The *crista acustica* is covered by a tectorial membrane (Mason, 1991). Despite the similarity to Tettigoniidae, the tibial organ of *C. monstrosa* is less acute at discriminating frequencies and can only determine if frequencies are high or low (Mason, 1999).

The morphology of the prothoracic spiracle resembles those that are found on other parts of the body and used for respiration (it is described as having valves, but the number is not specified), and internally it leads to three main tracheae (Mason, 1991). The most ventral of these tracheae (*trachea supraventralis*) connects the spiracle to the interior surfaces of the TM but no acoustic function has been described. The *trachea supraventralis* begins as an extended chamber, known as the auditory bulla (Fig. 15C; Anders, 1939 in Mason, 1991; Mason, 1991). The auditory bulla is 0.7 mm in diameter and advances for 4 mm dissipating into the tissue of the thorax. Two-thirds along the auditory bulla the *trachea supraventralis* forms branch which passes into the foreleg; the *trachea supraventralis* is the only trachea to enter the foreleg. (Fig. 15C; Mason, 1991). Upon reaching the femur, the *trachea supraventralis* splits into two tracheae of equal size (This condition is present in another prophalangopsid species, *Tarragoilus diuturnus*; Jonsson and Montealegre-Z, 2020) These two branches re-join each other after passing through two-thirds of the femur (Fig. 15C). This singular tube continues through the femoro-tibial joint, where it is constricted in radius. Once in the tibia, the trachea expands to form the proximal tracheal chamber (Fig. 15D), before splitting into the anterior and posterior branches (Fig. 15C; D). Here each branch forms the internal surface of their respective TM.

817 Upon stimulating the tympana with a free field FFT stimulus (500 Hz to 20 kHz),
818 Mason (1991) reports that the ear is neuronally tuned to 2 kHz – a mismatch when
819 compared to the 13 kHz carrier frequency of the calling song. This could be because the
820 frequency tuning of the TM reduces to 2 kHz when the prothoracic spiracle is closed (Sarria-
821 S and Montealegre-Z, 2020). Unlike in Gryllidae (Michelsen, Popov and Lewis, 1994) and
822 Tettigoniidae (Jonsson et al., 2016), the auditory system of *C. monstrosa* has been observed
823 to act as a pressure receiver (Mason, 1991).
824
825 **Tettigonioidea: Tettigoniidae**
826 Tettigoniids, otherwise known as bush-crickets or katydids (Fig. 16A), are a diverse
827 group of ensiferans that employ acoustic communication. With approximately 7000
828 described species, these insects are distributed across the globe and have adapted to
829 survive in a wide range of environments (Cigliano et al., 2020). Capturing and processing
830 sound is essential to the survival and reproduction of bush-crickets and occupying different
831 niches has resulted in high variation in their sound production and reception mechanisms.
832 Males typically produce mating calls to attract females and different species are known to
833 exploit a huge range of frequencies; from as low as 600 Hz to up to a record breaking 150
834 kHz (Montealegre-Z et al., 2017; Sarria-S et al., 2014). Consequently, the combined
835 members of this group possess an immense range of hearing. The ears of many species are
836 tuned to the carrier frequency of their conspecific's song but also retain some sensitivity to a
837 broader range of frequencies (Heinrich et al., 1993; Hummel et al., 2014; Jonsson et al.,
838 2016; Lewis et al., 1975). Both sexes benefit differently by hearing conspecifics: the females
839 to identify and assess and approach specific males, and the males to spatially distance
840 themselves and reduce aggressive intrasexual encounters. The ability to sense a broad
841 range of other frequencies enables bush-crickets to detect cues from potentially predators.
842 This includes the echolocation of hunting bats – which are known to heavily prey upon
843 tettigoniids (Belwood and Morris, 1987; Montealegre-Z et al., 2012; Römer et al., 2010;

844 Schul et al., 2000; Schulze and Schul, 2001; ter Hofstede et al., 2017). Simply detecting
845 such sounds may be sufficient for initiating basic predator avoidance responses (including
846 crypsis, flight dives and leg kicks; Schulze and Schul, 2001; Kilmer et al., 2010; ter Hofstede
847 et al., 2010) but localisation of the sound source is key to performing directional responses,
848 and efficiently pinpoint prospective mates.

849 In order to effectively localise airborne sound, bush-crickets have evolved complex
850 ears. Compared to tetrapods, they have small interaural distances (Bierman et al., 2014;
851 Calford and Piddington, 1988; Christensen-Dalsgaard and Manley, 2005; Koka et al., 2011;
852 Heffner and Heffner, 1992). This means that bush-crickets suffer short interaural time
853 differences, along with reduced interaural amplitude differences (Robert, 2005). This
854 presents challenges for neuronally determining differences in the arrival time and sound
855 pressure of the stimulus. To overcome these obstacles, the tettigoniid ear has evolved to
856 become a pressure-difference receiver – a system where a single sound stimulus can enter
857 the ear via multiple sounds inputs, each differing in intensity (for more recent findings and
858 discussion of this definition, see Chapter Three; Fig 16B. Michelsen and Larsen, 2008;
859 Robert, 2005).

860 Sound can enter the ear via an external and internal input, with the both stimuli
861 interacting together at the TM (Jonsson et al., 2016). Two are situated on the proximal fore-
862 tibia (Fig. 16C). The external surfaces of the TMs are exposed to the environment
863 (sometimes covered by a cuticular flap), and the internal surfaces are backed by the
864 acoustic trachea (*trachea supraventralis*), here referred to as the EC. These are the internal
865 and external sound pathways, respectively. The EC begins at the permanently open
866 prothoracic spiracle, which is enlarged in diameter to facilitate sound transmission (Fig. 16B;
867 Heinrich et al., 1993; Lewis et al., 1974; Rössler et al., 1994). The spiracle directly leads to
868 the EC, which remains at a large diameter to form a space known as the auditory bulla (Fig.
869 16B). The diameter of the bulla decreases exponentially until it reaches the femur of the
870 foreleg (Heinrich et al., 1993; Lewis et al., 1974; Nowotny et al., 2010). It remains at a more
871 constant diameter until constricting at the femoro-tibial joint and expanding in the tibia. After

the brief expansion, the EC splits into an anterior and posterior branch, leading to ATM and PTM, respectively.

In the subfamilies Conocephalinae, Dectinae, Mecopodinae, Phaneropterinae and Tettigoniinae, the exponential horn shape is the defining characteristic of the EC. Many studies have documented species with such anatomy (Heinrich et al., 1993; Jonsson et al., 2016; Lewis, 1974; Nowotny et al., 2010; Shen, 1993). The auditory bulla plays a key role in amplifying the sound signal (Celiker et al., 2020). Across the literature it is frequently reported that the acoustic signal can gain 15-20 dB as it passes from the spiracle to the tympana (Jonsson et al., 2016; Michelsen, Heller, Stumpner, and Rohrseitz, 1994; Shen, 1993). In the model species *Copiphora gorgonensis* (Conocephalinae), the tracheal gain is greatest at frequencies similar to the conspecific calling song carrier frequency with an additional peak around 45 kHz – likely for detecting bat echolocation (Jonsson et al., 2016).

As in Gryllidae, a time delay has been reported for sound travelling through the tettigoniid EC (see Chapters Two and Chapter Three for more information; Jonsson et al., 2016). Bush-crickets can localise the position of an acoustic stimulus because the EC input is directionally dependent, i.e. the ipsilateral ear will perceive an amplified and delayed signal, whist the contralateral ear may only detect the lower amplitude external stimulus (Jonsson et al., 2016; Robert, 2005; Römer and Krusch, 2000)

Once a soundwave has excited the TM, it is transduced into fluid vibrations by the tympanal plate, which exhibits an antiphase motion in relation to the TM (Montealegre-Z and Robert, 2015). The fluid vibrations pass through the acoustic vesicle as a travelling wave – stimulating the *crista acustica* (Montealegre-Z et al., 2012; Montealegre-Z and Robert, 2015). The mechanoreceptors of the *crista acustica* are tonotopically organised, allowing for precise frequency discrimination of the travelling wave (Montealegre-Z et al., 2012; Stölting and Stumpner, 1998). In addition to the *crista acustica*, the tettigoniid complex tibial organ is comprised of the subgenual organ and intermediate organ (Lin et al., 1993; Strauß, 2019; Yack, 2004).

Summary of the ensiferan ear

Ensifera are a diverse suborder that includes both modern and relict lineages. This is reflected in the varied methods of sound production and different adaptations to detecting and processing auditory information. As demonstrated by previous studies (Desutter-Grandcolas, 2003; Gwynne, 1995), this review describes no parsimonious solution when matching the phylogeny to the sound production and reception anatomy (Fig. 7). The ancestral state of Ensifera seems to be well represented in Rhaphidophoridae. Signalling with tremulations and detecting vibrations with the subgenual and intermediate organs, there was no intraspecific need to detect airborne sounds or high frequencies. This is reflected in the lack of tympanal ears and a *crista acustica*. The latter of the two suggests a relation to Gryllidea, despite being placed in Tettigoniidea (Fig. 7). The innervation of the intermediate organ is also simple, with a single linear nerve supplying the anterior and posterior sensilla (Stritih and Strauß, 2015). The foreleg tracheation is not adapted for sound transmission and likely had a respiratory function (Jeram et al., 1995).

Sound production by stridulation is common among Ensifera, and some form is present in all families discussed – excluding Rhaphidophoridae (Ander, 1938, Bennet-Clark, 1970; 1999; Field and Bailey, 1997; Field and Rind, 1992; Gorochov, 2001; Mason, 1961; Sarria et. al., 2014). Of the nine families reviewed, abdominal stridulation is present in five, all of which are placed in Tettigoniidea (Ander, 1938; Field and Bailey, 1997; Field and Rind, 1992; Gorochov, 2001; Mason, 1961). When the auditory anatomy that has been detailed in this review is compared to the phylogeny (Song et al., 2015; Fig.7) it parsimoniously describes that femoro-abdominal stridulation evolved separately in Schizodactylidae, and either once in the Hagloidea-Stenopelmatoidea ancestor (with Prophalangopsidae incorporating the use of the metanotum as *plectra*) or separately in Stenopelmatoidea with Prophalangopsidae developing the Ander's organ.

Tegminal stridulation and tympanal hearing has convergently evolved at least twice in Ensifera: once in Grylloidea and once in Tettigonioidea (Gwynne, 1995). Due to the

placement of the brachypterous and atympanate Rhaphidophoridae, relative to Tettigoniidae (Fig. 7), one can observe that tegminal stridulation must have evolved separately in the tettigoniid lineage for the phylogeny to fit with the anatomy. Interestingly, this coincides with the tegminal arrangement during stridulation: modern gryllids typically place their right wing dorsally to the left (Masaki et al., 1987 in Chivers et al., 2017), tettigoniids typically place their left wing dorsally to the right (Montealgre-Z and Postles, 2010), and prophalangopsids have the ability to switch the arrangement of their wings – even mid-calling (Morris and Gwynne, 1978). Of course, this is merely an observation, and the author suggests a formal analysis as an appropriate next step.

The tracheation of the foreleg is varied in the thorax, femur and tibia. The tibial tracheation is conserved throughout Ensifera, with two tracheae/branches present at the level of the complex tibial organ/subgenual organ complex/tympanal organ (Ball and Field, 1981; Heinrich et al., 1993; Jeram et al., 1995; Strauß and Lakes-Harlan, 2008a; Strauß and Lakes-Harlan, 2008b; Strauß and Lakes-Harlan, 2010; Mason, 1991; Young and Ball, 1975). Members of Prophalangopsidae possess a unique femoral bifurcation in the trachea supraventralis but the purpose is unknown, since there is no acoustic function of the trachea. Both Gryllidae and Tettigoniidae possess an EC adapted for sound transmission (Jonsson, 2016; Michelsen, Heller, Stumpner, and Rohrseitz, 1994; Michelsen, Popov and Lewis, 1994). The key difference between two families is that the EC are acoustically isolated in Tettigoniidae but connected by a sound-permeable septum in Gryllidae. Regardless, both EC result in interaural amplitude differences and phase-shifts, due to the diffractive effects of the thorax (Jonsson et al., 2016; Larsen, 1981; Robert, 2005). This system is explored in Chapter Two and described as a pressure-time difference receiver in Chapter Three.

Conclusion

Acoustic communication in tetrapods and ensiferans is diverse and complex, yet the anatomy present in both groups has evolved to provide the key functions of sound reception,

impedance conversion and frequency discrimination. It must be noted that the ear of Tettigoniidae exhibits a striking convergence to that of mammals; from signal amplification in the outer ear, to the formation of travelling waves propagating through the inner ear fluid. In both tetrapods and ensiferans, the auditory anatomy works to provide directional cues to the receiver.

The underlying mechanism of sound localisation involves interaural differences in signal amplitude and time of reception. Tetrapods typically have the advantage of larger heads which increases the interaural time differences but, with the exception of mammals, they generally communicate using lower frequencies which attenuate less between each ear. They exploit the lack of attenuation by possessing acoustically connected ears; destructive interference occurs at the contralateral ear to increase the interaural amplitude differences. In Ensifera this process involves the computation of differences both within and between each of the ears.

It is clear that both airborne and vibratory signals play an important role in how ensiferans sense their environment. Unlike the widespread ability to sense vibrations, not all ensiferans are capable of detecting airborne sounds. The EC plays a vital role in this, either by directly amplifying a signal, or providing an air-filled space at in the foretibia, allowing the TM to oscillate in response to stimulation. The author of this thesis states that an ensiferan EC, which has adapted to directly enhance hearing, should include: 1) an opening in the prothorax, 2) an amplifying auditory bulla in the prothorax, 3) a tracheal branch that connects the two previous structures to the TM, 4) an expanded anterior and posterior branch adjacent to the internal surface of the TM.

The diversity of Ensifera (especially Gryllidae and Tettigoniidae) and the varying anatomy of the EC leaves much to be explored in terms of the role that the EC plays in hearing. Chapter Three details collaborative project that uses modern experimental, numerical and investigative techniques to describe the exponential horn ear of Tettigoniidae as a pressure-time difference receiver. The author recommends that these techniques are

981 combined with diverse set of taxa, in order to elucidate patterns in sound transmission
982 through the EC and the effect on hearing sensitivity and directional hearing.

References

Alvord, L.S. and Farmer, B.L., 1997. Anatomy and orientation of the human external ear. *Journal-American Academy of Audiology*, 8, 383-390.

Ander, K., 1938. Ein abdominales Stridulationsorgan bei Cyphoderris (Prophalangopsidae) und über die systematische Einteilung der Ensiferen (Saltatoria). *Opuscula Entomologica*, 193, 32-38.

Arak, A., 1983. Sexual selection by male–male competition in natterjack toad choruses. *Nature*, 306, 261-262.

Aydin, G. and Khomutov, A., 2008. The biology, nymphal stages, and life habits of the endemic sand dune cricket Schizodactylus inexpectatus (Werner, 1901) (Orthoptera: Schizodactylidae). *Turkish Journal of Zoology*, 32, 427-432.

Baird, I.L., 1974. Some aspects of the comparative anatomy and evolution of the inner ear in submammalian vertebrates. *Brain, Behavior and Evolution*, 10, 11-36.

Bailey, W.J., 1993. The tettigoniid (Orthoptera: Tettigoniidae) ear: multiple functions and structural diversity. *International Journal of Insect Morphology and Embryology*, 22, 185-205.

Baker, E., 2016. The burrow morphology of mole crickets (Orthoptera: Gryllotalpidae): terminology and comparisons. *PeerJ Preprints*, 4, p.e2664v1.

Ball, E.E. and Field, L.H., 1981. Structure of the auditory system of the weta Hemideina crassidens (Blanchard, 1851)(Orthoptera, Ensifera, Gryllacridoidea, Stenopelmatidae). *Cell and Tissue Research*, 217, 321-344.

Belwood, J.J. and Morris, G.K., 1987. Bat predation and its influence on calling behavior in neotropical katydids. *Science*, 238, 64-67.

Bennet-Clark, H.C., 1970. The mechanism and efficiency of sound production in mole crickets. *Journal of Experimental Biology*, 52, 619-652.

Bennet-Clark, H.C., 1999. Resonators in insect sound production: how insects produce loud pure-tone songs. *Journal of experimental Biology*, 202, 3347-3357.

Benson, M.F., 1939 Great Grig by Mary Foley Benson, Illustration of *Cyphoderris monstrosa*. *Singing Insects of North America*. Accessed: 19/09/2020 {https://orthsoc.org/sina/339dm.htm}.

Bierman, H.S. and Carr, C.E., 2015. Sound localization in the alligator. *Hearing Research*, 329, 11-20.

Bierman, H.S., Thornton, J.L., Jones, H.G., Koka, K., Young, B.A., Brandt, C., Christensen-Dalsgaard, J., Carr, C.E. and Tollin, D.J., 2014. Biophysics of directional hearing in the American alligator (Alligator mississippiensis). *Journal of Experimental Biology*, 217, 1094-1107.

Briefer, E., Aubin, T., Lehongre, K. and Rybak, F., 2008. How to identify dear enemies: the group signature in the complex song of the skylark Alauda arvensis. *Journal of Experimental Biology*, 211, 317-326.

1036 Briskie, J.V., Naugler, C.T. and Leech, S.M., 1994. Begging intensity of nestling birds varies
1037 with sibling relatedness. *Proceedings of the Royal Society of London. Series B: Biological*
1038 *Sciences*, 258, 73-78.
1039
1040 Buchanan, K.L. and Catchpole, C.K., 2000. Song as an indicator of male parental effort in
1041 the sedge warbler. *Proceedings of the Royal Society of London. Series B: Biological*
1042 *Sciences*, 267, 321-326.
1043
1044 Burghardt, G. M. (1977). Of iguanas and dinosaurs: social behavior and communication in
1045 neonate reptiles. *American Zoologist*. 17, 177-190.
1046
1047 Butler, R.A., 1986. The bandwidth effect on monaural and binaural localization. *Hearing*
1048 *Research*, 21, 67-73.
1049
1050 Calford, M.B. and Pettigrew, J.D., 1984. Frequency dependence of directional amplification
1051 at the cat's pinna. *Hearing Research*, 14, 13-19.
1052
1053 Calford, M.B. and Piddington, R.W., 1988. Avian interaural canal enhances interaural delay.
1054 *Journal of Comparative Physiology A*, 162, 503-510.
1055
1056 Cantwell, L.R. and Forrest, T.G., 2013. Response of Anolis sagrei to acoustic calls from
1057 predatory and nonpredatory birds. *Journal of Herpetology*, 47, 293-298.
1058
1059 Carr, C.E., Christensen-Dalsgaard, J. and Bierman, H., 2016. Coupled ears in lizards and
1060 crocodilians. *Biological Cybernetics*, 110, 291-302.
1061
1062 Cary, P.R., 1983. Diet of the ground weta Zealandosandrus gracilis (Orthoptera:
1063 Stenopelmatidae). *New Zealand Journal of Zoology*, 10, 295-297.

Catchpole, C.K., Dittami, J. and Leisler, B., 1984. Differential responses to male song repertoires in female songbirds implanted with oestradiol. *Nature*, 312, 563-564.

Celiker, E., Jonsson, T. and Montealegre-Z, F., 2020. The Auditory Mechanics of the Outer Ear of the Bush Cricket: A Numerical Approach. *Biophysical Journal*, 118, 464-475.

Chivers, B.D., Béthoux, O., Sarria-S, F.A., Jonsson, T., Mason, A.C. and Montealegre-Z, F., 2017. Functional morphology of tegmina-based stridulation in the relict species Cyphoderris monstrosa (Orthoptera: Ensifera: Prophalangopsidae). *Journal of Experimental Biology*, 220, 1112-1121.

Christensen-Dalsgaard, J., Ludwig, T.A. and Narins, P.M., 2002. Call diversity in an old world treefrog: level dependence and latency of acoustic responses. *Bioacoustics* 13, 21–35.

Christensen-Dalsgaard, J. and Manley, G.A., 2005. Directionality of the lizard ear. *Journal of Experimental Biology*, 208, 1209-1217.

Christensen-Dalsgaard, J., 2005. Directional hearing in nonmammalian tetrapods. In *Sound Source Localization*, 67-123.

Christensen-Dalsgaard, J., 2011. Vertebrate pressure-gradient receivers. *Hearing Research*, 273, 37-45.

Cigliano, M.M., Braun, H., Eades, D.C. and Otte, D., 2020. *Orthoptera Species File*. Version 5.0/5.0. Available at http://Orthoptera.SpeciesFile.org [Accessed 15/09/2020].

1091 Clack, J.A., 2002. Patterns and processes in the early evolution of the tetrapod ear. *Journal*
1092 *of Neurobiology*, 53, 251-264.
1093
1094 Coles, R.B. and Guppy, A., 1986. Biophysical aspects of directional hearing in the tammar
1095 wallaby, Macropus eugenii. *Journal of Experimental Biology*, 121, 371-394.
1096
1097 Desutter-Grandcolas, L., 2003. Phylogeny and the evolution of acoustic communication in
1098 extant Ensifera (Insecta, Orthoptera). *Zoologica Scripta*, 32, 525-561.
1099
1100 Di Russo, C., Rampini, M., Latella, L. and Cobolli, M., 2014. Measurements of the diet in two
1101 species of Troglophilus Krauss, 1879 cave crickets from Italian subterranean habitats
1102 (Orthoptera, Rhaphidophoridae). *Subterranean Biology*, 13, 45-54.
1103
1104 Eibl, E., 1978. Morphology of the sense organs in the proximal parts of the tibiae of *Gryllus*
1105 *campestris* L. And. *Gryllus bimaculatus* de Geer (Insecta, Ensifera). *Zoomorphologie*, 89,
1106 185-205.
1107
1108 Ekdale, E.G., 2016. The ear of mammals: From monotremes to humans. In *Evolution of the*
1109 *Vertebrate Ear*, 175-206.
1110
1111 Elie, J.E. and Theunissen, F.E., 2018. Zebra finches identify individuals using vocal
1112 signatures unique to each call type. *Nature Communications*, 9, 1-11.
1113
1114 Evans, R.M., 1992. Embryonic and neonatal vocal elicitation of parental brooding and
1115 feeding responses in American white pelicans. *Animal Behaviour*, 44, 667-675.
1116

1117 Feng, A.S., Gerhardt, H.C. and Capranica, R.R., 1976. Sound localization behavior of the
1118 green treefrog (Hyla cinerea) and the barking treefrog (H. gratiosa). J*ournal of Comparative*
1119 *Physiology*, 107, 241-252.
1120
1121 Feng, A.S., Narins, P.M. and Capranica, R.R., 1975. Three populations of primary auditory
1122 fibers in the bullfrog (Rana catesbeiana): their peripheral origins and frequency sensitivities.
1123 *Journal of Comparative Physiology*, 100, 221-229.
1124
1125 Feng, A.S. and Narins, P.M., 2008. Ultrasonic communication in concave-eared torrent frogs
1126 (Amolops tormotus). *Journal of Comparative Physiology A*, 194, 159-167.
1127
1128 Fenton, M.B. and Bell, G.P., 1981. Recognition of species of insectivorous bats by their
1129 echolocation calls. *Journal of Mammalogy*, 62, 233-243.
1130
1131 Field, L.H. ed., 2001. *The biology of wetas, king crickets and their allies*. CABI.
1132
1133 Field, L.H. and Bailey, W.J., 1997. Sound production in primitive Orthoptera from Western
1134 Australia: sounds used in defence and social communication in Ametrus sp. and
1135 Hadrogryllacris sp.(Gryllacrididae: Orthoptera). *Journal of Natural History*, 31, 1127-1141.
1136
1137 Field, L.H. and Rind, F.C., 1992. Stridulatory behaviour in a New Zealand weta, Hemideina
1138 crassidens. *Journal of Zoology*, 228, 371-394.
1139
1140 Fischer, F.P., Köppl, C. and Manley, G.A., 1988. The basilar papilla of the barn owl Tyto
1141 alba: A quantitative morphological SEM analysis. *Hearing Research*, 34, 87-101.
1142

1143 Fletcher, N.H. and Thwaites, S., 1979. Acoustical analysis of the auditory system of the
1144 cricket Teleogryllus commodus (Walker). *The Journal of the Acoustical Society of America*,
1145 66, 350-357.
1146
1147 Flynn, W.E. and Elliott, D.N., 1965. Role of the pinna in hearing. *The Journal of the*
1148 *Acoustical Society of America*, 38, 104-105.
1149
1150 Garrick, L.D., Lang, J.W. and Herzog, H.A., 1978. Social signals of adult American alligators.
1151 *Bulletin of the AMNH*; 160, 155-192.
1152
1153 Gleich, O., Manley, G.A., Mandl, A. and Dooling, R.J., 1994. Basilar papilla of the canary
1154 and zebra finch: A quantitative scanning electron microscopical description. *Journal of*
1155 *Morphology*, 221, 1-24.
1156
1157 Gorochov, A.V., 2001. *The higher classification, phylogeny and evolution of the superfamily*
1158 *Stenopelmatoidea. The biology of wetas, king crickets and their allies*, 3-33.
1159
1160 Gorochov, A.V., 2003. New data on taxonomy and evolution of fossil and Recent
1161 Prophalangopsidae (Orthoptera: Hagloidea). *Acta Zoological Cracoviensia*, 46, 117-127.
1162
1163 Griesser, M., 2008. Referential calls signal predator behavior in a group-living bird species.
1164 *Current Biology*, 18, 69-73.
1165
1166 Griesser, M., 2013. Do warning calls boost survival of signal recipients? Evidence from a
1167 field experiment in a group-living bird species. *Frontiers in Zoology*, 10, 49.
1168
1169 Griffin, M.J., Morgan-Richards, M. and Trewick, S.A., 2011. Is the tree weta Hemideina
1170 crassidens an obligate herbivore. *New Zealand Natural Sciences*, 36, 11-19.

1171

1172 Gu, J.J., Qiao, G.X. and Ren, D., 2011. A exceptionally-preserved new species of
1173 Barchaboilus (Orthoptera: Prophalangopsidae) from the Middle Jurassic of Daohugou,
1174 China. *Zootaxa*, 2909, 64-68.

1175

1176 Gwynne, D.T., 1995. Phylogeny of the Ensifera (Orthoptera): a hypothesis supporting
1177 multiple origins of acoustical signalling, complex spermatophores and maternal care in
1178 crickets, katydids, and weta. *Journal of Orthoptera Research*, 203-218.

1179

1180 Hale, R.J., 2000. Nest utilisation and recognition by juvenile gryllacridids (Orthoptera:
1181 Gryllacrididae). *Australian Journal of Zoology*, 48, 643-652.

1182

1183 Heads, S.W. and Leuzinger, L., 2011. On the placement of the Cretaceous orthopteran
1184 Brauckmannia groeningae from Brazil, with notes on the relationships of Schizodactylidae
1185 (Orthoptera, Ensifera). *ZooKeys*, 77, 17-30.

1186

1187 Heffner, R.S. and Heffner, H.E., 1982. Hearing in the elephant (Elephas maximus): absolute
1188 sensitivity, frequency discrimination, and sound localization. *Journal of Comparative and*
1189 *Physiological Psychology*, 96, 926-944.

1190

1191 Heffner, R.S. and Heffner, H.E., 1992. Evolution of sound localization in mammals. In *The*
1192 *evolutionary biology of hearing*, 691-715.

1193

1194 Heinrich, R., Jatho, M. and Kalmring, K., 1993. Acoustic transmission characteristics of the
1195 tympanal tracheae of bushcrickets (Tettigoniidae). II: comparative studies of the tracheae of
1196 seven species. *The Journal of the Acoustical Society of America*, 93, 3481-3489.

1197

1198 Hellström, S., Salén, B. and Stenfors, L.E., 1982. Anatomy of the rat middle ear. *Cells*
1199 *Tissues Organs*, 112, 346-352.
1200
1201 Henson, O.W., 1974. Comparative anatomy of the middle ear. In *Auditory System*, 39-110.
1202
1203 Hetherington, T.E., 1988. Biomechanics of vibration reception in the bullfrog, Rana
1204 catesbeiana. *Journal of Comparative Physiology A*, 163, 43-52.
1205
1206 Higgs, D., Brittan-Powell, E., Soares, D., Souza, M., Carr, C., Dooling, R. and Popper, A.,
1207 2002. Amphibious auditory responses of the American alligator (Alligator mississipiensis).
1208 *Journal of Comparative Physiology A*, 188, 217-223.
1209
1210 Hill, K.G., Lewis, D.B., Hutchings, M.E. and Coles, R.B., 1980. Directional hearing in the
1211 Japanese quail (*Coturnix coturnix japonica*): I. Acoustic properties of the auditory system.
1212 *Journal of Experimental Biology*, 86, 135-151.
1213
1214 ter Hofstede, H.M., Kalko, E.K. and Fullard, J.H., 2010. Auditory-based defence against
1215 gleaning bats in neotropical katydids (Orthoptera: Tettigoniidae). *Journal of Comparative*
1216 *Physiology A*, 196, 349-358.
1217
1218 ter Hofstede, H., Voigt-Heucke, S., Lang, A., Römer, H., Page, R., Faure, P. and Dechmann,
1219 D., 2017. Revisiting adaptations of neotropical katydids (Orthoptera: Tettigoniidae) to
1220 gleaning bat predation. *Neotropical Biodiversity*, 3, 41-49.
1221
1222 Hopson, J.A., 1987. The mammal-like reptiles: a study of transitional fossils. *The American*
1223 *Biology Teacher*, 49, 16-26.
1224

1225 Hopson, J.A., 1966. The origin of the mammalian middle ear. *American Zoologist*, 6, 437-
1226 450.
1227
1228 Howard, D.R., Mason, A.C. and Hill, P.S., 2008. Hearing and spatial behavior in Gryllotalpa
1229 major Saussure (Orthoptera: Gryllotalpidae). *Journal of Experimental Biology*, 211, 3613-
1230 3618.
1231
1232 Hoy, R.R., Pollack, G.S. and Moiseff, A., 1982. Species-recognition in the field cricket,
1233 Teleogryllus oceanicus: behavioral and neural mechanisms. *American Zoologist*, 22, 597-
1234 607.
1235
1236 Hudspeth, A.J., 1989. How the ear's works work. *Nature*, 341, 397-404.
1237
1238 Hummel, J., Wolf, K., Kössl, M. and Nowotny, M., 2014. Processing of simple and complex
1239 acoustic signals in a tonotopically organized ear. *Proceedings of the Royal Society B:*
1240 *Biological Sciences*, 281, p.20141872.
1241
1242 Hunt, R.H. and Watanabe, M.E., 1982. Observations on maternal behavior of the American
1243 alligator, Alligator mississippiensis. *Journal of Herpetology*, 16, 235-239.
1244
1245 Hyson, R.L., Overholt, E.M. and Lippe, W.R., 1994. Cochlear microphonic measurements of
1246 interaural time differences in the chick. *Hearing Research*, 81, 109-118.
1247
1248 Janik, V.M. and Slater, P.J., 1997. Vocal learning in mammals. *Advances in the Study of*
1249 *Behaviour*, 26, 59-100.
1250

1251 Jaslow, A.P., 1988. Structure and function of the amphibian middle ear; in *The evolution of*
1252 *amphibian auditory system* (eds) Fritzsch, B., Ryan, M., Wilczynski, W., Hetherington, T. and
1253 Walkowiak, W.
1254
1255 Jeram, S., Rössler, W., Čokl, A. and Kalmring, K., 1995. Structure of atympanate tibial
1256 organs in legs of the cave-living Ensifera, Troglophilus neglectus (Gryllacridoidea,
1257 Raphidophoridae). *Journal of Morphology*, 223, 109-118.
1258
1259 Jonsson, T., and Montealegre-Z, F., 2020. Conversation with Fernando Montealegre-Z.
1260 September 2020.
1261
1262 Jonsson, T., Montealegre-Z, F., Soulsbury, C.D., Robson Brown, K.A. and Robert, D., 2016.
1263 Auditory mechanics in a bush-cricket: direct evidence of dual sound inputs in the pressure
1264 difference receiver. *Journal of the Royal Society Interface*, 13, p.20160560.
1265
1266 Jørgensen, M.B. and Kanneworff, M., 1997. Middle ear transmission in the grass frog, Rana
1267 temporaria. *Journal of Comparative Physiology A*, 182, 59-64.
1268
1269 Jørgensen, M.B., Schmitz, B. and Christensen-Dalsgaard, J., 1991. Biophysics of directional
1270 hearing in the frog Eleutherodactylus coqui. *Journal of Comparative Physiology A*, 168, 223-
1271 232.
1272
1273 Jost, M.C. and Shaw, K.L., 2006. Phylogeny of Ensifera (Hexapoda: Orthoptera) using three
1274 ribosomal loci, with implications for the evolution of acoustic communication. *Molecular*
1275 *Phylogenetics and Evolution*, 38, 510-530.
1276
1277 Kavanagh, M.W. and Young, D., 1989. Bilateral symmetry of sound production in the mole
1278 cricket, Gryllotalpa australis. *Journal of Comparative Physiology A*, 166, 43-49.

Kelley, D.B., 2004. Vocal communication in frogs. *Current Opinion in Neurobiology*, 14, 751-757.

Kelly, C.D., 2005. Allometry and sexual selection of male weaponry in Wellington tree weta, Hemideina crassidens. *Behavioral Ecology*, 16, 145-152.

Kilmer, M.K., Barrus, B.B. and Schul, J., 2010. Ultrasound avoidance behaviors in two species of Neoconocephalus (Orthoptera, Tettigoniidae). *Journal of Orthoptera Research*, 81-88.

Kilner, R. and Johnstone, R.A., 1997. Begging the question: are offspring solicitation behaviours signals of need?. *Trends in Ecology & Evolution*, 12, 11-15.

Koka, K., Jones, H.G., Thornton, J.L., Lupo, J.E. and Tollin, D.J., 2011. Sound pressure transformations by the head and pinnae of the adult Chinchilla (Chinchilla lanigera). *Hearing Research*, 272, 135-147.

Ladich, F. and Winkler, H., 2017. Acoustic communication in terrestrial and aquatic vertebrates. *Journal of Experimental Biology*, 220, 2306-2317.

Lal, H., 1967. Operant control of vocal responding in rats. *Psychonomic Science*, 8, 35-36.

Larsen, O.N., 1981. Mechanical time resolution in some insect ears. *Journal of Comparative Physiology*, 143, 297-304.

Larsen, O.N., Christensen-Dalsgaard, J. and Jensen, K.K., 2016. Role of intracranial cavities in avian directional hearing. *Biological Cybernetics*, 110, 319-331.

Leisler, B. and Catchpole, C.K., 1996. Female aquatic warblers (Acrocephalus paludicola) are attracted by playback of longer and more complicated songs. *Behaviour*, 133, 1153-1164.

Leubner, F., Bradler, S. and Wipfler, B., 2017. The thoracic morphology of the wingless dune cricket Comicus calcaris (Orthoptera: Schizodactylidae): Novel apomorphic characters for the group and adaptations to sand desert environments. *Arthropod Structure & Development*, 46, 449-461.

Lewis, D.B., 1974. The Physiology of the Tettigoniid Ear: I. The Implications of the Anatomy of the Ear to Its Function in Sound Reception. *Journal of Experimental Biology*, 60, 821-837.

Lewis, D.B., Seymour, C. and Broughton, W.B., 1975. The response characteristics of the tympanal organs of two species of bush cricket and some studies of the problem of sound transmission. *Journal of Comparative Physiology*, 104, 325-351.

Lin, Y., Kalmring, K., Jatho, M., Sickmann, T. and Rössler, W., 1993. Auditory receptor organs in the forelegs of Gampsocleis gratiosa (Tettigoniidae): morphology and function of the organs in comparison to the frequency parameters of the conspecific song. *Journal of Experimental Zoology*, 267, 377-388.

Liu, X., Zhou, M., Bi, W. and Tang, L., 2009. New data on taxonomy of recent Prophalangopsidae (Orthoptera: Hagloidea). *Zootaxa*, 2026, 53-62.

Lomas, K., Montealegre-Z, F., Parsons, S., Field, L.H. and Robert, D., 2011. Mechanical filtering for narrow-band hearing in the weta. *Journal of Experimental Biology*, 214, 778-785.

1335 Maestripieri, D. and Call, J., 1996. Mother-infant communication in primates. In *Advances in*
1336 *the Study of Behavior*, 25, 613-642.
1337
1338 Maier, W., 1989. Phylogeny and ontogeny of mammalian middle ear structures. *Netherlands*
1339 *Journal of Zoology*, 40, 55-74.
1340
1341 Manley, G.A. and Clack, J.A., 2004. An outline of the evolution of vertebrate hearing organs.
1342 In *Evolution of the Vertebrate Auditory System*, 1-26.
1343
1344 Manley, G.A., 2000. Cochlear mechanisms from a phylogenetic viewpoint. *Proceedings of*
1345 *the National Academy of Sciences*, 97, 11736-11743.
1346
1347 Manley, G.A., 2002. Evolution of structure and function of the hearing organ of lizards.
1348 *Journal of Neurobiology*, 53, 202-211.
1349
1350 Manley, G.A., 2010. An evolutionary perspective on middle ears. *Hearing Research*, 263, 3-
1351 8.
1352
1353 Marcellini, D., 1977. Acoustic and visual display behavior of gekkonid lizards. *American*
1354 *Zoologist*, 17, 251-260.
1355
1356 Mason, M.J. and Narins, P.M., 2002a. Vibrometric studies of the middle ear of the bullfrog
1357 Rana catesbeiana I. The extrastapes. *Journal of Experimental Biology*, 205, 3153-3165.
1358
1359 Mason, A.C., 1991. Hearing in a primitive ensiferan: the auditory system of Cyphoderris
1360 monstrosa (Orthoptera: Haglidae). *Journal of Comparative Physiology A*, 168, 351-363.
1361

Mason, A.C., Forrest, T.G. and Hoy, R.R., 1998. Hearing in mole crickets (Orthoptera: Gryllotalpidae) at sonic and ultrasonic frequencies. *Journal of Experimental Biology*, 201, 1967-1979.

Mason, A.C., Morris, G.K. and Hoy, R.R., 1999. Peripheral frequency mis-match in the primitive ensiferan Cyphoderris monstrosa (Orthoptera: Haglidae). *Journal of Comparative Physiology A*, 184, 543-551.

Mason, J.B., 1961. Stridulatory Mechanism in the Family Schizodactylidae (Orth. Gryllacridoidea).

Mason, M.J. and Narins, P.M., 2002b. Vibrometric studies of the middle ear of the bullfrog Rana catesbeiana II. The operculum. *Journal of Experimental Biology*, 205, 3167-3176.

Michelsen, A. and Larsen, O.N., 2008. Pressure difference receiving ears. *Bioinspiration & Biomimetics*, 3, p.011001.

Michelsen, A., Heller, K.G., Stumpner, A. and Rohrseitz, K., 1994. A new biophysical method to determine the gain of the acoustic trachea in bushcrickets. *Journal of Comparative Physiology A*, 175, 145-151.

Michelsen, A., Popov, A.V. and Lewis, B., 1994. Physics of directional hearing in the cricket Gryllus bimaculatus. *Journal of Comparative Physiology A*, 175,153-164.

Molliver, M.E., 1963. Operant control of vocal behavior in the cat 1. *Journal of the Experimental Analysis of Behavior*, 6, 197-202.

1389 Montealegre-Z, F., Jonsson, T., Robson-Brown, K.A., Postles, M. and Robert, D., 2012.
1390 Convergent evolution between insect and mammalian audition. *Science*, 338, 968-971.
1391
1392 Montealegre-Z, F., Ogden, J., Jonsson, T. and Soulsbury, C.D., 2017. Morphological
1393 determinants of signal carrier frequency in katydids (Orthoptera): a comparative analysis
1394 using biophysical evidence of wing vibration. *Journal of Evolutionary Biology*, 30, 2068-2078.
1395
1396 Montealegre-Z, F. and Postles, M., 2010. Resonant sound production in Copiphora
1397 gorgonensis (Tettigoniidae: Copiphorini), an endemic species from parque nacional natural
1398 gorgona, Colombia. *Journal of Orthoptera Research*, 347-355.
1399
1400 Montealegre-Z, F. and Robert, D., 2015. Biomechanics of hearing in katydids. *Journal of*
1401 *Comparative Physiology A*, 201, 5-18.
1402
1403 Morris, G.K. and Gwynne, D.T., 1978. Geographical distribution and biological observations
1404 of Cyphoderris (Orthoptera: Haglidae) with a description of a new species. *Psyche*, 85, 147-
1405 167.
1406
1407 Morton, S.R. and Rentz, D.C.F., 1983. Ecology and taxonomy of fossorial, granivorous
1408 gryllacridids (Orthoptera: Gryllacrididae) from arid central Australia. *Australian Journal of*
1409 *Zoology*, 31, 557-579.
1410
1411 Musicant, A.D. and Butler, R.A., 1984. The influence of pinnae-based spectral cues on
1412 sound localization. *The Journal of the Acoustical Society of America*, 75, 1195-1200.
1413
1414 Myers, S.A., Horel, J.A. and Pennypacker, H.S., 1965. Operant control of vocal behavior in
1415 the monkey Cebus albifrons. *Psychonomic Science*, 3, 389-390.
1416

1417 Nishino, H., Domae, M., Takanashi, T. and Okajima, T., 2019. Cricket tympanal organ
1418 revisited: morphology, development and possible functions of the adult-specific chitin core
1419 beneath the anterior tympanal membrane. *Cell and Tissue Research*, 377, 193-214.
1420
1421 Nishino, H. and Field, L.H., 2003. Somatotopic mapping of chordotonal organ neurons in a
1422 primitive ensiferan, the New Zealand tree weta Hemideina femorata: II. Complex tibial organ.
1423 *Journal of Comparative Neurology*, 464, 327-342.
1424
1425 Nocke, H., 1975. Physical and physiological properties of the tettigoniid ("grasshopper") ear.
1426 *Journal of Comparative Physiology*, 100, 25-57.
1427
1428 Nowotny, M., Hummel, J., Weber, M., Möckel, D. and Kössl, M., 2010. Acoustic-induced
1429 motion of the bushcricket (Mecopoda elongata, Tettigoniidae) tympanum. *Journal of*
1430 *Comparative Physiology A*, 196, 939-945.
1431
1432 Otte D, Alexander RD (1983) *The Australian Crickets (Orthoptera: Gryllidae)*, Academy of
1433 Natural Sciences of Philadelphia.
1434
1435 Otte, D., 1990. The relation between hearing and flying in crickets. *Entomological News*,
1436 101, 29-34.
1437
1438 Otte, D., 1992. Evolution of cricket songs. Journal of orthoptera research, (1), pp.25-49.
1439 Pascoal, S., Cezard, T., Eik-Nes, A., Gharbi, K., Majewska, J., Payne, E., Ritchie, M.G., Zuk,
1440 M. and Bailey, N.W., 2014. Rapid convergent evolution in wild crickets. *Current Biology*, 24,
1441 1369-1374.
1442

1443 Phillips, D.P., Calford, M.B., Pettigrew, J.D., Aitkin, L.M. and Semple, M.N., 1982.
1444 Directionality of sound pressure transformation at the cat's pinna. *Hearing Research*, 8, 13-
1445 28.
1446
1447 Poole, J.H., Payne, K., Langbauer, W.R. and Moss, C.J., 1988. The social contexts of some
1448 very low frequency calls of African elephants. *Behavioral Ecology and Sociobiology*, 22, 385-
1449 392.
1450
1451 Purgue, A.P. and Narins, P.M., 2000. Mechanics of the inner ear of the bullfrog (Rana
1452 catesbeiana): the contact membranes and the periotic canal. *Journal of Comparative*
1453 *Physiology A*, 186, 481-488.
1454
1455 Puria, S. and Steele, C., 2010. Tympanic-membrane and malleus–incus-complex co-
1456 adaptations for high-frequency hearing in mammals. *Hearing Research*, 263, 183-190.
1457
1458 Rayner, J., Aldridge, S., Montealegre-Z, F. and Bailey, N.W., 2019. A silent orchestra:
1459 convergent song loss in Hawaiian crickets is repeated, morphologically varied, and
1460 widespread. *Ecology*, p.e02694.
1461
1462 Rentz, D.C., 1996. *Grasshopper country: the abundant orthopteroid insects of Australia*.
1463 UNSW Press.
1464
1465 Richards, A.M., 1954. The systematics and ecology of the genus Macropathus Walker, 1869
1466 (Orthoptera, Rhaphidophoridae). In *Transactions of the Royal Society of New Zealand*, 82,
1467 739-762).
1468
1469 Robert, D., 2005. Directional hearing in insects. In *Sound Source Localization*, 6-35.
1470

1471 Robillard, T. and Desutter-Grandcolas, L., 2004. High-frequency calling in Eneopterinae
1472 crickets (Orthoptera, Grylloidea, Eneopteridae): adaptive radiation revealed by phylogenetic
1473 analysis. *Biological Journal of the Linnean Society*, 83, 577-584.
1474
1475 Rodríguez-Vázquez, J.F., 2005. Development of the stapes and associated structures in
1476 human embryos. *Journal of Anatomy*, 207, 165-173.
1477
1478 Römer, H. and Krusch, M., 2000. A gain-control mechanism for processing of chorus sounds
1479 in the afferent auditory pathway of the bushcricket Tettigonia viridissima (Orthoptera;
1480 Tettigoniidae). *Journal of Comparative Physiology A*, 186, 181-191.
1481
1482 Römer, H., Lang, A. and Hartbauer, M., 2010. The signaller's dilemma: a cost–benefit
1483 analysis of public and private communication. *PLoS One*, 5, p.e13325.
1484
1485 Rose, J.E., Brugge, J.F., Anderson, D.J. and Hind, J.E., 1967. Phase-locked response to
1486 low-frequency tones in single auditory nerve fibers of the squirrel monkey. *Journal of*
1487 *Neurophysiology*, 30, 769-793.
1488
1489 Rosowski, J.J., Carney, L.H. and Peake, W.T., 1988. The radiation impedance of the
1490 external ear of cat: Measurements and applications. *The Journal of the Acoustical Society of*
1491 *America*, 84, 1695-1708.
1492
1493 Rössler, W., Hübschen, A., Schul, J. and Kalmring, K., 1994. Functional morphology of
1494 bushcricket ears: comparison between two species belonging to the Phaneropterinae and
1495 Decticinae (Insecta, Ensifera). *Zoomorphology*, 114, 39-46.
1496
1497 Ruiz-Monachesi, M.R. and Labra, A., 2020. Complex distress calls sound frightening: the
1498 case of the weeping lizard. *Animal Behaviour*, 165, 71-77.

Ruta, M. and Coates, M.I., 2007. Dates, nodes and character conflict: addressing the lissamphibian origin problem. *Journal of Systematic Palaeontology*, 5, 69-122.

Saino, N. and Fasola, M., 1996. The function of embryonic vocalization in the little tern (Sterna albifrons). *Ethology*, 102, 265-271.

Sakaluk, S.K. and Belwood, J.J., 1984. Gecko phonotaxis to cricket calling song: a case of satellite predation. *Animal Behaviour*, 32, 659-662.

Salzinger, K. and Waller, M.B., 1962. The operant control of vocalization in the dog 1. *Journal of the Experimental Analysis of Behavior*, 5, 383-389.

Sarria-S, F.A, and Montealegre-Z, F., 2020. Conversation with Fernando Montealegre-Z. September 2020.

Sarria-S, F.A., Morris, G.K., Windmill, J.F., Jackson, J. and Montealegre-Z, F., 2014. Shrinking wings for ultrasonic pitch production: hyperintense ultra-short-wavelength calls in a new genus of neotropical katydids (Orthoptera: Tettigoniidae). *PLoS One*, 9, p.e98708.

Saunders, J. C., Duncan, R. K., Doan, D. E. and Werner, Y. L. (2000). The middle ear of reptiles and birds. In *Comparative Hearing: Birds and Reptiles* (ed. R. J. Dooling, R. R. Fay and A. N. Popper), 13-69.

Schmidt, A.K. and Römer, H., 2013. Diversity of acoustic tracheal system and its role for directional hearing in crickets. *Frontiers in Zoology*, 10, 1-9.

1526 Schmitz, B., Scharstein, H. and Wendler, G., 1983. Phonotaxis in Gryllus campestris L.
1527 (Orthoptera, Gryllidae). *Journal of Comparative Physiology*, 152, 257-264.
1528
1529 Schoffelen, R.L., Segenhout, J.M. and Van Dijk, P., 2008. Mechanics of the exceptional
1530 anuran ear. *Journal of Comparative Physiology A*, 194, 417-428.
1531
1532 Schul, J., Matt, F. and Helversen, O.V., 2000. Listening for bats: the hearing range of the
1533 bushcricket Phaneroptera falcata for bat echolocation calls measured in the field.
1534 *Proceedings of the Royal Society of London. Series B: Biological Sciences*, 267, 1711-1715.
1535
1536 Schulze, W. and Schul, J., 2001. Ultrasound avoidance behaviour in the bushcricket
1537 Tettigonia viridissima (Orthoptera: Tettigoniidae). *Journal of Experimental Biology*, 204, 733-
1538 740.
1539
1540 Seagraves, K.M. and Hedwig, B., 2014. Phase shifts in binaural stimuli provide directional
1541 cues for sound localisation in the field cricket Gryllus bimaculatus. *Journal of Experimental*
1542 *Biology*, 217, 2390-2398.
1543
1544 Semple, S. and McComb, K., 2000. Perception of female reproductive state from vocal cues
1545 in a mammal species. *Proceedings of the Royal Society of London. Series B: Biological*
1546 *Sciences*, 267, 707-712.
1547
1548 Shen, J.X., 2018. Ultrasonic Vocalization in Amphibians and the Structure of Their Vocal
1549 Apparatus. In *Handbook of Behavioral Neuroscience*, 25, 481-491.
1550
1551 Shen, J.X., 1993. A peripheral mechanism for auditory directionality in the bushcricket
1552 Gampsocleis gratiosa: acoustic tracheal system. *The Journal of the Acoustical Society of*
1553 *America*, 94, 1211-1217.

Shute, C.C.D. and Bellairs, A.D.A., 1955. The external ear in Crocodilia. In *Proceedings of the Zoological Society of London*, 124, 741-749.

Song, H., Amédégnato, C., Cigliano, M.M., Desutter-Grandcolas, L., Heads, S.W., Huang, Y., Otte, D. and Whiting, M.F., 2015. 300 million years of diversification: elucidating the patterns of orthopteran evolution based on comprehensive taxon and gene sampling. *Cladistics*, 31, 621-651.

Spencer, K.A., Buchanan, K.L., Goldsmith, A.R. and Catchpole, C.K., 2003. Song as an honest signal of developmental stress in the zebra finch (Taeniopygia guttata). *Hormones and Behavior*, 44, 132-139.

Spooner, J.D., 1973. Sound production in Cyphoderris monstrosa (Orthoptera: Prophalangopsidae). *Annals of the Entomological Society of America*, 66, 4-5.

Stölting, H. and Stumpner, A., 1998. Tonotopic organization of auditory receptors of the bushcricket Pholidoptera griseoaptera (Tettigoniidae, Decticinae). *Cell and Tissue Research*, 294, 377-386.

Strauß, J., 2019. What determines the number of auditory sensilla in the tympanal hearing organs of Tettigoniidae? Perspectives from comparative neuroanatomy and evolutionary forces. *Journal of Orthoptera Research*, 28, 205-219.

Strauß, J. and Lakes-Harlan, R., 2008a. Neuroanatomy of the complex tibial organ of Stenopelmatus (Orthoptera: Ensifera: Stenopelmatidae). *Journal of Comparative Neurology*, 511, 81-91.

1582 Strauß, J. and Lakes-Harlan, R., 2008b. Neuroanatomy and physiology of the complex tibial
1583 organ of an atympanate Ensiferan, Ametrus tibialis (Brunner von Wattenwyl,
1584 1888)(Gryllacrididae, Orthoptera) and evolutionary implications. *Brain, Behavior and*
1585 *Evolution*, 71, 167-180.
1586
1587 Strauß, J. and Lakes-Harlan, R., 2009. The evolutionary origin of auditory receptors in
1588 Tettigonioidea: the complex tibial organ of Schizodactylidae. *Naturwissenschaften*, 96, 143-
1589 146.
1590
1591 Strauß, J. and Lakes-Harlan, R., 2010. Neuroanatomy of the complex tibial organ in the
1592 splay-footed cricket Comicus calcaris Irish 1986 (Orthoptera: Ensifera: Schizodactylidae).
1593 *Journal of Comparative Neurology*, 518, 4567-4580.
1594
1595 Strauß, J., Lomas, K. and Field, L.H., 2017. The complex tibial organ of the New Zealand
1596 ground weta: sensory adaptations for vibrational signal detection. *Scientific Reports*, 7, 1-15.
1597
1598 Strauß, J., Stritih, N. and Lakes-Harlan, R., 2014. The subgenual organ complex in the cave
1599 cricket Troglophilus neglectus (Orthoptera: Rhaphidophoridae): comparative innervation and
1600 sensory evolution. *Royal Society Open Science*, 1, p.140240.
1601
1602 Stritih, N. and Čokl, A., 2012. Mating behaviour and vibratory signalling in non-hearing cave
1603 crickets reflect primitive communication of Ensifera. *PloS one*, 7, p.e47646.
1604
1605 Stritih, N. and Strauß, J., 2015. Tremulation signalling and sensory neuroanatomy of cave
1606 crickets (Rhaphidophoridae: Troglophilus) are consistent with ancestral vibrational
1607 communication in Ensifera. *Mitt Dtsch Ges Allg Angew Ent*, 20, 333-336.
1608

1609 Todd, N.P.M., 2007. Estimated source intensity and active space of the American alligator
1610 (Alligator Mississippiensis) vocal display. *The Journal of the Acoustical Society of America*,
1611 122, 2906-2915.
1612
1613 Tollin, D.J. and Koka, K., 2009. Postnatal development of sound pressure transformations by
1614 the head and pinnae of the cat: monaural characteristics. *The Journal of the Acoustical*
1615 *Society of America*, 125, 980-994.
1616
1617 Tollin, D.J., Ruhland, J.L. and Yin, T.C., 2009. The vestibulo-auricular reflex. *Journal of*
1618 *Neurophysiology*, 101, 1258-1266.
1619
1620 Tonndorf, J. and Khanna, S.M., 1971. The tympanic membrane as a part of the middle ear
1621 transformer. *Acta Oto-Laryngologica*, 71, 177-180.
1622
1623 Toxopeus, J., Lebenzon, J.E., McKinnon, A.H. and Sinclair, B.J., 2016. Freeze tolerance of
1624 Cyphoderris monstrosa (Orthoptera: Prophalangopsidae). *The Canadian Entomologist*, 148,
1625 668-672.
1626
1627 Vandergast, A.G., Weissman, D.B., Wood, D.A., Rentz, D.C., Bazelet, C.S. and Ueshima,
1628 N., 2017. Tackling an intractable problem: Can greater taxon sampling help resolve
1629 relationships within the Stenopelmatoidea (Orthoptera: Ensifera)?. *Zootaxa*, 4291, 1-33.
1630
1631 Vergne, A.L., Pritz, M.B. and Mathevon, N., 2009. Acoustic communication in crocodilians:
1632 from behaviour to brain. *Biological Reviews*, 84, 391-411.
1633
1634 Volman, S.F. and Konishi, M., 1989. Spatial selectivity and binaural responses in the inferior
1635 colliculus of the great horned owl. *Journal of Neuroscience*, 9, 3083-3096.
1636

1637 Voss, S.E. and Allen, J.B., 1994. Measurement of acoustic impedance and reflectance in the
1638 human ear canal. *The Journal of the Acoustical Society of America*, 95, 372-384.
1639
1640 Wang, H., Fang, Y., Zhang, Q.Q., Lei, X.J., Wang, B., Jarzembowski, E.A. and Zhang, H.C.,
1641 2017. New material of Sigmaboilus (Insecta, Orthoptera, Prophalangopsidae) from the
1642 Jurassic Daohugou Beds, Inner Mongolia, China. *Earth and Environmental Science*
1643 *Transactions of the Royal Society of Edinburgh*, 107, 177-183.
1644
1645 Webster, D.B., 1966. Ear structure and function in modern mammals. *American Zoologist*, 6,
1646 451-466.
1647
1648 Weissman, D.B. and Bazelet, C.S., 2013. Notes on southern Africa Jerusalem crickets
1649 (Orthoptera: Stenopelmatidae: Sia). *Zootaxa*, 3616, 49-60.
1650
1651 Weissman, D.B., 2005. Jerusalem! cricket?(Orthoptera: Stenopelmatidae: Stenopelmatus);
1652 origins of a common name. *American Entomologist*, 51, 138-139.
1653
1654 Wendler, G. and Löhe, G., 1993. The role of the medial septum in the acoustic trachea of the
1655 cricket Gryllus bimaculatus. *Journal of Comparative Physiology A*, 173, 557-564.
1656
1657 Wilson, B.S., Finley, C.C., Lawson, D.T. and Wolford, R.D., 1988. Speech processors for
1658 cochlear prostheses. *Proceedings of the IEEE*, 76, 1143-1154.
1659
1660 Woodrow, C., Judge, K.A., Pulver, C., Jonsson, T. and Montealegre-Z (2020) The Ander's
1661 Organ: a mechanism for anti-predator ultrasound in a relict ensiferan. *Journal of*
1662 *Experimental Biology*. In press.
1663

1664 Xu, C., Fang, Y. and Wang, H., 2020. A new mole cricket (Orthoptera: Gryllotalpidae) from
1665 mid-Cretaceous Burmese amber. *Cretaceous Research*, p.104428.
1666
1667 Yack, J.E., 2004. The structure and function of auditory chordotonal organs in insects.
1668 *Microscopy Research and Technique*, 63, 315-337.
1669
1670 Young, A.M., 1983. Patterns of Distribution and Abundance in Small Samples of Litter-
1671 Inhabiting Orthoptera in Some Costa Rican Cacao Plantations. *Journal of the New York*
1672 *Entomological Society*, 91, 312-327.
1673
1674 Young, B.A., 2016. Anatomical influences on internally coupled ears in reptiles. *Biological*
1675 *Cybernetics*, 110, 255-261.
1676
1677 Young, D. and Ball, E., 1974. Structure and development of the auditory system in the
1678 prothoracic leg of the cricket Teleogryllus commodus (Walker). *Zeitschrift für Zellforschung*
1679 *und Mikroskopische Anatomie*, 147, 293-312.
1680
1681 Zhou, Z., Zhao, L., Liu, N., Guo, H., Guan, B., Di, J. and Shi, F., 2017. Towards a higher-
1682 level Ensifera phylogeny inferred from mitogenome sequences. *Molecular Phylogenetics and*
1683 *Evolution*, 108, 22-33.
1684
1685 Zuk, M., Rotenberry, J.T. and Tinghitella, R.M., 2006. Silent night: adaptive disappearance
1686 of a sexual signal in a parasitized population of field crickets. *Biology letters*, 2, 521-524.

Figures

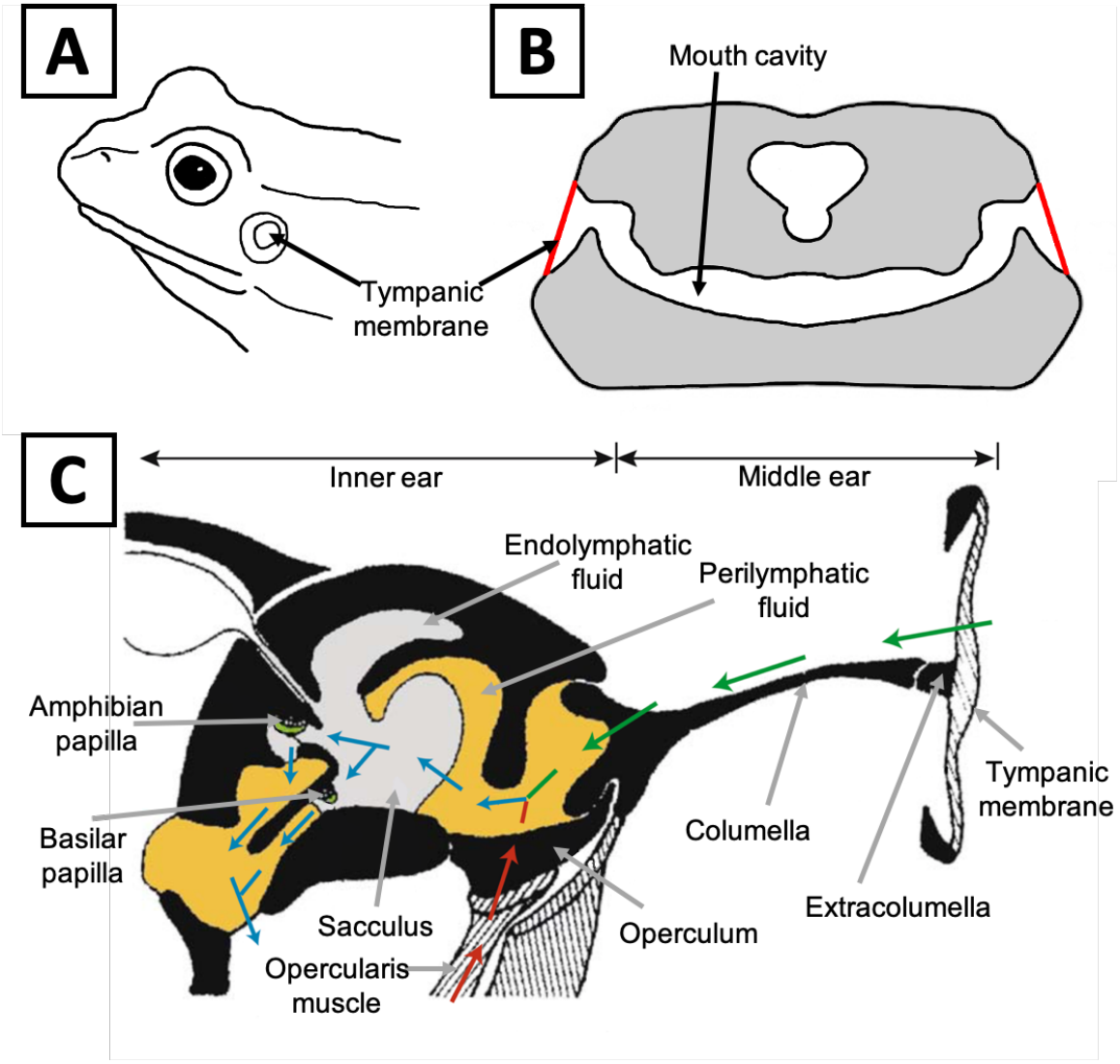

Figure 1. The anuran ear as seen in a frog. **A**) The placement of the ear on the head of *Rana temporaria*, demonstrating the lack of outer ear. **B**) Cross-section of *Rana sphenocephala* at the placement of the ear. The mouth cavity enables sound to pass internally to the tympanic membrane of the other ear. **C**) The anatomy of the middle and inner ear. Airborne sound reaches the perilymphatic fluid via the green arrow pathway and substrate vibrations transmit via the red arrow pathway. Once in the perilymphatic fluid, sound passes travels via the blue pathway to the papillae and out of the ear. (**A** is illustrated

by the author; **B** was modified from Christensen-Dalsgaard, 2005; **C** was modified from Schoffelen et al., 2008).

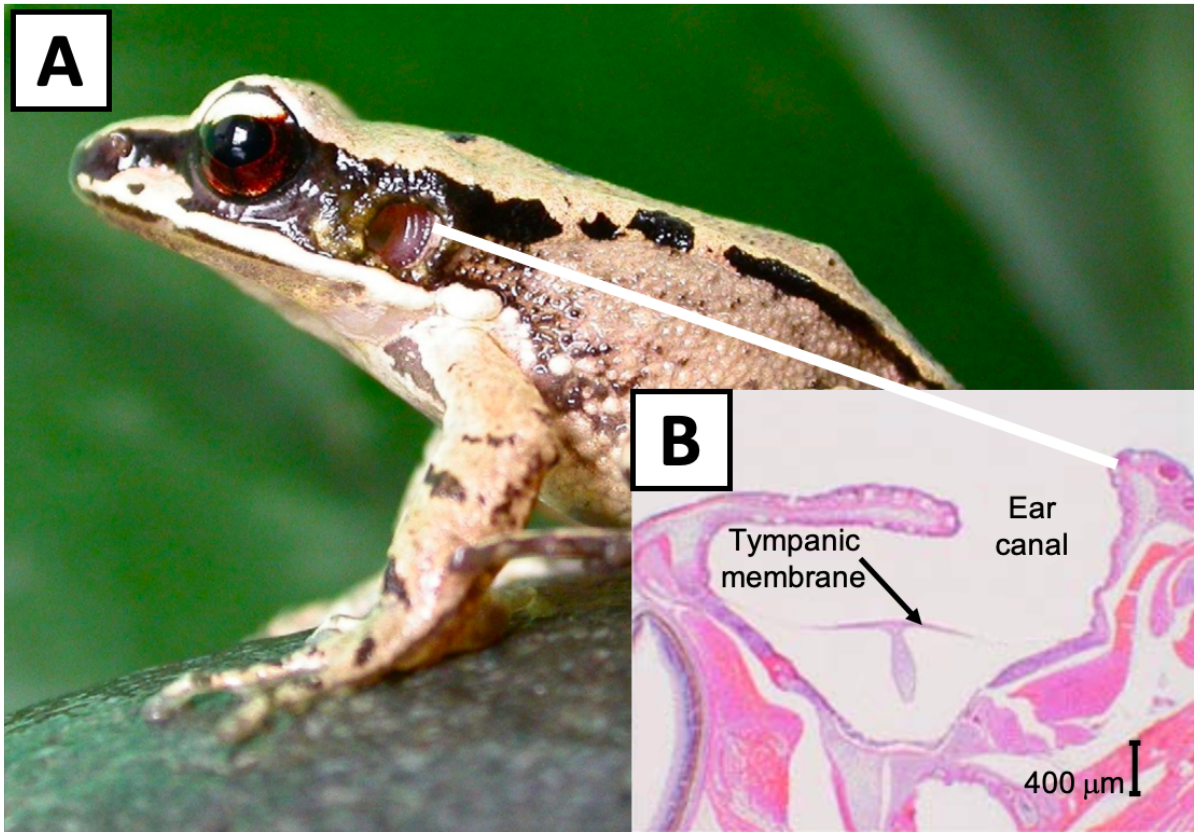

Figure 2. The unique outer ear of an *Odorrana tormota* male. **A**) A male displaying its ear canal, **B**) Low-power photomicrograph of a horizontal cross-section of the right ear (stained with hematoxylin and eosin) through the right ear of a male. The white line indicates the placement of the cross-sectional view on the animal. (**A** is from Shen, 2018; **B** was modified from Feng and Narins, 2008)

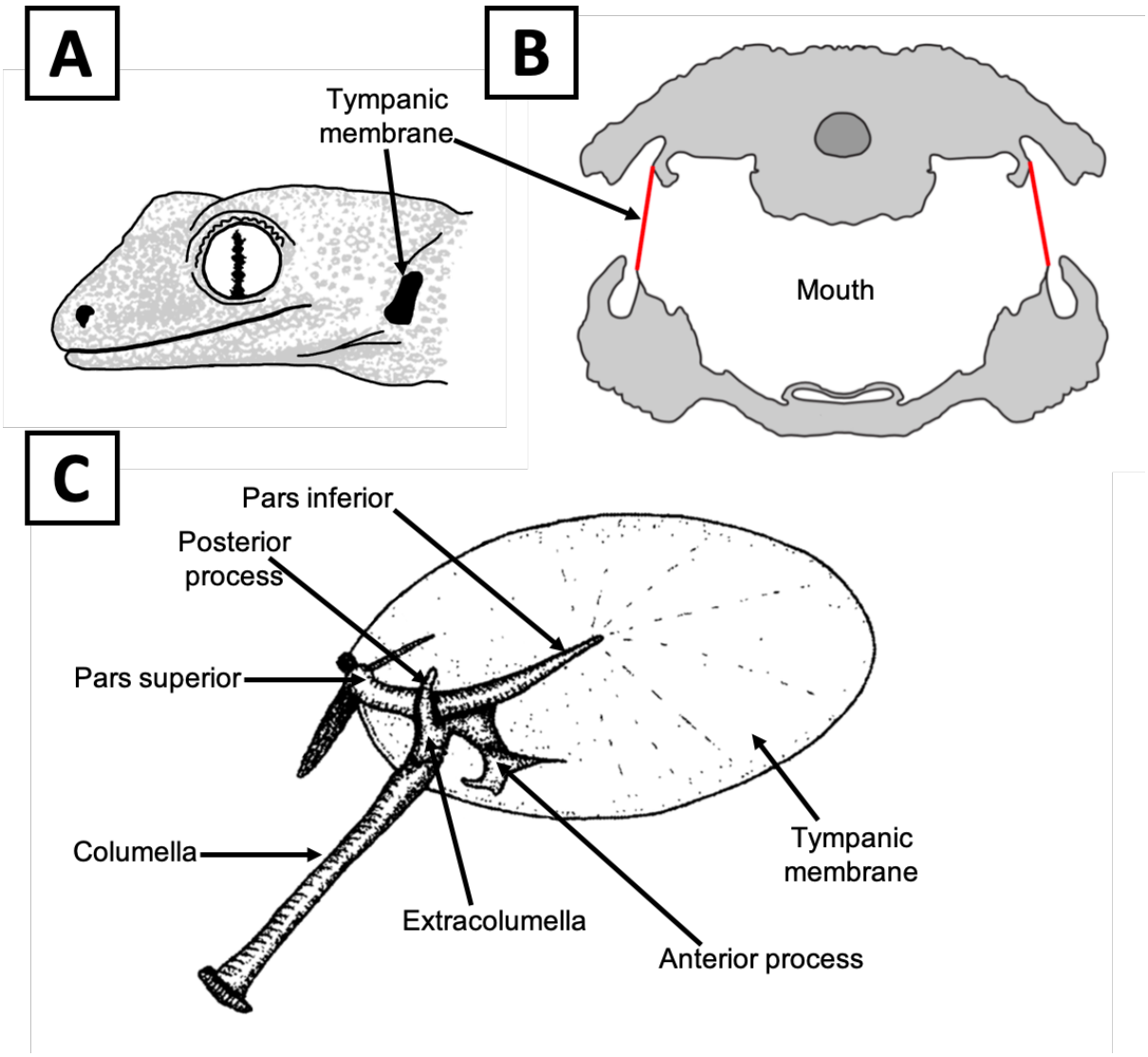

Figure 3. The squamate ear, as seen in the tokay gecko (*Gekko gecko*). **A**) The position of the shallow outer ear on the head. **B**) A cross-section of the head at the ear position. Sound can travel internally, to the contralateral tympanic membrane, via mouth cavity. **C**) The anatomy of the middle ear. The pars inferior and pars superior connects the tympanic membrane to the anterior and posterior processes on the extracolumella. Sound passes through these structures, the columella and into the inner ear. (**A** and **C** were modified from Saunders et al., 2000; **B** modified from Carr et al., 2016).

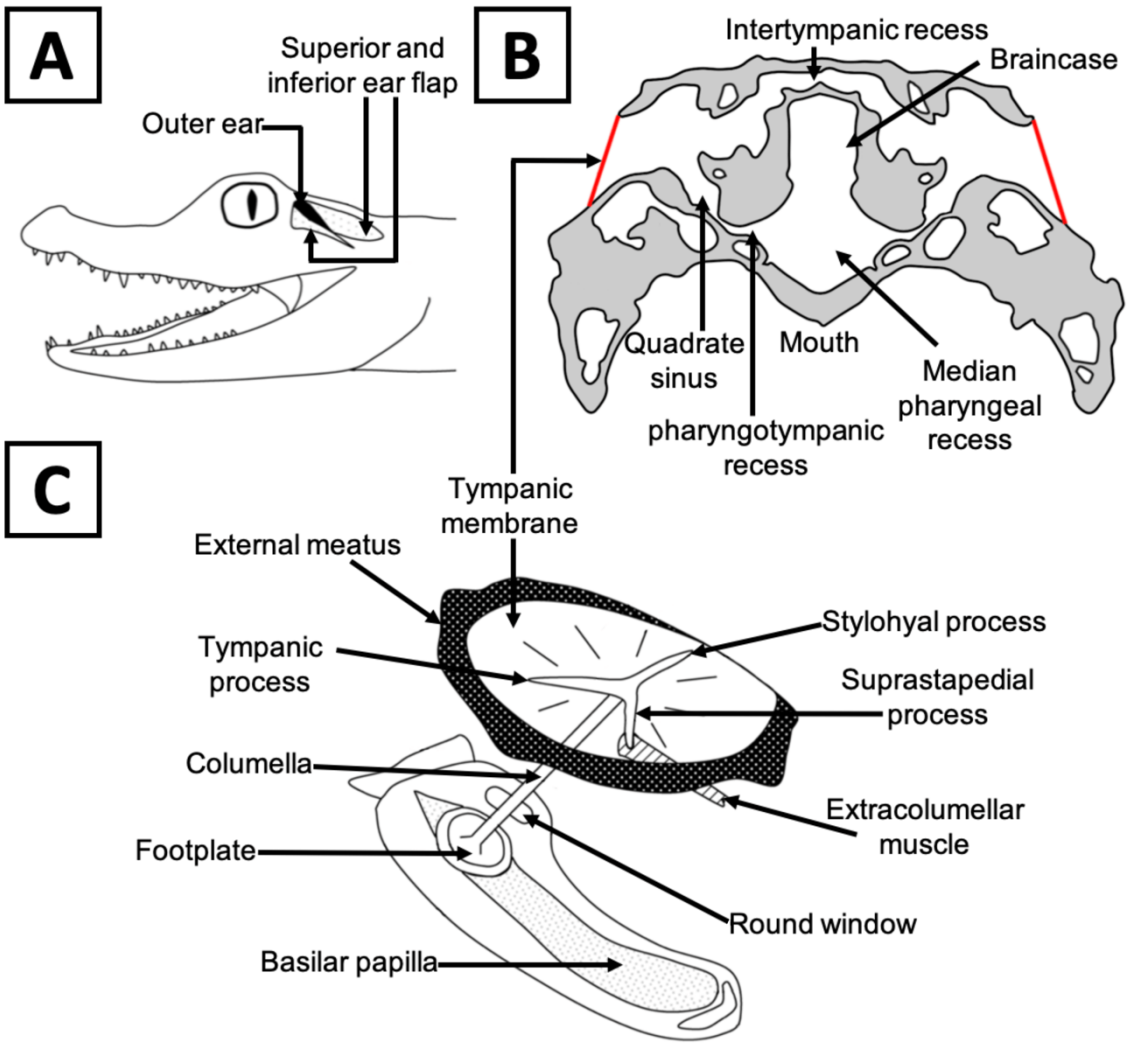

1714

1715 **Figure 4.** The crocodilian ear, as seen in the American alligator (*Alligator mississippiensis*).
1716 **A**) The position of the outer ear on the head, the superior and inferior ear flaps close to
1717 protect the ear when underwater. **B**) A cross-section of the head at the ear position; the
1718 lower jaw and ear flaps are not illustrated. Sound can pass internally to the contralateral
1719 tympanic membrane via the intertympanic recess or through the quadrate sinuses,
1720 pharyngotympanic sinuses and median pharyngeal recess. **C**) the middle and inner ear
1721 anatomy. The tympanic, stylohyal, and suprastapedial processes attach the columella to the
1722 tympanic membrane. Sound passes through these structures and into reach the basilar
1723 papilla for frequency discrimination. (**A** and **C** were modified from Vergne and Mathevon,
1724 2009; **B** was modified from Carr and Bierman, 2015, and Bierman et al., 2014).

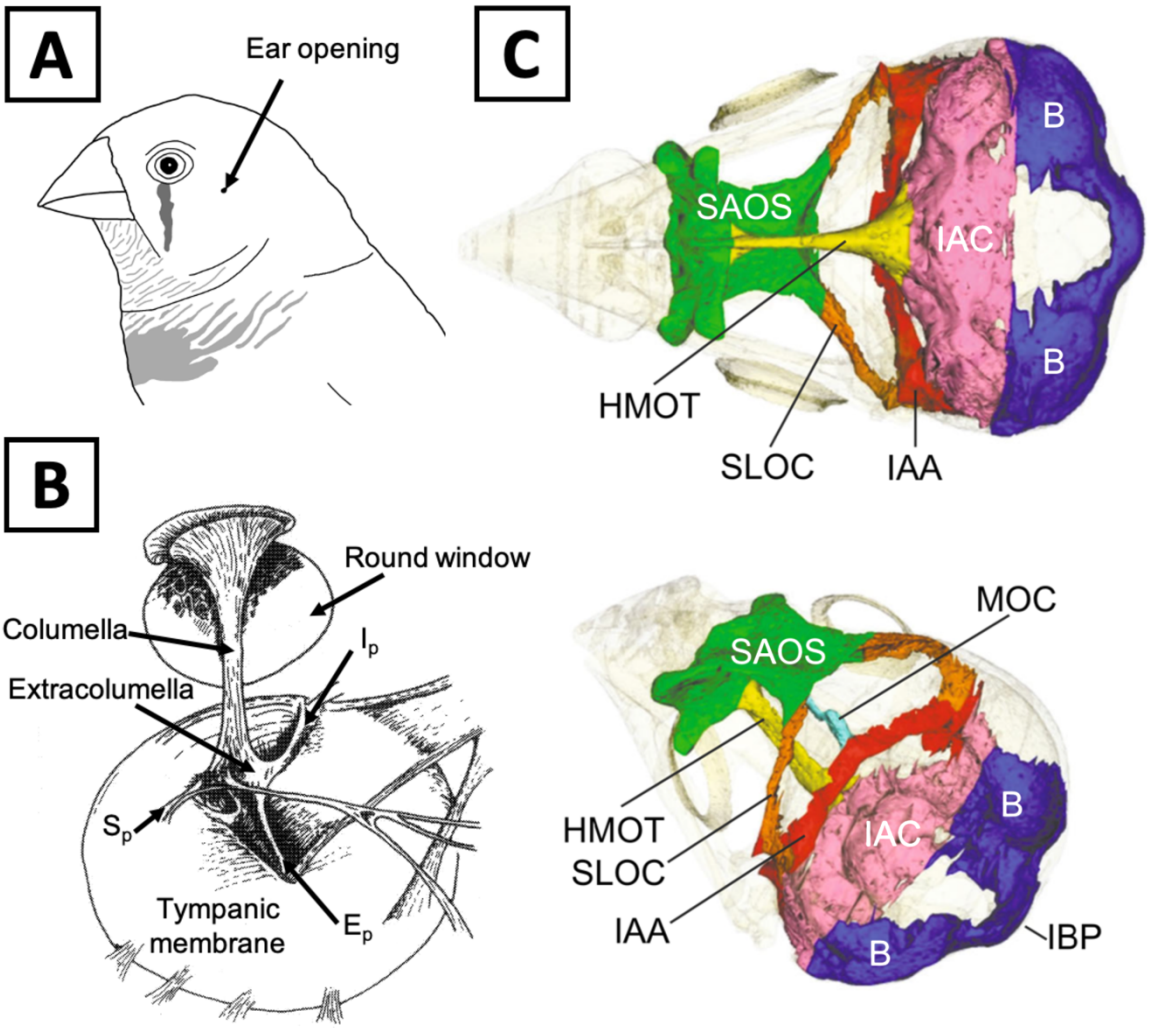

1725

1726 **Figure 5.** The avian ear. **A**) The placement of the ear opening on a zebra finch (*Taeniopygia*
1727 *guttata*). Feathers cover the entrance to a shallow ear canal, where the middle ear sits. **B**)
1728 The middle ear of a parakeet viewed from the internal perspective. Sound vibrations are
1729 captured by the tympanic membrane and transmit to the inner ear via the columella. E_p =
1730 extrastapedial process; I_p = inferiorstapedial process; S_p = superiorstapedial process. **C**)
1731 Micro-CT reconstruction of the air-filled pathways in the skull of *T. guttata*. Above image:
1732 view from directly beneath the specimen, which does not possess a lower beak. Below
1733 image: posterior view from slightly left of the specimen. B = bulla; IAA = interaural arc; IAC =
1734 interaural canal; IBP = inter-bullae passage; HMOT = hypomedial orbital tube; MOC =
1735 medio-orbital canal; SAOS = superoantero-orbital sinus; SLOC = superolateral orbital canal.
1736 (**B** was modified from Saunders et al., 2000; **C** was slightly modified from Larsen et al.,
1737 2016)

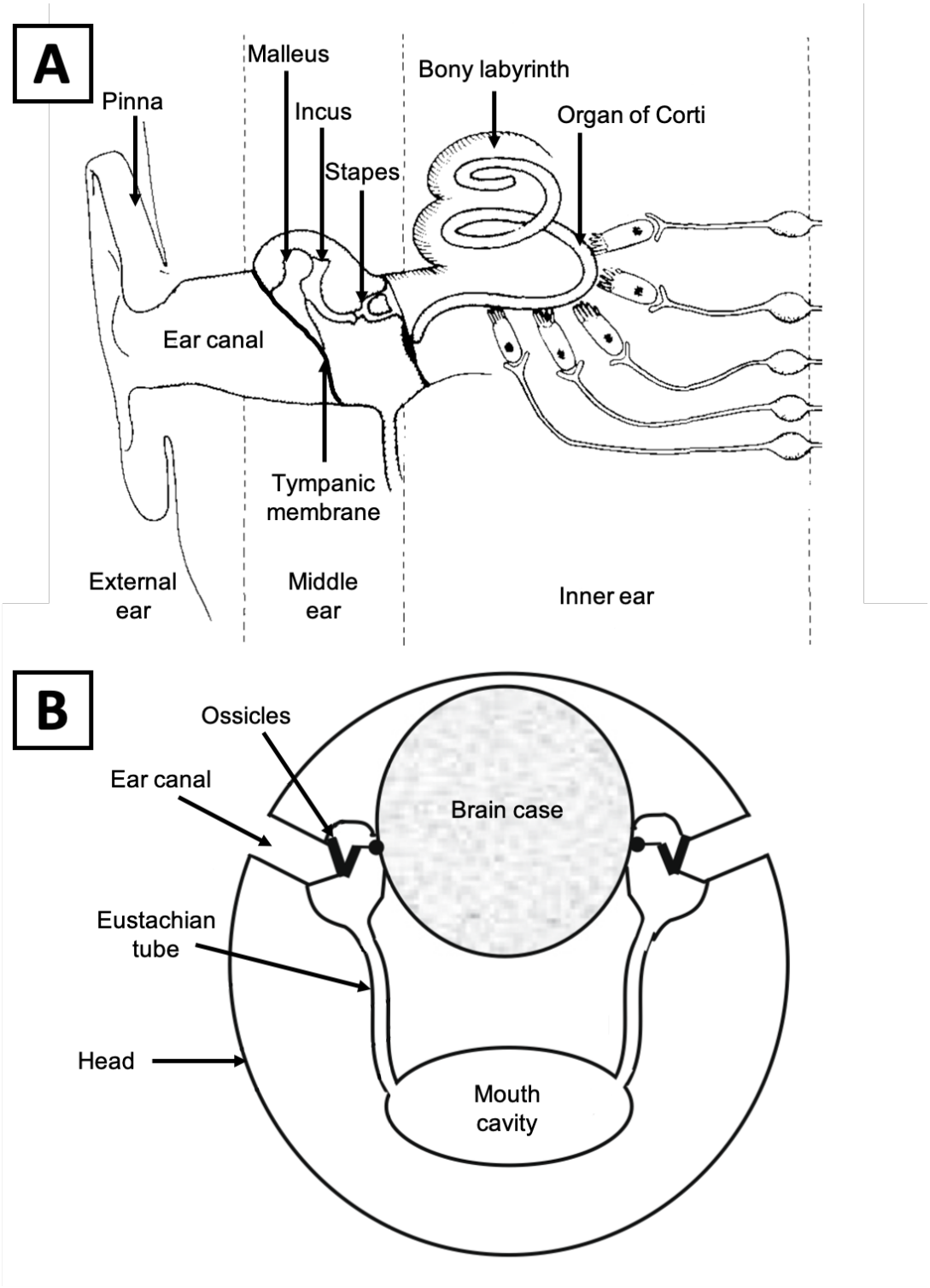

1738

1739 **Figure 6.** The mammalian ear, as seen in a human (*Homo sapiens*). **A**) The human ear (not
1740 to scale). The pinna and ear canal function to detect, filter and amplify sound, the tympanic
1741 membrane and ossicles capture the airborne soundwaves and transduce them into fluid
1742 vibrations, and the organ of Corti classifies the frequencies present in a sound. **B**) Schematic
1743 of the mammalian interaural connection. The length and small diameter of the eustachian

1744 tubes mean that sound cannot transit between ears internally. This makes the mammalian
1745 ear a pressure receiver system. (**A** was modified from Wilson et al., 1988; **B** was modified
1746 from Manley, 2010).
1747

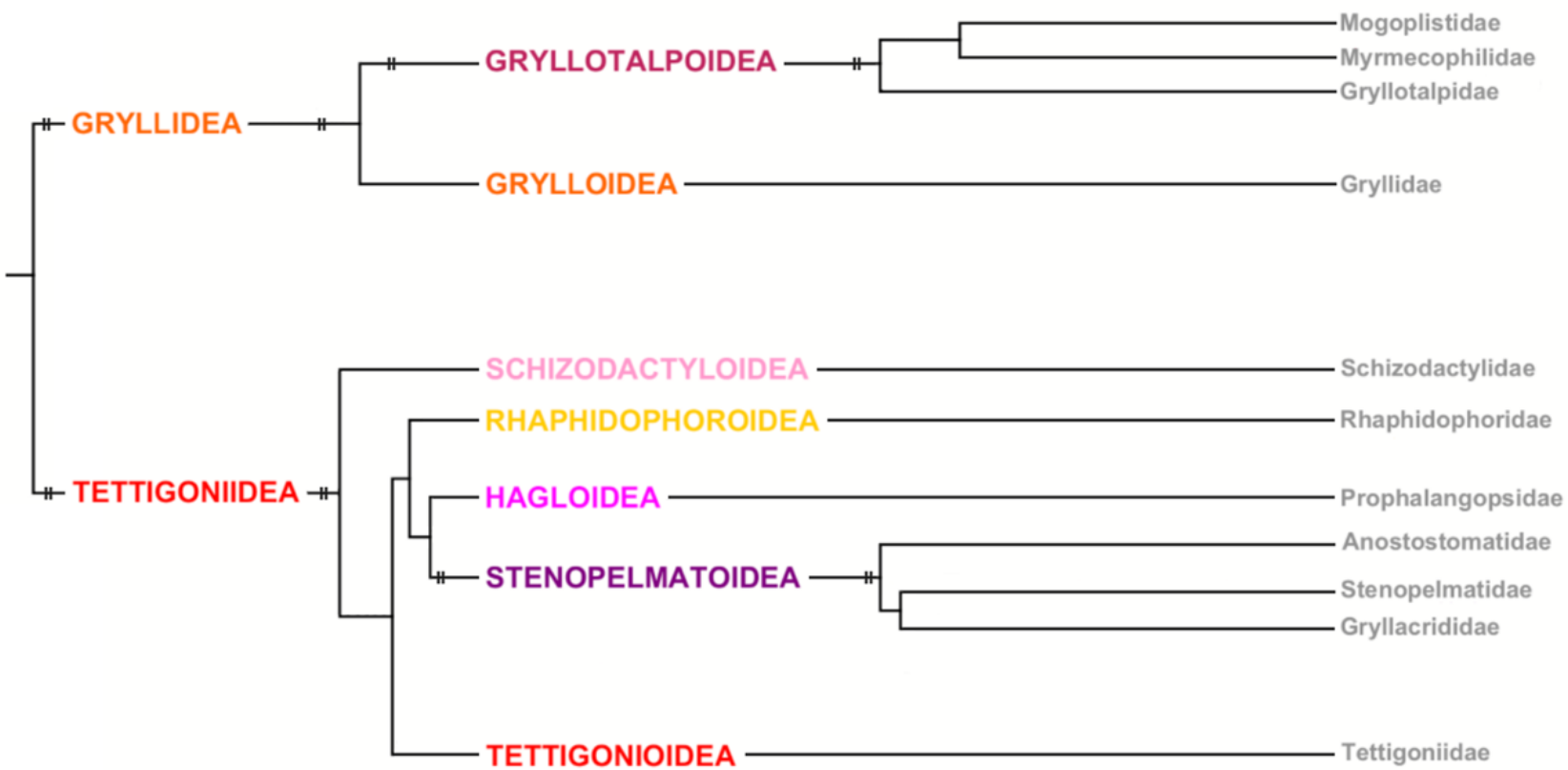

1748

1749 **Figure 7.** The phylogeny of Ensifera, from infraorder to family level. The complexity of the auditory system anatomy (or homologous structures)

1750 in each family is not parsimonious. Sound production and reception is thought to have occurred multiple times within Ensifera. A pair of two

1751 vertical lines indicates that no time has passed between the pair. (This figure is modified from Song et al., 2015).

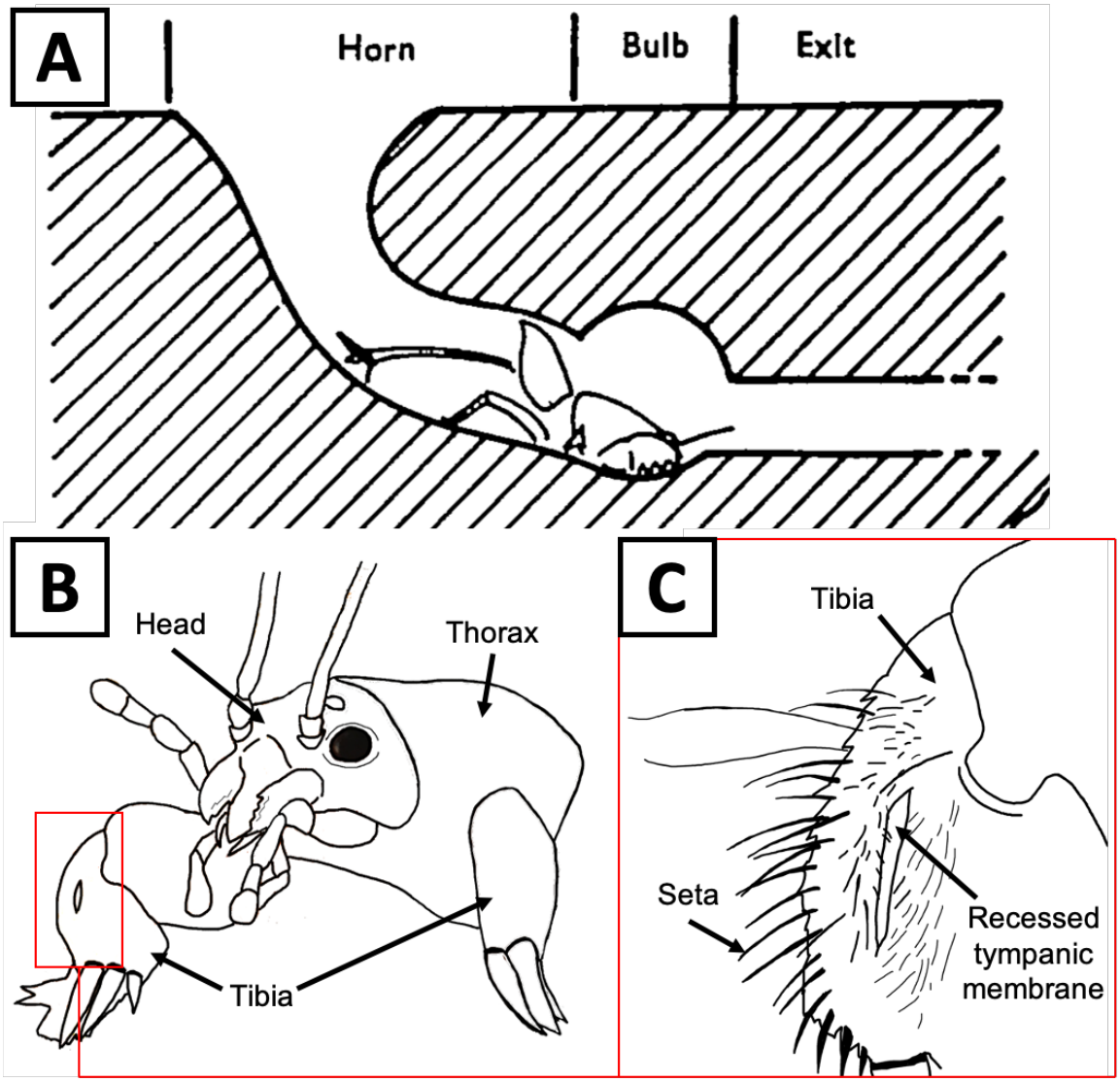

Figure 8. Gryllotalpidae burrow and anatomy. **A**) The burrow of a *Gryllotalpa vinae* male. Both sexes use these when foraging for plant roots, and mating. Males construct a special horn-shaped entrance to amplify their calling song. **B**) Head, thorax and forelegs of *Gryllotalpa sp*. The tibiae are robust and adapted for digging. **C**) Magnified view of the tibia. The tympanic membrane is situated on the anterior side of the tibia and 'covered' (held inside a recession in the cuticle). No posterior recession was observed. Long setae protrude from the dorsal tibia, and short setae surround the entrance to the recession, extending anteriorly. The setae may function in preventing substrate from blocking the tympanic membrane. (**A** is from Bennet-Clark, 1970; **B** and **C** are illustrated by the author).

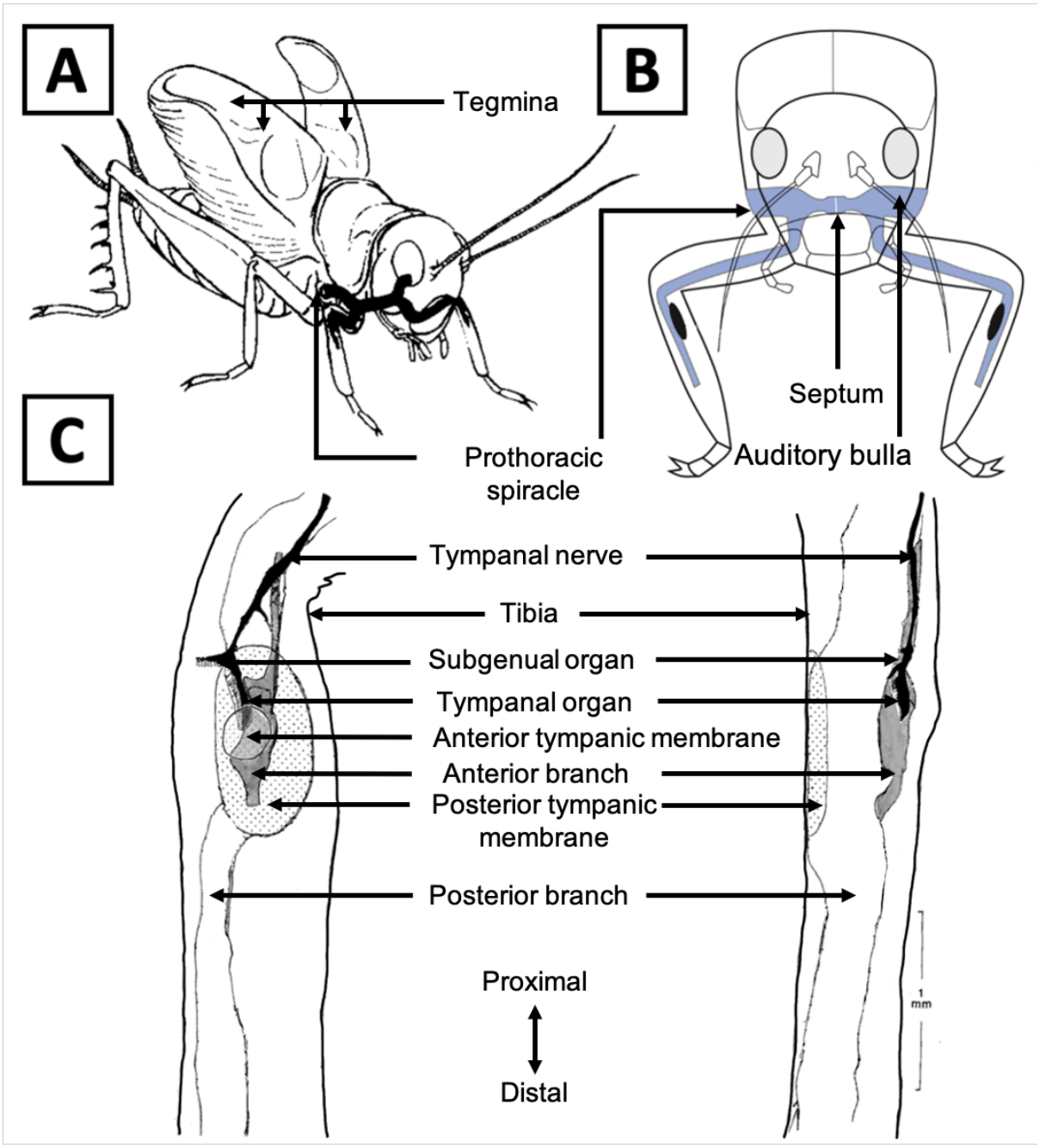

1763

1764 **Figure 9.** Anatomy of Gryllidae, as seen in *Gryllus bimaculatus*. **A**) A male *G. bimaculatus*
1765 sings using tegminal stridulation. The prothoracic tracheal system is coloured black. **B**)
1766 Anterior view of *G. bimaculatus*. The prothoracic tracheal system is coloured in blue,
1767 demonstrating the auditory bulla and septum, which enables sound to pass between the left
1768 and the right auditory systems. **C**) The proximal tibia of *G. bimaculatus*. After passing the
1769 into the tibia, the ear canal splits into an anterior and posterior branch. The subgenual organ
1770 and tibial organ are closely associated with the anterior branch. (**A** was modified from

1771 Michelsen, Popov and Lewis, 1994; **B** was modified from Schmidt and Römer, 2013; **C** was

1772 modified from Eibl, 1978).

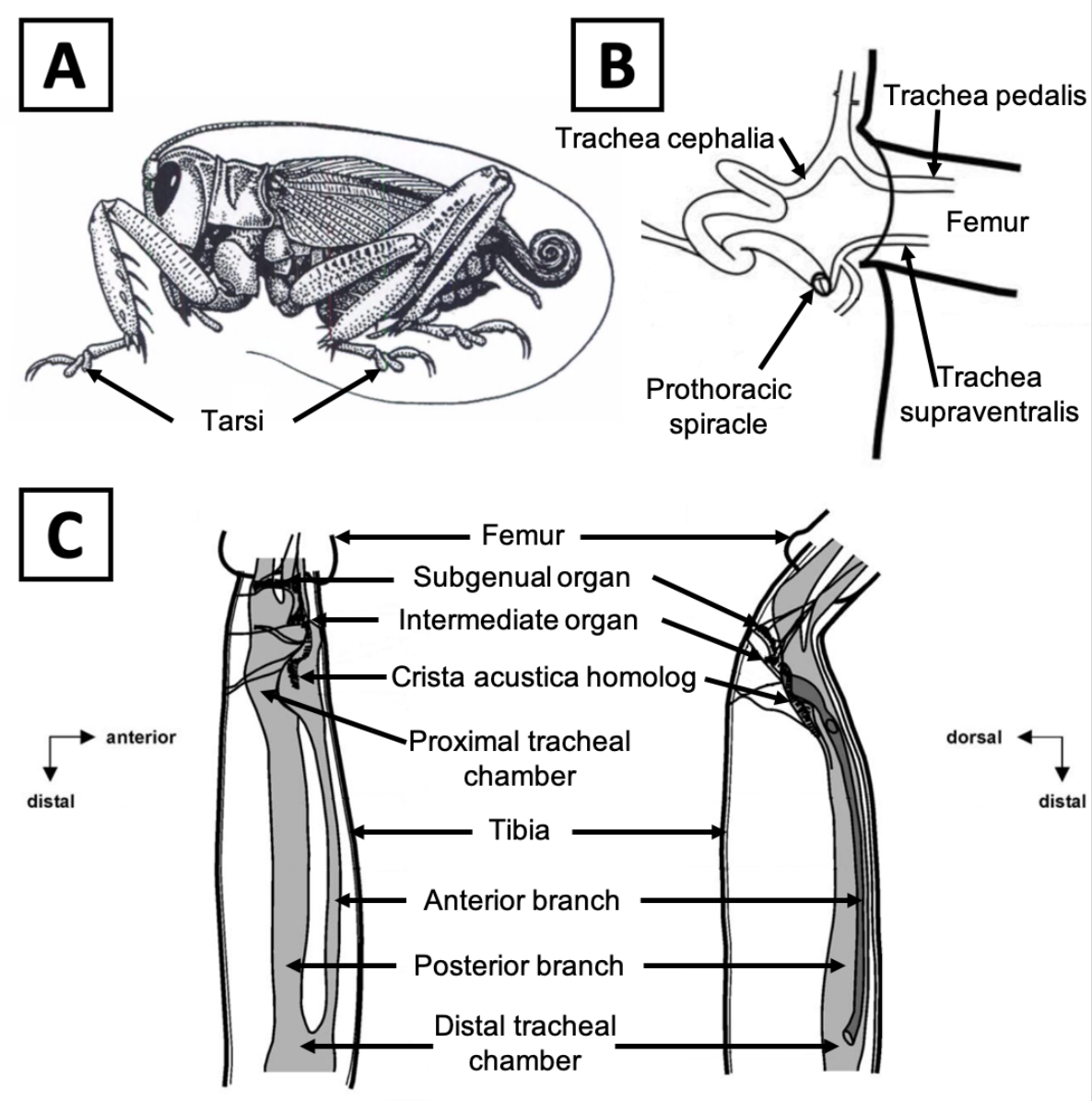

Figure 10. Anatomy of Shizodactylidae, also known as splay-footed crickets. **A**) A *Schizodactylus hesperus* male with tarsi adapted for walking on sand. **B**) The prothoracic tracheal system of *Comicus calcaris*. The *trachea pedalis* and *trachea supraventralis* enter the foreleg and extend to the tibia. **C**) The tibial organ complex and the tracheae of proximal tibia, in *C. calcaris*, from two different vantage points. Both the *trachea pedalis* and *trachea supraventralis* enter the tibia before fusing. The tibial organ complex consists of a subgenual organ, intermediate organ and a set of receptors homologous to the *crista acustica* of tettigonids. (**A** is an illustration from Gorochov, 2001; **B** and **C** were modified from Strauß and Lakes-Harlen, 2010).

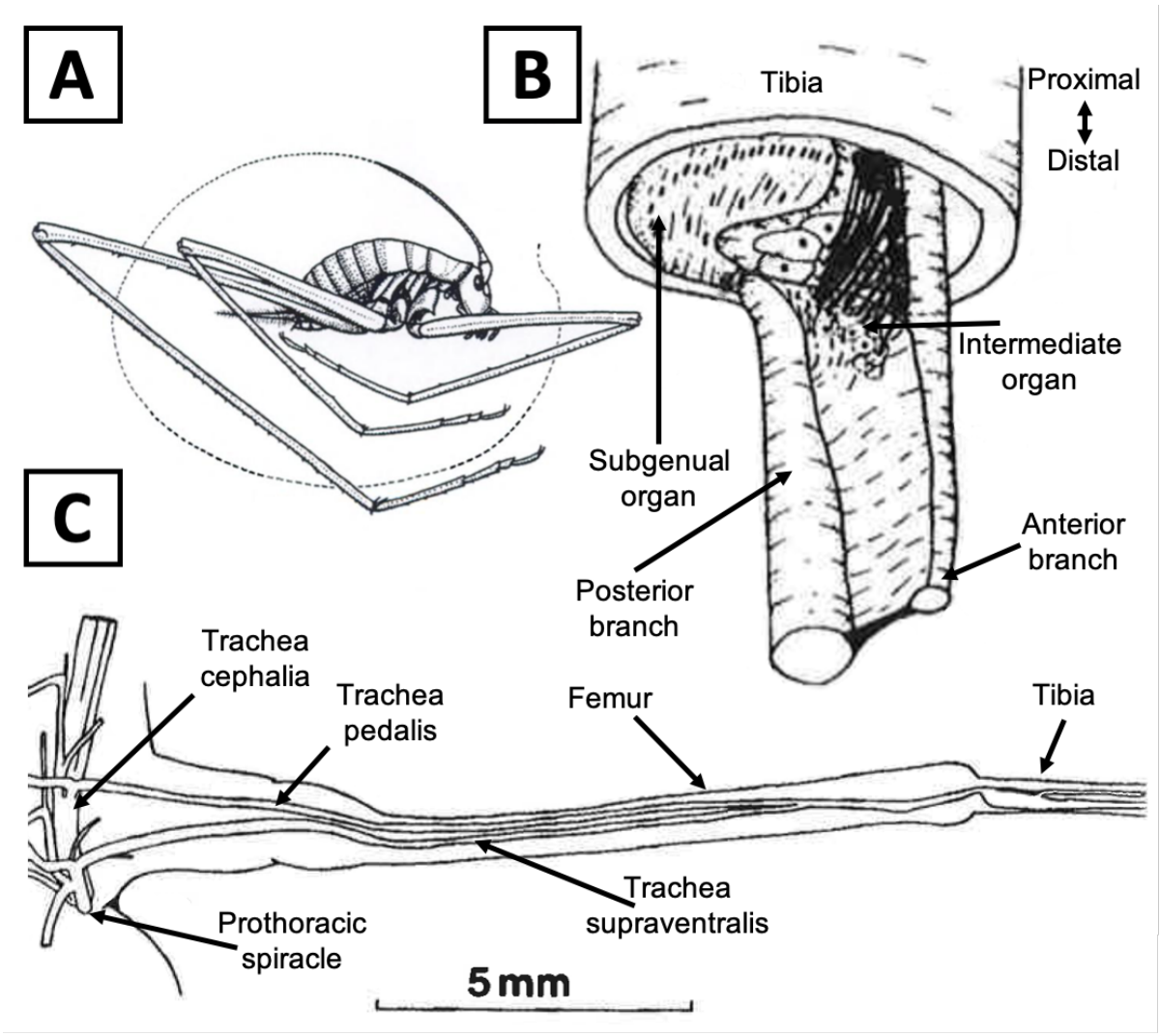

Figure 11. Anatomy of Rhaphidophoridae, also known as cave crickets. **A**) *Macropathus filifer* male. **B**) The tibial organ complex and the tracheae of proximal tibia, in *Troglophilus neglectus*. Only the subgenual organ and intermediate organ are present, suggesting that Rhaphidophoridae represent a primitive. The tibial organ resides on the anterior branch. **C**) The tracheae of the prothorax and foreleg, in *T. neglectus*. The *trachea pedalis* and *trachea supraventralis* enter the femur before fusing into one. This trachea branches into two in the tibia. (**A** is an illustration from Gorochov, 2001; **B** and **C** were modified from Jeram et al., 1995).

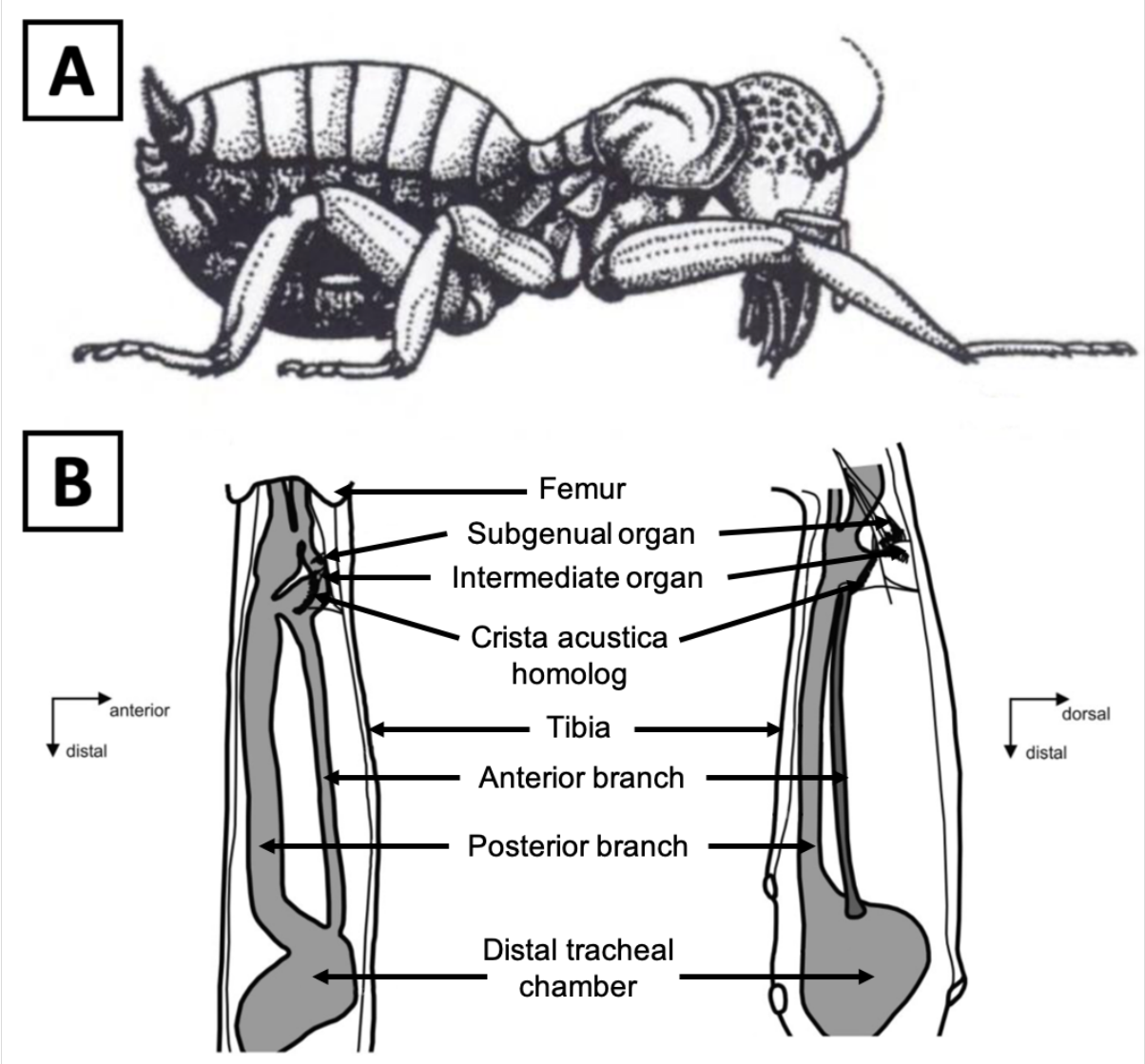

1792

1793 **Figure 12.** Anatomy of Stenopelmatidae, also known as stone crickets. **A**) *Oryctopterus*
1794 *lagenipes* female. **B**) The tibial organ complex and tracheation of the fore-tibia of
1795 *Stenopelmatus sp*. Two tracheae enter the tibia and promptly fuse, split, and fuse again.
1796 This forms an anteriorly facing protrusion where the *crista acustica* homolog is positioned.
1797 After the protrusion the trachea split into the. anterior and posterior branch. The anterior
1798 branch is reduced in width compared to the posterior. (**A** is an illustration from Gorochov,
1799 2001; **B** is modified from Strauß and Lakes-Harlan, 2008).

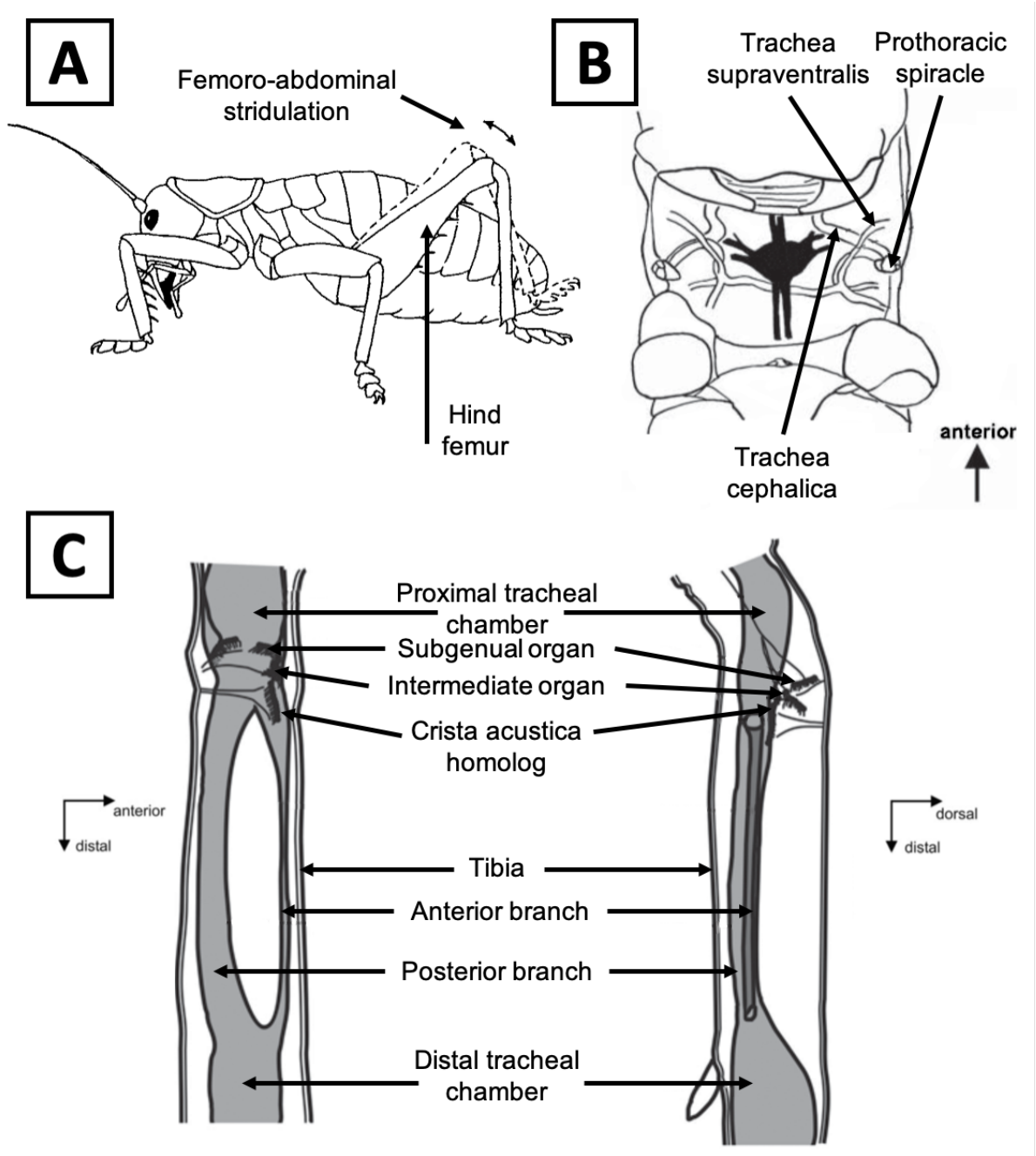

1800

1801 **Figure 13.** Anatomy of Gryllacrididae, seen in *Ametrus sp*. **A**) Femoro-abdominal stridulation
1802 in *Ametrus sp*. By scraping a series of pegs on the abdomen with a cuticular ridge on the
1803 hind femur, a broadband sound is produced. This is used as a defence mechanism. **B**)
1804 Tracheation of the thorax in *Ametrus tibialis*. Two tracheae emerge from the prothoracic
1805 spiracle: one branches into the *trachea supraventralis*, which enters the foreleg; the other is
1806 the *trachea cephalica*. The *trachea pedalis* (not pictured) also enters the foreleg, possibly
1807 arising from the *trachea cephalica*. **C**) The tibial organ complex and tracheation of the fore-

tibia of *A. tibialis*. The *trachea supraventralis* enters the tibia, forms the posterior tracheal chamber and divides into the anterior and posterior branches. The *crista acustica* homolog associates with the anterior branch. (**A** is from Field and Bailey, 1997; **B** and **C** are modified from Strauß and Lakes Harlan, 2008).

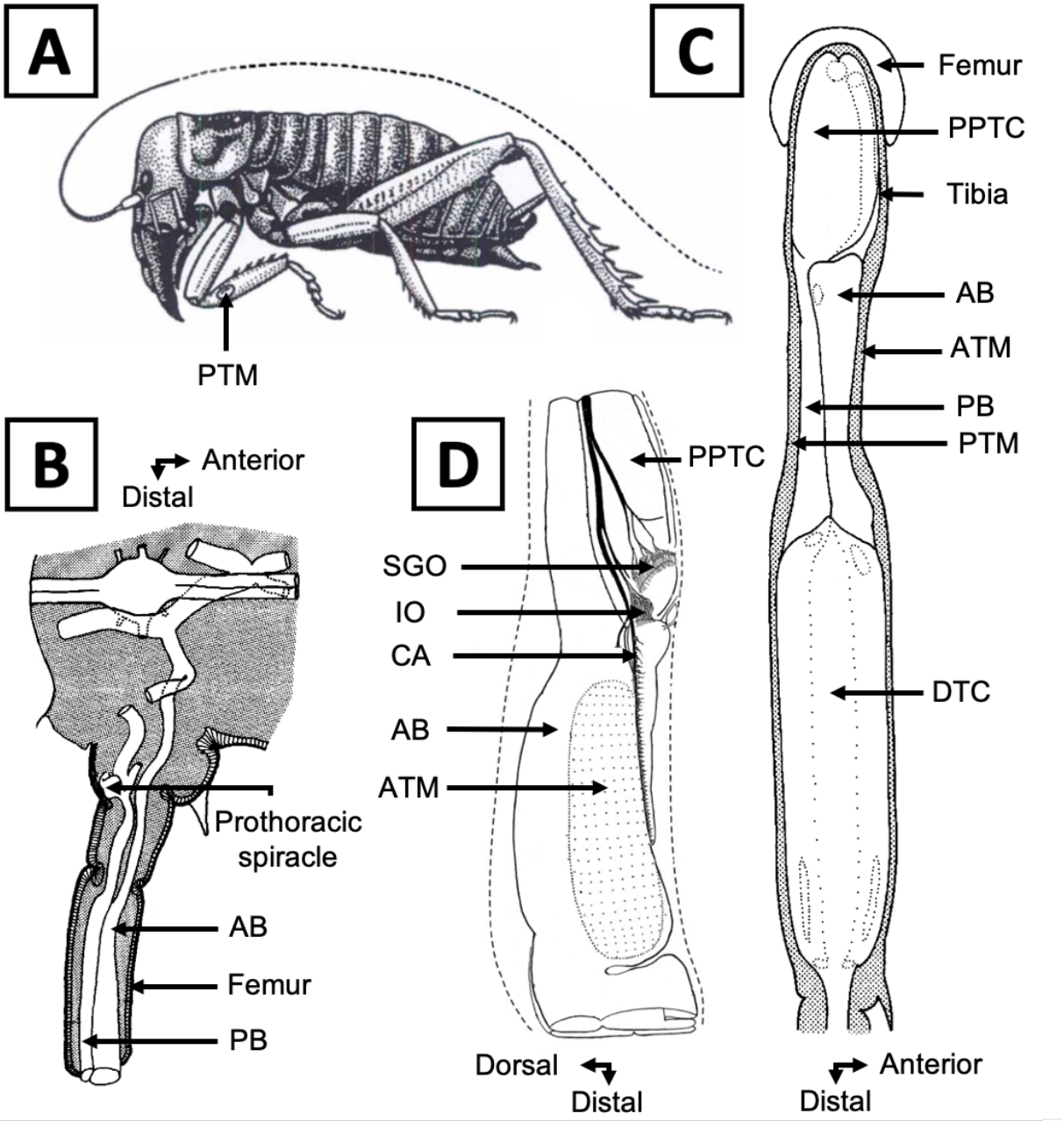

Figure 14. Anatomy of Anostostomatidae, as seen in *Hemideina* spp. **A**) *Hemideina maori*. Posterior tympanic membrane is visible. **B**) Tracheation of the thorax to the femur in *H. crassidens*. The posterior trachea emerges directly from the prothoracic spiracle (as the *trachea supraventralis*); the anterior trachea enters the femur from the thorax. **C**) Dorsal view of the tibial tracheation in *Hemideina crassidens*. Unlike in other Ensifera, the anterior and posterior tracheae remain separate until a foramen in the anterior and posterior branch. The anterior and posterior branches each join the distal tracheal chamber twice: once as the distal chamber forms, and again at the distal tibia. **D**) The complex tibial organ at the

proximal tibia of *Hemideina femorata*. The subgenual organ, intermediate organ and *crista acustica* are all present. The *crista acustica* is associated with the anterior branch and the anterior tympanic membrane. AB = anterior branch, ATM = anterior tympanic membrane, CA = *crista acustica*, DTC = distal tracheal chamber, IO = intermediate organ, PB = posterior branch, PPTC = proximal posterior tracheal chamber, PTM = posterior tympanic membrane, SGO = subgenual organ. (**A** is from Gorochov, 2001; **B** and **C** were modified from Ball and Field, 1981; **D** is from Nishino and Field, 2003).

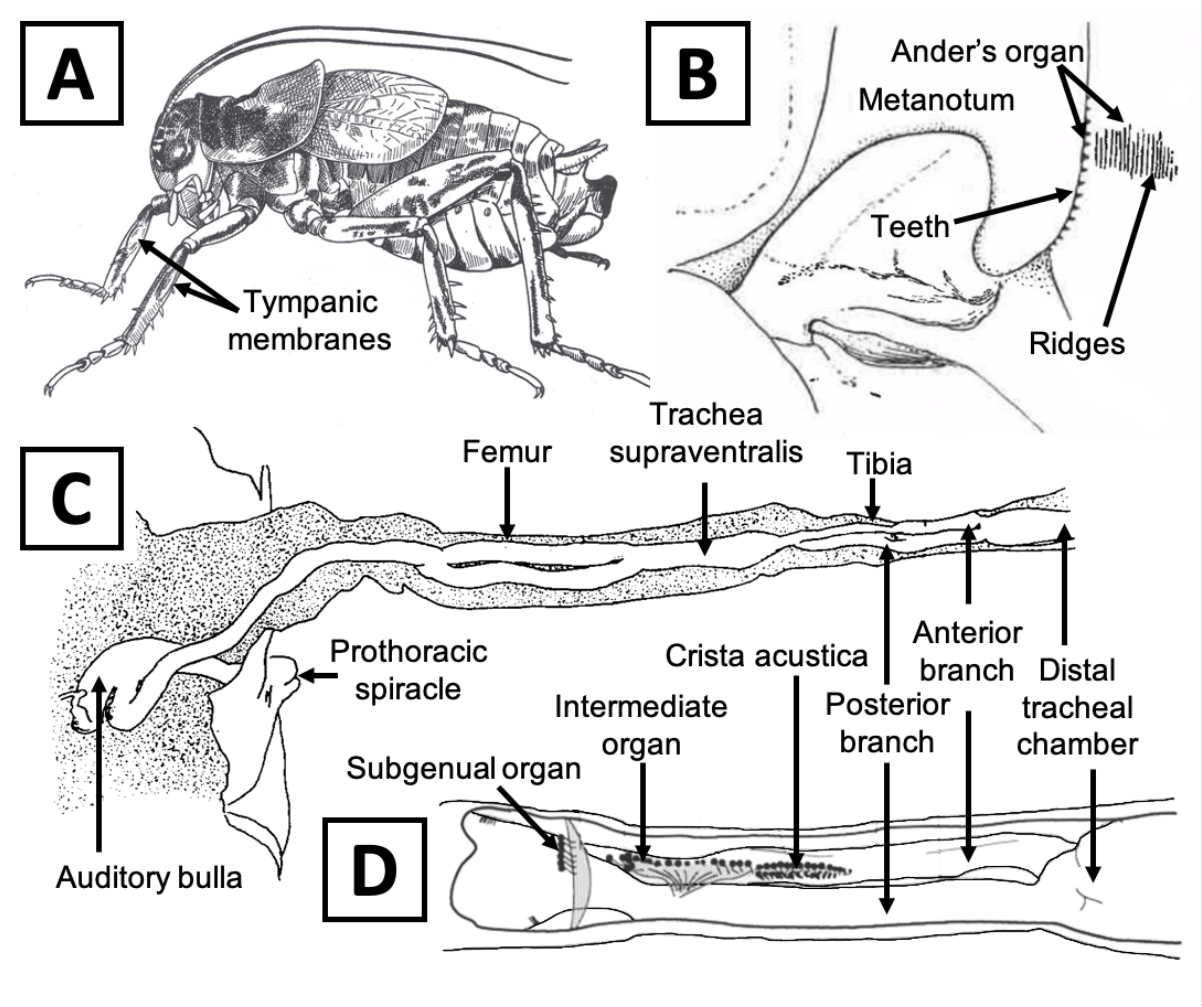

Figure 15. Anatomy of *Cyphoderris monstrosa*, representing Prophalangopsidae – also known as grigs. **A**) *C. monstrosa* male. Tympanic membranes are present on the anterior and posterior of the forelegs. **B**) Ander's organ. A sound producing organ comprised of thoracic teeth and abdominal ridges. Females and nymphs, which lack fully developed tegmina, utilise this organ to produce sound. **C**) The anatomy of the *trachea supraventralis*, from the prothoracic spiracle to the tympanic membranes (not illustrated). The tracheal bifurcation in the femur is a unique trait to Prophalangopsidae. The anterior and posterior branch arise in the tibia. **D**) Illustration of the tibial organ complex, and tracheation, within the fore-tibia. Prophalangopsidae possess a tibial organ complex comparable to that of Tettigoniidae; a subgenual organ, intermediate organ and a *crista acustica* are all present. (**A** is Great Grig by M.F. Benson, 1939; **B** was modified from Ander, 1938; **C** and **D** were modified from Mason, 1991).

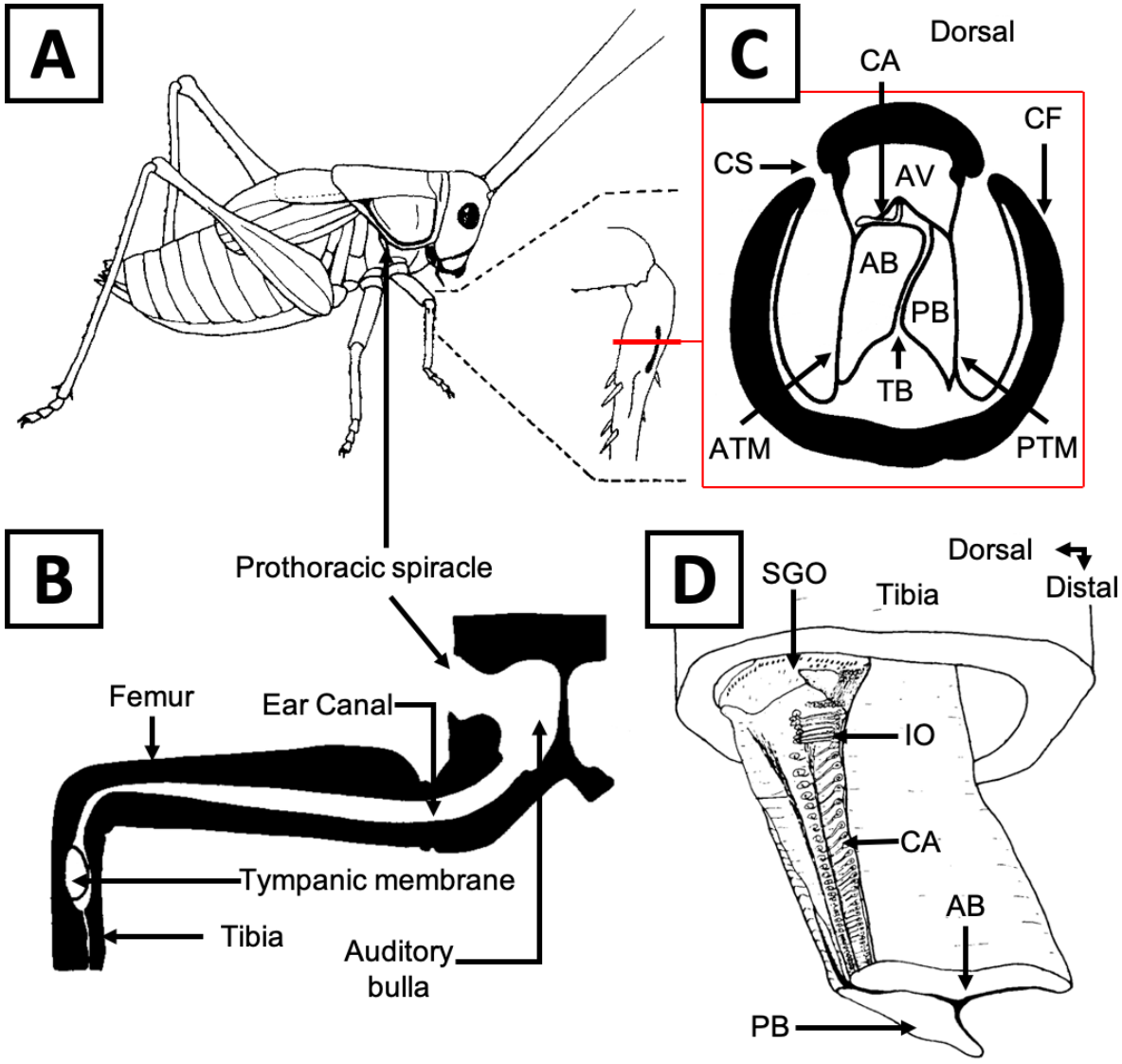

Figure 16. Anatomy of Tettigoniidae, as seen in *Gampsocleis gratiosa*. **A**) *Gampsocleis gratiosa* with foreleg further magnified. This species has cuticular flaps covering the tympanic membrane and sound enters the ear externally through the cuticular slits. The prothoracic spiracle, the internal sound input of the ear, is labelled. **B**) Schematic of the ear canal. Beginning at the prothoracic spiracle, the ear canal passes through the femur and into the tibia, where it reaches the internal surface of the tympanic membrane. The auditory bulla amplifies sound as it transmits into the foreleg. **C**) Cross-section of the proximal tibia. The *crista acustica* borders the anterior branch and is held within the fluid-filled acoustic vesicle. The anterior and posterior branches are separated by the tracheal bifurcation, bordering the anterior and posterior tympanic membranes, respectively. The cuticular flaps which form the

cuticular slits, are clearly visible. **D**) The complex tibial organ, comprised of the subgenual organ, intermediate organ and *crista acustica,* which is situated at the proximal tibia. The *crista acustica* is heavily associated with the anterior branch. AB = anterior branch, ATM = anterior tympanic membrane, AV = acoustic vesicle, CA = *crista acustica*, CF = cuticular flap, CS = cuticular slit, IO = intermediate organ, PB = posterior branch, PTM = posterior tympanic membrane, SGO = subgenual organ, TB = tracheal bifurcation. (**A** and **D** were modified from Lin et al., 1993; **B** and **C** were modified from Bailey, 1993).

Chapter Two:

Sound Propagation in a Plastic Linear Tube

Foreword

The main aim of this MSc research project is to build upon a study conducted by Jonsson et al. (2016), and to provide an understanding of what causes reduction in sound velocity as it passes through the ear canal of bush-crickets (Orthoptera: Tettigoniidae), using *Copiphora gorgonensis* as a model species. This species belongs to the subfamily Conocephalinae and is endemic to a small island, in the Pacific Ocean of Colombia, known as Natural National Park Gorgona (Montealegre-Z and Postles, 2010). The only captive colony is established at the University of Lincoln, UK, and therefore preserving this population is paramount for future research. It was essential that each insect used in the experiment was returned to their vivarium in breeding condition, ideally having undergone as little stress as possible. Developing and practicing the method was an important step in ensuring this.

Introduction

Capturing and processing sound is essential to the survival and reproduction of bush-crickets. As a group, they possess an immense range of hearing, and across species, the males are known to exploit a huge range of frequencies for their mating calls; from as low as 600 Hz to up to a record breaking 150 kHz (Montealegre-Z et al., 2017; Sarria-S et al., 2014). Many individual species can also hear a broad range of frequencies, enabling them to detect the echolocation of hunting bats, which are known to heavily prey upon them (Belwood and Morris, 1987; ter Hofstede et al., 2017; Montealegre-Z et al., 2017; Römer et al., 2010; Schul et al., 2000; Schulze and Schul, 2001). In order to successfully evade

predation, and find a mate, these insects need to localise the source of these sounds effectively (ter Hofstede et al., 2010; Schulze and Schul, 2001). They achieve such directional acuity because their ears are located in the forelegs, separated enough to create small time and pressure differences which enable them to perceive the spatial characteristics and three-dimensional position of the sound from the original source. The bush-cricket ear is located in the proximal part of the tibia, and each ear is endowed with two tympanic membranes (TM). These work in synchrony to transmit the airborne-sound vibrations to the mechanoreceptors – forming a system known as the complex tibial organ.

In bush-crickets, the complex tibial organ is comprised of outer, middle and inner ear components. The outer ear consists of an ear canal (EC) that connects the prothoracic spiracle to the TM (see Chapter One for further details). Sound can stimulate the TM both externally, through the environment, and internally, via the ear canal (Heinrich eet al., 1993; Hoffman and Jatho, 1994; Jonsson et al., 2016; Kalmring and Jatho, 1994; Larsen, 1981; Michelsen and Larsen, 2008). Such an ear design is known as pressure-difference receiver. The defining characteristic of a pressure-difference receiver is that the same signal differs in intensity between the external and internal pathway (Michelsen and Larsen, 2008; Robert, 2005). In *C. gorgonensis*, both experimental and numerical evidence show that the exponential horn shape of the ear canal causes a gain of approximately 15 dB, enabling a pressure gradient across the membrane (Celiker et al., 2020; Jonsson et al., 2016). Furthermore, a time-delay appears in the transmission of the signal through the internal pathway – with the acoustic signal slowing to around 255 m/s and arriving close to 60 μs later (see Chapter Three for further discussion; Jonsson et al., 2016). The combination of the time and amplitude differences, between the external and internal inputs, means that the TM receives the external signal before the interference occurs. Despite its significance, the mechanism behind the reduction in sound velocity remains unknown, although it is speculated to result from the geometry of the EC or possibly even the accumulation of respiratory gases. Chapter Three of this thesis will address the underlying mechanism of

sound velocity reduction in the EC, whilst the current chapter documents the preliminary experiment.

Michelsen et al. (1994) initially proposed isolating the TM from the internal sound input of the ear canal by using a barrier of beeswax around the insect. In order to seal the barrier, the beeswax would have been melted onto the insect, likely burning the animal. Jonsson et al. (2016) proposed a non-invasive method of using a Perspex mount, resembling a medieval pillory, and liquid latex to seal any gaps in the barrier. In this thesis, the procedure for investigating the observed reduction in EC sound velocity will follow the set-up of Jonsson et al. (2016), with the addition of a novel apparatus enabling the manipulation of gas composition within the EC.

This can be summarised in six simple steps: 1) mount the insect in a customised platform that isolates the external and internal sound input (see Chapter Three and Jonsson et al., 2016 for further details), 2) position a probe-speaker and modified syringe near and into the prothoracic spiracle, respectively (see Chapter Three), 3) deliver sound into the EC, 4) use a laser Doppler vibrometer (LDV) to measure the time taken for the signal to reach the TM (Jonsson et al., 2016), 5) repeat measurement whilst the EC is filled with carbon dioxide (CO_2), 6) divide the EC length by the time taken for sound to propagate through the EC, to calculate sound velocity. The first aim of this chapter is to test the proposed method using non-organic tubing materials. The second aim is to quantify the purity of the CO_2 gas to be used in the experiments on live animals.

Materials and Methods

General set-up

All experiments were performed on a vibration isolation table (Pneumatic Vibration Isolation Table with a B120150B - Nexus Breadboard, 1200 mm x 1500 mm x 110 mm, M6 x 1.0 Mounting Holes; and a PFA52507 - 800 mm Active Isolation Frame 900 x 1200 mm, Thorlabs Inc., Newton, New Jersey, US) placed inside an acoustic booth (IAC Acoustics,

Series 120a, internal dimensions of 2.8 m x 2.7 m x 2 m). All experiments were conducted at room temperature within the range of 24-27°C.

A sound level calibrator (Bruel Kjaer, 4231; Nærum, Denmark) was used to calibrate the sensitivity of a 1/8" (3.2 mm) microphone (Bruel Kjaer, 4138). Before the beginning of each experiment, a reference point was recorded in order to standardise the experimental results.

In order to provide accurate positioning of the laser beam, the LDV was combined with a close-up unit (PSV-A-410) and a 300 mm lens (PSV-A-CL-300).

Generating the acoustic stimulus

Acoustic stimuli were created by a function generator (SDG1000 Series Function/Arbitrary Waveform Generator, Siglent Technologies Co. Ltd., Shenzhen, P.R. China), that was synchronised with a laser Doppler vibrometer (PSV-500, Polytec, Waldbronn, Germany) internal data acquisition board (PCI-4451; National Instruments, Austin, TX, USA). The signal was generated as a four-cycle pulse at a sound pressure of 1 Pa (= 94 dB; peak to peak). Frequency was controlled via the function generator, and either 20 or 23 kHz was used. It was then transmitted to an RZ6-A 1 Z-Series Bioacoustic System, with an attenuator connected to MF1-S 1 Multi Field Speaker (Tucker Davis Technologies, Alachua, FL, USA). This speaker included a closed-field configuration option, which involves a CF adaptor and an exponential tip with a reduced tip of 3 mm (Tucker Davis Technologies, Alachua, FL, USA). A polypropylene tube (length: 35mm, external diameter: 3 mm, internal diameter: 2 mm) was inserted and served as a probe to deliver sound stimuli directly into the linear tube.

Apparatus for gas delivery

A gas delivery system was constructed and used throughout all experiments. First, a micropipette puller (P30; Sutter Instruments, Novato, CA, USA) was used to rework a

borosilicate glass tubing (Fig. 1A; external diameter: 1.2 mm, internal diameter: 0.9 mm; B120-69-8, Linton Instruments, Norfolk, England) into produce a microinjection needle (Fig. 1B). The glass needle was then carefully shortened using tweezers (Fig. 1C). This increased the volume of air able to pass through the capillary tube, whist also maintaining the smaller size required for inserting the glass tube into the prothoracic spiracle. The microcapillary was fixed into a PicoNozzle kit (5430-ALL, World Precision Instruments, Inc., Sarasota, FL, USA), which was connected to PVC tubing (external diameter: 3 mm, internal diameter 1.5 mm). This provided a precise yet robust system for delivering CO_2 gas into a small target area. CO_2 was dispensed using a cartridge and dispenser system (Genuine Innovations, San Luis Obispo, California, USA). To allow for the smooth joining of the dispenser to the PVC tubing, an extension was required. This was achieved by sealing a pump needle adapter, with the threaded fixing removed, to the dispenser using Blu Tac.

Measuring free field sound velocity in the natural air composition of the room

To act as a control, the sound propagation velocity through the natural gas composition was measured in a free field environment.

The microphone was mounted in a micromanipulator (World Precision Instruments, Inc., Sarasota, FL, USA) and placed 300 mm from the centre of the MF1-S 1 Multi Field Speaker (Fig. 2A). A 23 kHz 4-cycle pulse was produced, and the LDV recorded time taken for the microphone to receive the signal. This measurement acted as a reference recording. The microphone was then moved towards the speaker by 40 mm. A second recording was taken. For both of these recordings, the minimum of the first wavelength was used to obtain a time value for each measurement. The time difference between each recording was calculated, and the sound propagation velocity determined by dividing the distance the signal had travelled, by the time difference. Both the reference and measurement points were repeated seven times, and the mean sound velocity determined. The room temperature was 24°C and relative humidity at 60 %.

Sound propagation in a linear tube with an open end

The central idea was to recreate the insect's EC and TM in its most simple form. Plastic tubing was cut and sealed at one end, with the membrane of an inflated balloon and Super Glue (Loctite, Düsseldorf, Germany). Removing the remaining balloon and sealing the excess material to the side of the tube resulted in a flat, stretched elastic membrane with the ability to capture sound energy. This resulted in a hollow tube (length: 99.03 mm, external diameter: 7 mm, internal diameter: 4 mm), with one end open to the environment, and one end sealed with the elastic membrane simulating a TM (Fig. 2B).

Following the method from the literature (Jonsson et al., 2016), the acoustic signal was delivered into the opening of the tube from a distance of 2mm. In order to measure the time taken for the stimulus to travel the entire length of the tube, a reference point was required to standardise the measurements. The MF1-S 1 Speaker, with the closed-field configuration probe attached, was positioned 2 mm away from the microphone, a 23 kHz signal was produced, and the time taken for the microphone to receive the signal was recorded. This was the reference recording. The closed-end linear tube was mounted horizontally in a micromanipulator. The speaker-probe system was then positioned 2 mm away from the opening of the tube. The gas delivery system was mounted in a clamp and then a micromanipulator, the needle carefully manoeuvred between the speaker-probe and into the opening of the linear tube. The laser beam from the LDV was positioned on the exterior of the stretched membrane of the 'TM' and focused. The acoustic signal was generated. The balloon membrane captured the sound energy and the LDV recorded the response in time. This measurement was then repeated with the addition of CO_2 into the linear tube. CO_2 gas was manually dispensed into the tube for 10 seconds and the time measurement instantly taken. In total, ten measurements were taken in the natural air composition, and seven measurements taken in CO_2.

Sound propagation velocity was determined by calculating the time difference between the reference and linear tube recordings (Fig. 3), and then dividing the length of the linear tube by this time difference. The time value of each recording was determined by the position of the local minimum of the first wavelength. This first wavelength pattern was consistent between recordings, ensuring that the time value is correct (Fig. 3).

Sound Propagation in a sealed linear tube

A plastic tube (length: 101 mm, external diameter: 12 mm, internal diameter: 10 mm) was sealed by attaching two stretched balloon membranes, following the procedure above. To allow the diffusion of gas in and out of the tube, two 3 mm airflow holes were drilled in the middle of the length; one dorsal, one ventral (Fig. 2C). The laser beam from the LDV and another laser beam from a compact sensor head (OFV-534, Polytec, Waldbronn, Germany) were each placed on an opposing balloon membrane, monitoring any vibrations (Fig. 2C). An MF1-S 1 Multi Field Speaker was placed facing a membrane, and a 20 kHz acoustic stimulus was produced. The laser beams recorded the arrival time of the signal at each membrane, allowing us to calculate the time difference between sound arrival. To ensure that no sound waves were passing the far membrane via an external route, a barrier of acoustic foam (Studiofoam Pyramids, Auralex Acoustics, Inc., Indianopolis, United States) was used to attenuate the free field signal (Fig. 2C).

For the normal gas composition measurements, the airflow holes were covered with Parafilm (Sigma-Aldrich, Dorset, UK) ensuring the system was closed. Carbon dioxide was added via the gas delivery system; the syringe perforated the parafilm, keeping the barrier airtight. The less dense gas composition of the room was allowed to escape through the dorsal airflow hole – which was then sealed with Blu Tack. A total of five laser recordings occurred in air, and nine in carbon dioxide. The time difference between the signal reaching each membrane was then calculated. Sound velocity was determined by dividing the length

of the tube by the time difference. These measurements occurred at 27°C and 55 % relative humidity.

Determining the expected sound velocity in air and carbon dioxide

At 20°C and under standard atmospheric pressure (1 atm), the mean sound velocity of an acoustic signal transmitting through CO_2 is approximately 267 m/s (Zuckerwar, 2002). Sound velocity in air, at a given temperature (between 0-30°C) and humidity, can be calculated by using the following equations:

First, the ratio of specific heats (γ), in dry air at temperature (t; in Celsius), is calculated using the equations (1) and (2; Wong and Embleton, 1984):

$$\gamma = 1.39984 - A_t(0.125), \quad (1)$$

where A_t is an expression of the coefficient of temperature, and

$$A_t = 5.2 \times 10^{-4} + 5.2 \times 10^{-5}\, t + 5.2 \times 10^{-7}\, t^2 + 5.2 \times 10^{-8}\, t^3. \quad (2)$$

This value is then substituted into equation (3).

In an ideal gas at a constant pressure, the sound velocity (c) at a given temperature, (T_0; in Kelvins) is,

$$c = [\left(\frac{\gamma}{M}\right) RT_0]^{1/2}, \quad (3)$$

where γ, M and R are the specific heat ratio of dry air, molar mass of dry air and the universal gas constant, respectively. This calculation excludes humidity. The approximate

ratio of sound velocity in a humid gas (c_h) to the sound velocity in a dry gas (c_0) can be given by equation (4; Wong and Embleton, 1985):

$$\frac{c_h}{c_0} = 1 + h(9.66 \times 10^{-4} + 7.2 \times 10^{-5}\, t\, + 1.8 \times 10^{-6}\, t^2 + 7.2 \times 10^{-8}\, t^3 + 6.5 \times 10^{-11}\, t^4), \quad (4)$$

where h is relative humidity. With the correct conversion of T_0, in kelvins, to t, in Celsius, c and c_0 can be assumed to equal. Therefore, the sound velocity in a gas with humidity h, and temperature t, can be denoted as c_h and expressed in the equations (5) or (6):

$$c_h = c \times \frac{c_h}{c_0} \quad (5)$$

or

$$c_h = \left[\left(\frac{\gamma}{M}\right) RT_0\right]^{\frac{1}{2}} \times [1 + h(9.66 \times 10^{-4} + 7.2 \times 10^{-5} t\, + 1.8 \times 10^{-6}\, t^2 + 7.2 \times 10^{-8}\, t^3 + 6.5 \times 10^{-11}\, t^4)], \quad (6)$$

To enable a comparison between the experimental and theoretical data, the theoretical sound velocity was calculated using the equation (6) and values in Table 1. Welch Two-Sample t Tests were conducted on the velocity data using R Version 3.6.1 (R Core Team, 2019).

Results

The unknown variables from each equation were solved and are reported in Table 2**.** The experimental results are reported in Table 3.

The mean sound velocity in free field air, at 24°C and 60 % was only 0.006 % greater than the theoretical prediction. This provides confidence that the method for measuring sound in free field air is accurate. In the open-end linear tube, the mean sound velocity of air was significantly different to that measured in the free field (Welch Two-Sample t Test: t = 25.09, DF = 9.23, P < 0.001). Within the sealed linear tube, however, the mean sound velocity in air was statistically similar to that recorded in free field air (Welch Two-Sample t Test: t = -0.21, DF = 6, P = 0.839). Compared to the value in the literature, the mean sound velocity in CO_2, in the open-end and sealed linear tube, were 4.787 % and 1.843 % lower than the expected value of 267 m/s, respectively. The velocity recorded in the open-end linear tube and sealed linear tube were significantly different (Welch Two-Sample t Test: t = 4.24, DF = 10.101, P = 0.002).

Discussion

Measuring the mean sound velocities, through air and CO_2, in the open-end linear tube saw the completion of the first aim of this chapter. The set-up operated just as planned, providing an insight into the more complex procedure of performing the study in live insects. Sound propagated through the open-ended tube at a significantly lower velocity than in free field air. This means that the velocity measurement for sound propagating through CO_2 was likely also be reduced, and therefore does not accurately represent the mean sound velocity in free field CO_2. It is noted that the sound also reduces in velocity as it passes through the EC of the bush-cricket ear (Jonsson et al., 2016). Perhaps the reduction of sound velocity is a process that occurs when it travels through a conduit with an elastic membrane sealing one end. In the sealed linear tube, the mean sound velocity in air is statistically similar to that recorded in the free field. Perhaps this is due to the presence of the second membrane, causing this to be a closed system. The measurements of sound velocity in air, in the sealed linear tube, were also incredibly consistent – with no variation at all.

In CO_2, the experimental mean sound velocities were lower than 267 m/s, the value suggested in the literature (Zuckerwar, 2002). This could be due to the low temperature of the gas. Before being released, the CO_2 was stored as a liquid, in a cartridge. When released from the cartridge, it evaporates into gas form – an endothermic process. To the touch, the gas felt colder than the ambient temperature, although this was not quantified. Sound propagated at a lower velocity in the open-end tube than in the sealed tube, following the trend in air. Whatever the cause in reduction, this set-up accurately measured the sound propagation velocity through the CO_2 gas dispensed from the canister – completing the second aim of this chapter.

In addition to the unusual effect that the linear tube with a single closed end has on sound velocity, it is possible that this tube overflows with CO_2 gas. With no barrier to prevent diffusion, any excess gas dispensed into the tube could have leaking into the space between the linear tube and the probe of the speaker. This space would otherwise be occupied by air, and therefore changing gas composition of this space would affect the time it takes for sound to propagate through it, therefore invalidating the reference signal. Since the experimental set-up simulates the EC of an insect, this issue could occur when experimenting on a real bush-cricket EC. Thought must be given to the volume of CO_2 gas dispensed into the insect EC to avoid unwanted overflow.

Conclusion

The research conducted has satisfied the two aims of this chapter. By practicing a preliminary version of the main experiment for this thesis, valuable experience in equipment use was gained. Efficient use of micromanipulators and gas dispensation will play a key role in reducing stress to the insects used in the next experiment. The sound velocity in air and CO_2 were successfully measured as 346.66 ± 0.00 m/s and 262.08 ± 2.73 m/s, respectively. These values will act as a reference, when measuring the effect of different gas compositions, on the sound propagation velocity in the EC of *C. gorgonensis*.

References

Belwood, J.J. and Morris, G.K., 1987. Bat predation and its influence on calling behavior in neotropical katydids. *Science*, 238, 64-67.

Celiker, E., Jonsson, T. and Montealegre-Z, F., 2020. The Auditory Mechanics of the Outer Ear of the Bush Cricket: A Numerical Approach. *Biophysical Journal*, 118, 464-475.

Gatley, D.P., Herrmann, S. and Kretzschmar, H.J., 2008. A twenty-first century molar mass for dry air. *HVAC&R Research*, 14, 655-662.

Heinrich, R., Jatho, M. and Kalmring, K., 1993. Acoustic transmission characteristics of the tympanal tracheae of bushcrickets (Tettigoniidae). II: comparative studies of the tracheae of seven species. *The Journal of the Acoustical Society of America*, 93, 3481-3489.

Hoffmann, E. and Jatho, M., 1995. The acoustic trachea of tettigoniids as an exponential horn: theoretical calculations and bioacoustical measurements. *The Journal of the Acoustical Society of America*, 98, 1845-1851.

Jonsson, T., Montealegre-Z, F., Soulsbury, C.D., Robson Brown, K.A. and Robert, D., 2016. Auditory mechanics in a bush-cricket: direct evidence of dual sound inputs in the pressure difference receiver. *Journal of the Royal Society Interface*, 13, p.20160560.

Kalmring, K. and Jatho, M., 1994. The effect of blocking inputs of the acoustic trachea on the frequency tuning of primary auditory receptors in two species of tettigoniids. *Journal of Experimental Zoology*, 270, 360-371.

Larsen, O.N., 1981. Mechanical time resolution in some insect ears. *Journal of Comparative Physiology*, 143, 297-304.

Michelsen, A. and Larsen, O.N., 2008. Pressure difference receiving ears. *Bioinspiration & Biomimetics*, 3, p.011001.

Michelsen, A., Heller, K.G., Stumpner, A. and Rohrseitz, K., 1994. A new biophysical method to determine the gain of the acoustic trachea in bushcrickets. *Journal of Comparative Physiology A*, 175, 145-151.

Mohr, P.J. and Taylor, B.N., 1999. CODATA recommended values of the fundamental physical constants: 1998. *Journal of Physical and Chemical Reference Data*, 28, 1713-1852.

Montealegre-Z, F. and Postles, M., 2010. Resonant sound production in Copiphora gorgonensis (Tettigoniidae: Copiphorini), an endemic species from parque nacional natural gorgona, Colombia. *Journal of Orthoptera Research*, 347-355.

Montealegre-Z, F., Jonsson, T., Robson-Brown, K.A., Postles, M. and Robert, D., 2012. Convergent evolution between insect and mammalian audition. *Science*, 338, 968-971.

Montealegre-Z, F., Ogden, J., Jonsson, T. and Soulsbury, C.D., 2017. Morphological determinants of signal carrier frequency in katydids (Orthoptera): a comparative analysis using biophysical evidence of wing vibration. *Journal of Evolutionary Biology*, 30, 2068-2078.

R Core Team. 2019. *R: A language and environment for statistical computing. R Foundation for Statistical Computing*, Vienna, Austria. https://www.R-project.org/.

2194 Römer, H., Lang, A. and Hartbauer, M., 2010. The signaller's dilemma: a cost–benefit
2195 analysis of public and private communication. *PLoS One*, 5, p.e13325.
2196
2197 Sarria-S, F.A., Morris, G.K., Windmill, J.F., Jackson, J. and Montealegre-Z, F., 2014.
2198 Shrinking wings for ultrasonic pitch production: hyperintense ultra-short-wavelength calls in a
2199 new genus of neotropical katydids (Orthoptera: Tettigoniidae). *PLoS One*, 9, p.e98708.
2200
2201 Schul, J., Matt, F. and Helversen, O.V., 2000. Listening for bats: the hearing range of the
2202 bushcricket Phaneroptera falcata for bat echolocation calls measured in the field.
2203 *Proceedings of the Royal Society of London. Series B: Biological Sciences*, 267, 1711-1715.
2204
2205 Schulze, W. and Schul, J., 2001. Ultrasound avoidance behaviour in the bushcricket
2206 Tettigonia viridissima (Orthoptera: Tettigoniidae). *Journal of Experimental Biology*, 204, 733-
2207 740.
2208
2209 ter Hofstede, H., Voigt-Heucke, S., Lang, A., Römer, H., Page, R., Faure, P. and Dechmann,
2210 D., 2017. Revisiting adaptations of neotropical katydids (Orthoptera: Tettigoniidae) to
2211 gleaning bat predation. *Neotropical Biodiversity*, 3, 41-49.
2212
2213 ter Hofstede, H.M., Kalko, E.K. and Fullard, J.H., 2010. Auditory-based defence against
2214 gleaning bats in neotropical katydids (Orthoptera: Tettigoniidae). *Journal of Comparative*
2215 *Physiology A*, 196, 349-358.
2216
2217 Wong, G.S. and Embleton, T.F., 1984. Variation of specific heats and of specific heat ratio in
2218 air with humidity. *The Journal of the Acoustical Society of America*, 76,555-559.
2219
2220 Wong, G.S. and Embleton, T.F., 1985. Variation of the speed of sound in air with humidity
2221 and temperature. *The Journal of the Acoustical Society of America*, 77, 1710-1712.

Figures

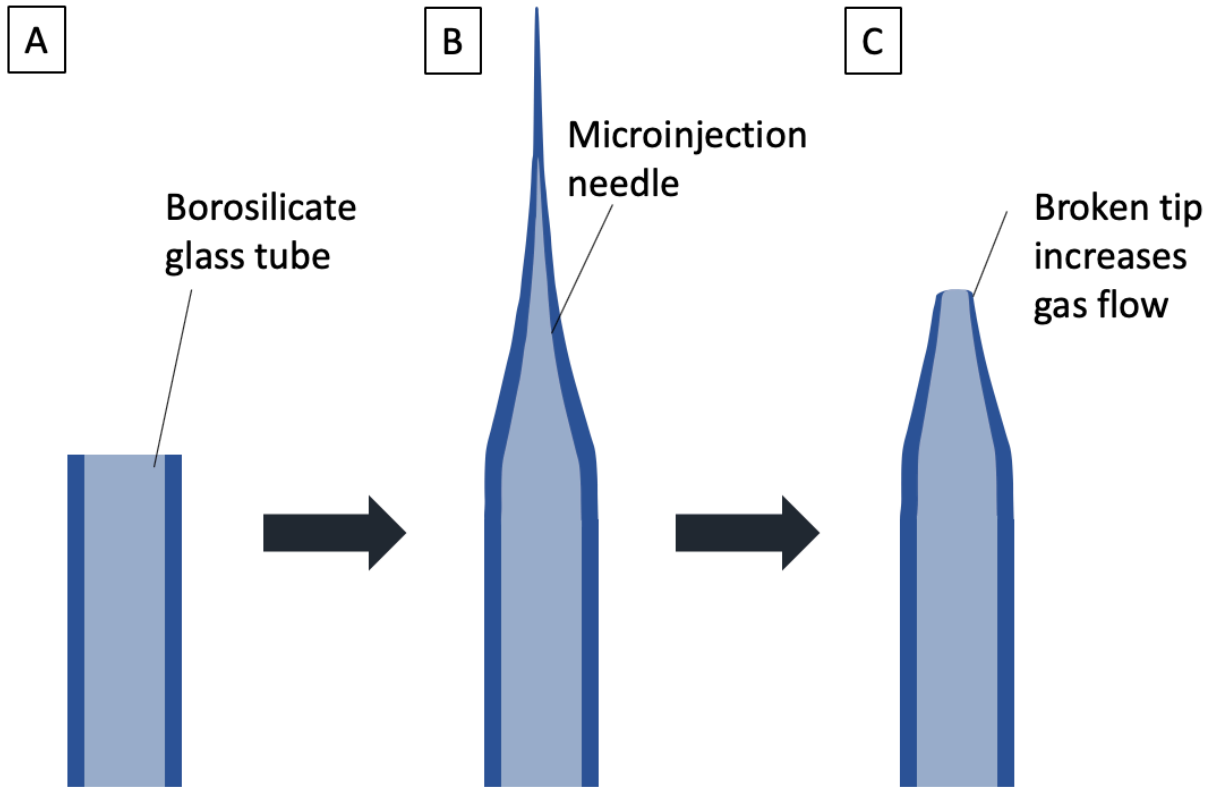

Figure 1. Process of forming the needle used as part of the gas delivery system. **A-B**) The borosilicate glass tube is re-shaped into a microinjection needle. **B-C**) the gas delivery needle is formed by breaking the tip of the needle.

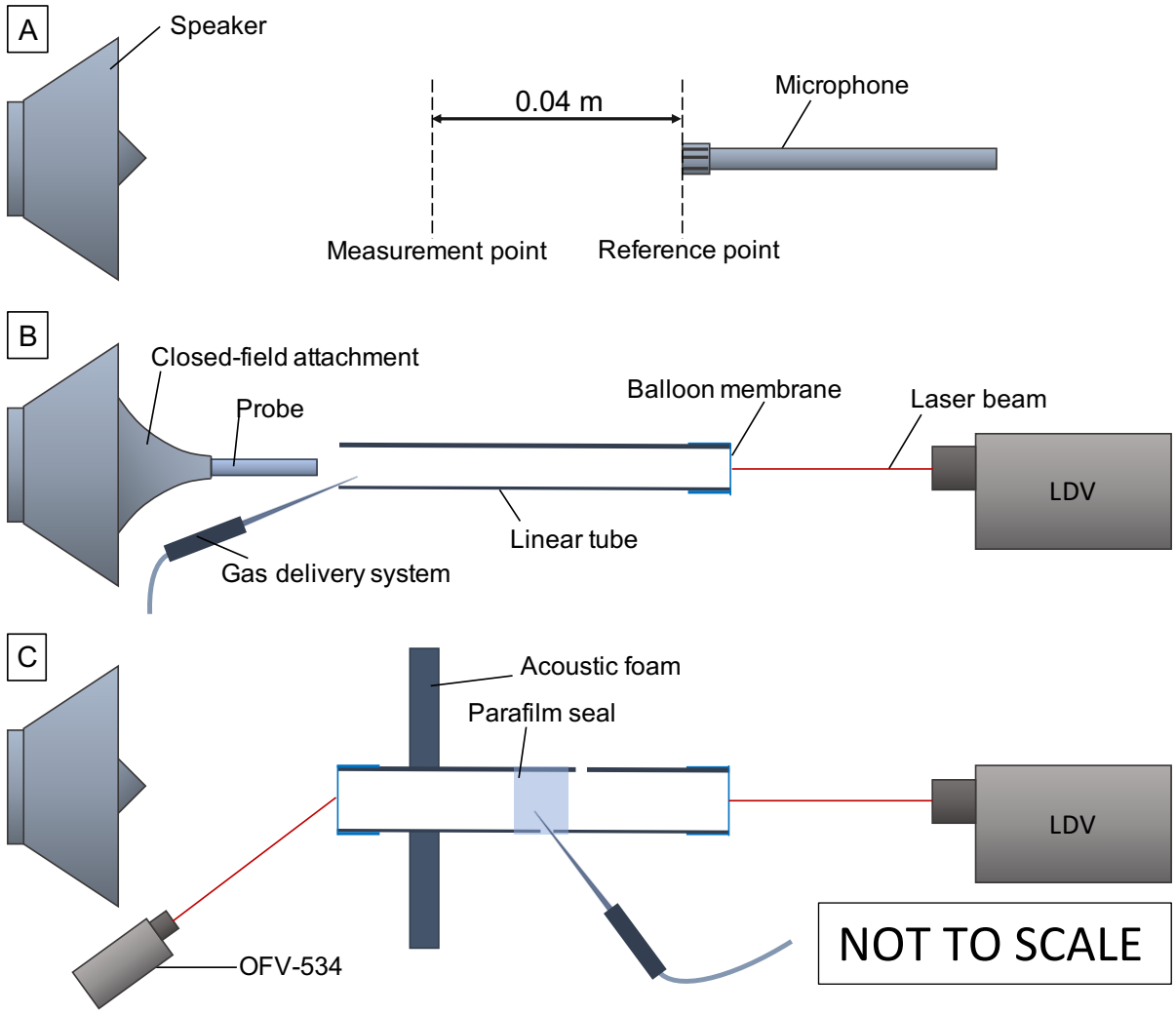

Figure 2. Set-up for each experiment performed. **A**) Measuring the sound propagation velocity in free field air. **B**) Measuring the sound propagation velocity in air and carbon dioxide, in a linear tube with an open end. **C**) Measuring the sound propagation velocity in air and carbon dioxide, in a sealed linear tube.

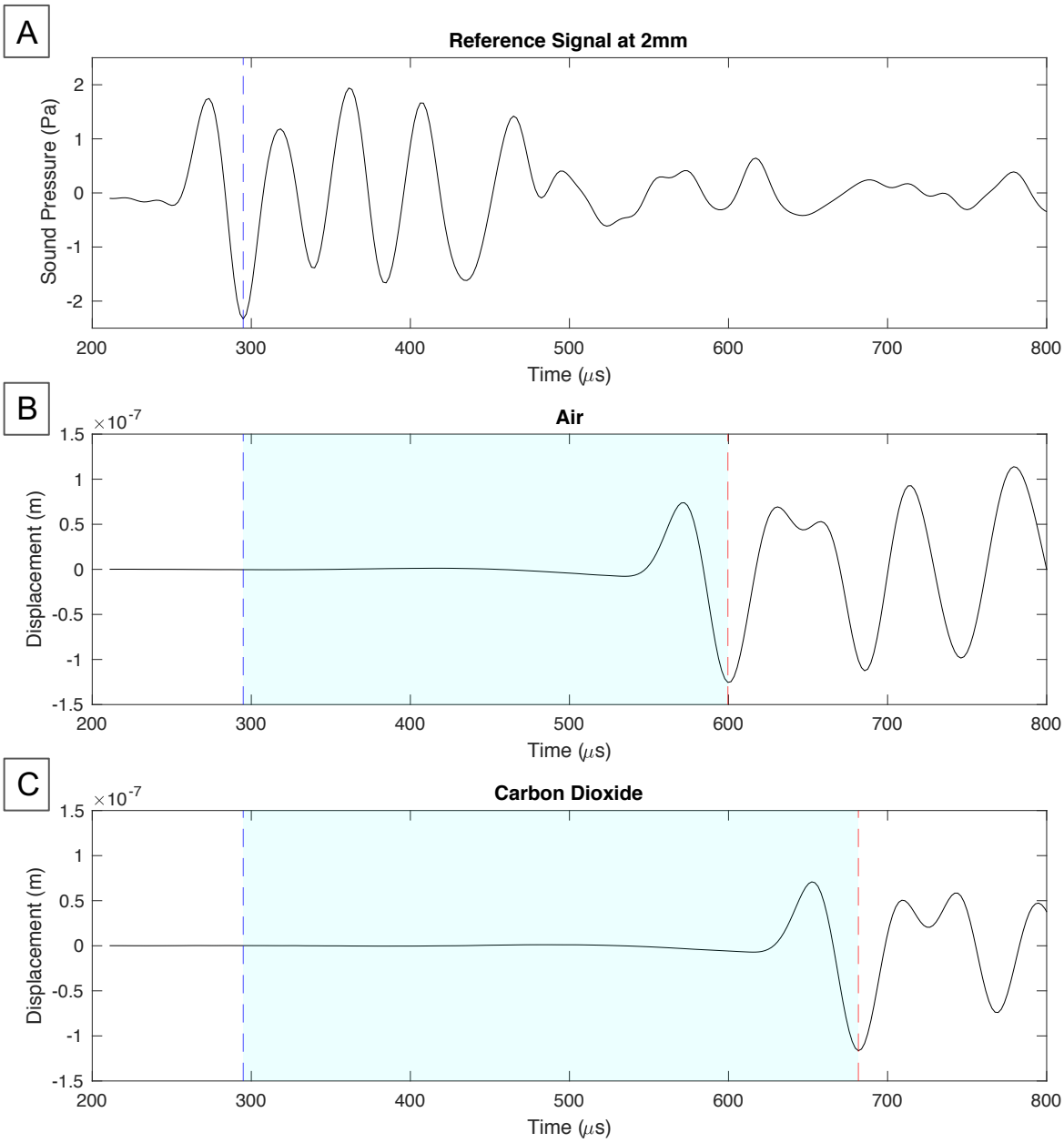

Figure 3. Oscillogram showing the 4-cycle 23 kHz pulse in the time domain. **A**) The time taken for the signal to travel a distance of 2mm, from the speaker-probe, to the microphone; the first minimum of the pulse is used as the reference time (**blue line**). **B**) The **red line** denotes the arrival time of the pulse at the end of the open-end linear tube, after propagating through air. **C**) The **red line** denotes the arrival time of the pulse at the end of the open-end linear tube, after propagating through carbon dioxide. The time taken for sound to propagate through the tube (the difference between the reference time and measurement time) is denoted by the shaded area.

2243 # Tables

2244 **Table 1**. Values used to calculate sound velocity in air, at 24°C and 60 % relative humidity.

Term	Variable	Value and Units	Literature
Universal gas constant	R	8.314472 J mol^{-1} K^{-1}	Mohr and Taylor, 1999
Molar mass for dry air	M	0.028965369 kg mol^{-1}	Gatley et al., 2008
Temperature in Kelvins	T_0	297.15 K	-
Temperature in Celsius	t	24	-
Relative humidity	h	0.6	-

2245

Table 2. Solution to the unknown variables from equations to derive the sound propagation velocity, at 24°C and 60 % relative humidity.

Term	Variable	Value and Units
Ratio of specific heats in dry air	γ	1.39984
Sound velocity in dry air	c	345.50595 m/s
Ratio of sound velocities in dry humid air	$\frac{c_{\mathrm{h}}}{c_0}$	1.002845
Sound velocity in humid air	c_{h}	346.48892 m/s

Table 3. Mean sound velocity (± standard deviation), in air and CO_2, for each experimental set-up.

	Sound Velocity Mean (± standard deviation; m/s)	
	Air	Carbon dioxide
Free field air composition	346.51 ± 1.87	–
Open-end linear tube	326.47 ± 1.11	254.22 ± 4.18
Sealed linear tube	346.66 ± 0.00	262.08 ± 2.73

Chapter Three:

A narrow ear canal reduces sound velocity to create additional acoustic inputs in a micro-scale insect ear

Foreword

This chapter details a collaborative project in the form of a manuscript. At the time of thesis submission, this manuscript is in the second round of review at the Proceedings of the National Academy of Sciences of the United States of America. Formatting is consistent with the previous chapters and Supplementary Materials provided at the end of the manuscript.

Author Contributions, Competing Interests and Acknowledgements

Daniel Veitch[a,1], Emine Celiker[a,1,2], Sarah Aldridge[a], Christian Pulver[a], Carl Soulsbury[a], Thorin Jonsson[b], Charlie Woodrow [a], and Fernando Montealegre-Z[a,2]

[a] University of Lincoln, School of Life Sciences, Joseph Banks Laboratories, Lincoln, LN6 7TS, United Kingdom,

[b] Institute of Biology, Karl-Franzens-University Graz, Graz, Austria.

[1] D.V. and E.C. contributed equally to this work.

[2] To whom correspondence should be addressed. E-mail: eceliker@lincoln.ac.uk, fmontealegrez@lincoln.ac.uk

F.M.Z conceived the idea for the project. D.V, C.P, C.W and F.M.Z were involved in collecting experimental data. E.C developed and performed all numerical simulations. D.V and S.A conducted μ-CT scans and D.V, S.A and T.J processed this data. D.V, E.C, C.S, T.J and F.M.Z developed the conceptual framework, interpreted the results and C.S performed statistical analysis. D.V, E.C and F.M.Z wrote the first draft of the manuscript, with C.S and T.J contributing to later versions. D.V and C.W designed and illustrated figures. All authors commented on and agreed with the final version of the manuscript. The authors declare that they have no competing interests.

This study is funded by the European Research Council, Grant ERCCoG- 334 2017-773067 awarded to F.M.Z. for the project “The Insect Cochlea”.

Data and Materials Availability

Laser Doppler vibrometry recordings, Comsol model files and 332 micro-CT .stl files are available in Dryad, under DOI:10.5061/dryad.2547d7wnn.

Abstract

Located in the forelegs, katydid ears are unique among arthropods in having outer, middle and inner components, analogous to the mammalian ear. Unlike mammals, sound is received externally via two tympanic membranes in each ear, and internally via a narrow ear canal (EC) derived from the respiratory tracheal system. Inside the EC sound travels slower than in free air, causing temporal and pressure differences between external and internal inputs. The delay was suspected to arise as sound propagation changes from adiabatic to isothermal, imposed by EC geometry. If true, a reduction in sound velocity should persist independently of the gas composition in the EC. Integrating laser Doppler vibrometry, micro-

CT scanning, and numerical analysis on 3D geometries of each experimental animal ear, we demonstrate that the narrowing radius of the EC is the main factor reducing sound velocity. The numerical simulations of the sound propagation use the precise 3D geometry of the EC and take into account the viscous and thermal boundary layers formed near the wall of the EC; whose thickness also depend on the tube radius. Likewise, the EC is asymmetrically bifurcated at the tympana organ location (one branch for each tympanic membrane) creating two additional internal sound paths and imposing different sound velocities for each tympanic membrane. Therefore, external and internal inputs add up to four auditory paths for each ear (to compare, only one for humans). Implication of findings in avian directional hearing and potential applications in acoustic triangulation devices are discussed.

Introduction

Tetrapod auditory perception is based on sound capturing, transformation of airborne vibrations into fluid vibrations, and mechanical frequency decomposition followed by the transduction of the mechanical energy into electro-chemical signals by the auditory receptor neurons (Gefland, 2005). Adaptations for the first step - the efficient capture of the sound waves - vary across taxa and have evolved independently in mammals, reptiles and birds (Lombard, 1979; Tucker, 2017). In terrestrial mammals, for instance, sound capture involves the pinna and the ear canal, which vary in morphology depending on a species' hearing abilities (Heffner and Hefner, 2016). The symmetrical arrangement of the components of the outer ear enhances directional hearing, and therefore improves the localisation of a sound source.

An analogue mechanism of hearing has been reported in katydids (bush-crickets; Orthoptera, Tettigoniidae), which also exhibit the three basic steps of hearing reported in mammals (Montealegre-Z et al., 2012). These insects use hearing for mate (Montealegre-Z et al., 2012) and predator detection (Hartbauer and Römer, 2014; Robert, 2005; Yack, 2004), both of which require precise auditory perception and orientation. Different to

tetrapods, the katydid ear, also known as the tympanal organ, is located in the fore-tibia (Yack, 2004). Each ear possesses two tympanic membranes (TM), called the anterior and posterior TM (ATM and PTM, respectively) (Bailey and Stephen, 1978; Rajaraman et al., 2012). Both ATM and PTM are exposed to airborne sound arriving externally to the legs, but they are also backed internally by an air-filled pipe, the acoustic trachea, which is derived from the insect's respiratory system and opens in a large spiracle at the side of the thorax (Hoffman and Jatho, 1995; Shen, 1993; Yack, 2004). Sound travels into the prothoracic spiracle and through the acoustic trachea to reach the inside of the tympanic membranes in the forelegs (Fig. 1A-C). Here the acoustic trachea fulfils the role of an ear canal, and will therefore be called EC from here on. The EC has considerable variation in morphology across the ca. 7000 living species of katydids (Bailey, 1996), and this research focuses on the common type, which involves a large thoracic entrance (acoustic spiracle) and a canal that gradually tapers as it approaches the tympanal organ (Fig. 1C; Celiker et al., 2020; Jonsson et al., 2016; Michelsen et al., 1994).

The symmetrical arrangement of the outer ear in katydids is not enough to enable the localisation of sound – the insects are usually too small for their ears to detect interaural differences in time and amplitude for the relevant sounds in nature (Hartbauer and Römer, 2014). However, they overcome this problem: a) ears located in the legs allow more spatial separation than if they were positioned on the head, thorax or abdomen, b) the dual acoustic inputs form a pressure difference receiver at the TMs, caused by the convergence of the internal and external sound inputs.

As a pressure difference receiver, we define a system that creates a gradient in sound pressure across a membrane. In katydids this is formed by the two sound inputs (external and internal) to the TMs (Robert, 2005), and via the fact that the sound wave coming through the internal part, the EC, is both amplified and slowed down compared to the external input (Celiker et al., 2020; Jonsson et al., 2016).

The reduction in sound velocity was first reported and inferred in Michelsen, Popov and Lewis (1994) and Larsen (1981). This was later experimentally quantified (Jonsson et

al., 2016). However, the underlying assumptions of the interpretation of results, such as adiabatic thermal processes, the effect of the respiratory gases in the EC and propagation of sound in highly narrowing tubes being the cause of reduction of sound velocity (Jonsson et al., 2016; Michelsen and Larsen, 2008), have never been analysed in detail.

Here, we experimentally determine the velocity of sound propagation inside the EC of the katydid *Copiphora gorgonensis* (Tettigoniidae, Conocephalinae) and test the hypothesis that changes in EC diameter are the primary cause of any observed changes in sound velocity. Furthermore, to corroborate results, we investigate sound propagation velocity when the EC filled with different gases, under the expectation that sound velocity will decrease in a narrow tube independent of the gas. Adding to the experimental results, we applied finite element analysis (FEA) to simulate the propagation of sound in the precise geometry of all experimental EC (Fig. 1C), obtained through micro-computer tomography (μ-CT). Both the experimental and numerical results demonstrate that EC geometry is the primary cause of sound velocity reduction within the katydid middle ear.

Results

We investigated factors leading to the reduction of sound velocity in the EC o*f C. gorgonensis* in comparison to sound velocity in free air conditions (Jonsson et al., 2016), both experimentally and numerically. In particular, we considered the effect of the gas composition within both the left and right EC of the specimen, on the velocity reduction in three different categories: alive insects, dead insects and numerical models. For each insect status, in addition to the gas composition inside the EC, we also analysed whether the reduction of sound propagation velocity was affected by length of the EC, and the location of recording on the ATM or PTM. We calculated the velocity of sound propagation through the EC by dividing the length of the EC with the time taken for a sound signal to transmit though it, to the TM. To measure the time of sound transmission, the insect was mounted on a special platform that separates the internal and external sound inputs (Fig. 2). Sound was

generated into the EC, whilst the TM was monitored with a laser Doppler vibrometer (LDV; PSV-500, Polytec, Waldbronn, Germany). The gas composition of the EC was manipulated by dispensing carbon dioxide gas (CO_2) into the acoustic spiracle via a microcapillary needle (see Section 1 of Supplementary Materials for details). CO_2 was used because the EC is derived from the respiratory system and therefore the gas could be present in naturally high concentrations; it is also known that sounds travels slower in CO_2 (see Section 2 of Supplementary Materials for details). When compared to free-field sound velocity in air, sound velocity within the EC across live, dead and numerically modelled data was significantly slower ($F(2,45.16) = 68.19$, $P < 0.001$; Fig. 3; Table 1). Both live and dead insects did not differ in their velocity reduction of 17.05 % (alive vs. dead: t-ratio = 1.88, $P = 0.158$), but numerical data predicted a significantly greater velocity reduction than was found in alive or dead insects, in air (vs alive: t-ratio = 10.76, $P < 0.001$; vs. dead: t-ratio = 9.09, $P < 0.001$; Fig. 3A; Table 1). EC length did not affect the sound velocity reduction ($F(1,8.13) = 1.60$, $P = 0.241$), but reduction of velocity was greater at the ATM ($F(1,41.25) = 4.14$, $P = 0.048$).

Sound velocity data in the EC from all three insect statuses were significantly slower in CO_2 in comparison to free-field CO_2 sound velocity, but there was no significant difference amongst the different statuses ($F(1,37.854) = 0.37$, $P = 0.696$; Fig. 3B; Table 1). More precisely, sound velocity of dead and alive insects was 31.56 % slower than free-field CO_2 sound velocity. Neither EC length ($F(1,6.43) = 2.61$, $P = 0.154$) nor sound velocity, at either tympanum, was significantly related to sound velocity with CO_2 present ($F(1,36.41) = 0.54$, $P = 0.467$).

To explore the effect of the EC radius on the sound propagation velocity inside of the ear in more detail, we also carried out numerical simulations after manipulating the EC geometry by changing its radius. Considering the tube to be filled with air or CO_2, we obtained the sound velocity from ECs with median radii 75-600 μm. The results are presented in Fig. 4, from which it is evident that, regardless of the gas composition inside the tube, for smaller EC radius the sound velocity reduces.

Discussion

Review of findings

This study tests the hypothesis that sound velocity reduction in the katydid EC is caused by the canal's geometry. Using LDV, μ-CT and FEA we have demonstrated, both experimentally and numerically, that sound propagation velocity was always reduced in relation to the expected free-field propagation velocity under normal conditions (Table 1), independent of gas composition in the trachea. This suggests that the tracheal geometry, namely the narrow radius of the EC, is the major factor that contributes to the observed reduction in velocity. This is further verified from the numerical results presented in Fig. 4, which demonstrate a decreasing sound propagation velocity in narrower EC. This is consistent with the narrow tube theory developed in Benade (1968) and Tijdeman (1975), which states that the sound velocity reduces in narrow tubes. The narrow section of the EC, starting in the femur and ending in the base of the tibia (Fig. 1), has a relatively uniform radius of approximately 150 μm (Fig. 5), small enough to affect sound propagation velocity.

The ear of *C. gorgonensis* is believed to have at least two acoustic inputs. Amplitude differences of around 15 dB are produced between the internal and external surfaces of the TMs and measured in this research, supporting the findings in Jonsson et al., 2016 (Jonsson et al., 2016). Our own results show an internal time delay of 59.5 ± 5.45 μs in live insects (Table 1). These insects determine the direction of the sound source through auditory differences in their independent ears; the differences, however, are caused by the interaction of an acoustic signal with its internally amplified and delayed counterpart, at the TM, as opposite to the external low-amplitude and faster stimulus arriving externally. Given that the signal delay in this system is further enhanced by the structure of the EC, we propose that this mechanism is included in the definition of the pressure difference receiver ears. Therefore, we redefine these ears as pressure-time difference receivers.

Through additional investigation, it has been observed that the gas composition contributes to the rate of velocity reduction. The numerical results show that sound propagation slows down 32.47 % in air and 28.19 % in CO_2, when compared to its respective free-field velocity under normal conditions (Table 1). These results imply that the rate of reduction in air is 4.3 % less compared to that in CO_2. We believe that these discrepancies are associated with the physical properties of each gas and to corroborate this we ran numerical simulations where the EC was filled with helium (He). This also projected a reduction in sound velocity (see Section 3 of Supplementary Materials; Table S1).

As a further demonstration that different gases will interact with EC geometry in different ways, we also consider the theoretical solution developed in Benade (1968) for the phase velocity in a narrow tube. This is defined by,

$$v = c \cdot 1 - \left(\frac{1}{r_v \sqrt{2}} - \frac{\gamma - 1}{r_t \sqrt{2}}\right) \quad (1)$$

where c is the speed of sound in open space, γ is the ratio of specific heats, and r_v, r_t are variables proportional to the ratio of the tube radius to the viscous and thermal boundary layer thickness, respectively, and are strongly dependent on gas density. We have assumed the propagation velocity for three different gases (air, helium (He) and CO_2) taking the tube radius to be equal to the median trachea radius of 150 μm, and the sound stimulus to be at 23 kHz. The variables used for calculating the phase velocity have been outlined in Table S1 in the Supplementary Materials.

The results in Table S1 show that in air there is a reduction of 7.3 % from free-field propagation. In CO_2 this reduction was around 4.5 %, whereas for He it was 24.7 %. There is an expected difference in the numerical results obtained in the EC and with the use of formula (1) since the tube for which formula (1) holds has a uniform radius and is assumed to have a rigid wall.

Formula (1) demonstrates that the reduction of sound velocity in tubes are also affected by the thickness of the viscous and thermal boundary layers formed near the tube wall, which in turn depend on the tube radius and the gas properties. Based on the theoretical results, it can be concluded that differing rates of velocity reduction obtained in the EC for different gas compositions result from the viscous and thermal boundary layers formed near the EC wall.

When the experimental results are compared to the numerical model, the relationship between the sound propagation velocity in two gases is not as clear. In CO_2, there is a consistent reduction in velocity, in air however, the numerical model predicts a greater decrease in sound velocity than what we observed experimentally. Furthermore, the reduction rate obtained in air (16.24 % in alive insects and 17.60 % in dead insects) is not as large as the results obtained in Jonsson et al. (2016), where velocity reduction was 25 %. This is attributable to our study utilising precise and consistent µ-CT measurements to determine the tracheal length, whereas the previous study used multiple approaches (Jonsson et al., 2016). The higher variation displayed in the sound velocity measurements in CO_2 likely results from random error in gas dispensation.

Differences between the experimental and numerical results can be attributed to some simplifying assumptions applied in the model. For instance, we assumed that the lumen of the EC is smooth. Instead, the EC is derived from the respiratory trachea built up of taenidia, which generally take the form of spiral thickenings of the tracheal walls joined by soft material, forming an irregular sinuous surface. In the model the gas is also assumed to be quiescent, which in reality is not since the tracheal tube is part of the respiratory system of the insect. Finally, in the models, the air and CO_2 gas that fill the EC are assumed to be under standard conditions, although during the experiment the trachea is filled with the ambient atmospheric gas composition. Nonetheless, both the experimental and numerical results show that even though the gas composition inside the EC play a part in the rate of velocity reduction inside the tube, the key component causing it is the complex EC geometry.

Dual-input ears in the animal kingdom

Pressure-time difference receivers are present in other insects too, for example, the cricket (Gryllidae). Related to katydids, crickets also possess narrow ear canals (Schmidt and Römer, 2013). Fittingly, when a signal passes through the cricket EC, it gains in amplitude and reduces in velocity (Larsen, 1981; Michelsen et al., 1994). This velocity reduction is comparable with our measurement of approximately 290 m/s in *C. gorgonensis* (under normal conditions; Table 1). The EC sound velocity in *Teleogryllus commodus* is shown to be 263 m/s (Larsen, 1981), and that in *Gryllus bimaculatus* is reported to be 264 m/s (Michelsen et al., 1994).

Other animals, including some insects and tetrapods, utilise pressure difference receivers to localise sound. These include grasshoppers (Michelsen and Rohrseitz, 1995), lizards (Christensen-Dalsgaard and Manley, 2005), crocodilians (Carr et al., 2009) and birds. Unlike in katydids, the pressure difference in these animals occurs between the membranes of two internally coupled ears. A signal transmitting internally from one tympanic membrane to another may suffer attenuation or, depending on the interaural distance and frequency of the signal, a time delay. This mechanism can present problems for smaller organisms such as the grasshopper (Acrididae). Grasshopper ears are located at lateral surfaces of the almost cylindrical body, exactly on the first abdominal segment. The tympana are connected by a series of sound-guiding air sacs (Michelsen and Rohrseitz, 1995), permitting sound to internally travel from one TM to the other. The vibration of the TMs, measured using LDV recordings, show the occurrence of nulls, i.e. frequencies where eardrum vibration is cancelled because its two surfaces receive sounds with an identical amplitude and phase (Michelsen and Larsen, 2008). Measurements of the neuronal response to sound stimulation show that the grasshopper hearing system provides sufficient interaural amplitude differences for accurate sound localisation (Schul et al., 1999).

The katydid outer ear reported here shows similarities with some bird ears. Firstly, the time for a sound signal to pass through the katydid EC (59.5 ± 5.45 μs; Table 1) is similar to the interaural neuron response time differences that are displayed in the barn owl (*Tyto alba*; 51 ± 12 μs; Volman and Konishi, 1989). This demonstrates a potential biological feasibility for the katydid to detect a stimulus travelling via both the external and internal sound inputs of the same ear. Secondly, avian ears are located at the side of the head, and evidence suggests that some species utilise pressure-time difference receivers to localise sound (Calford and Piddington, 1988; Larsen et al., 2006; Rosowski and Saunders, 1980). Across taxa, the documented anatomy of the avian ear canal varies from the basic interaural canal of the *T. alba* (Kettler et al., 2016), to the complex network of tubes described in the zebra finch (*Taeniopygia guttata*; Larsen et al., 2016). *Taeniopygia guttata* overcomes the size limitations of sound localisation through a delayed interaural signal (Calford and Piddington, 1988). The mechanism behind this delay is unknown but could result from a series of narrow tubes that internally connect each ear (Larsen et al., 2016). The TMs of *T. guttata* are directly connected by an interaural canal; but are also interconnected by several narrow canals (see Figure in Larsen et al., 2016). Perhaps the most significant of the narrow pathways are the superolatero-orbital canals. These begin above the interaural canal, at the sides of the head, arching upwards to join together in a sinus on the forehead (superoantero-orbital sinus). The end result is a 27 mm long canal with a cross-sectional area of 400 μm2 (radius = 11.3 μm). The superoantero-orbital sinus also associates with other narrow canals, both of which run down the longitudinal plane of the head. Resembling an exponential horn, the 5 mm long hypomedial-orbital tube connects the sinus to the interaural canal. Near the sinus, at its most narrow point, the cross-sectional area is 400 μm2. The narrowest tube is 7 mm long and has a cross-sectional area of 100 μm2 (radius = 5.6 μm). This extends from the sinus to a medium sized tube that runs parallel to the interaural canal. Proposed to be air-filled (Larsen et al., 2016), these narrow tubes resemble the geometry of the katydid EC. If sound does indeed reach these canals, then our models display the potential effect they

could have on signal transmission through the internal pathways in birds, and any role in sound localisation and potential signal delay warrant investigation.

Another relevant aspect of narrowing tubes and the reduction in sound velocity in katydids (Fig. 4), is the potential effect of the EC division at the position of the tympanal organ. The EC divides into two branches prior to reaching the inner ear: an anterior branch leads to the ATM, and a posterior branch to the PTM (see Fig. 6). Our results show that the anterior branch has a reduced sound velocity compared to the posterior one. The anterior branch is narrower in width than the posterior branch and is also adjacent to the auditory sensilla (Bangert et al., 1998). The asymmetric morphology of each branch suggests that the EC input is split into two signals with marginally different sound velocity. Taking into account the two external inputs at each TM, each ear may face a total of four acoustic inputs (only one for the human ear). The role of these branches along with the neural processing of the combined inputs should be investigated further.

The pressure-time difference receiver system reported here could also inspire acoustic detection sensors. Analogous processes for the development of direction-finding systems have been simulated in circuit models using mammals (Hubbard et al., 2009; Liu et al., 2009), and in insect-inspired robots mainly designed as biological models or for use in engineering (Reeve and Webb, 2003; Reeve et al., 2007; Webb, 1996). These models can be further developed by incorporating the sound processing capability of the outer ear of the katydid.

Materials and Methods

Experimental design

This research combines experimental and numerical approaches to infer the cause of sound velocity reduction inside the acoustic trachea of katydids. The experimental aspect involves measuring the time for an acoustic signal to transmit through the EC of a katydid and determining the length of the EC. This enables sound velocity to be calculated by

dividing the length of the EC by the time it takes the sound stimulus to reach the TM. To achieve this a special platform that isolates the external and internal auditory inputs is utilised (Jonsson et al., 2016; Montealegre-Z et al., 2012), along with an array of probe-loudspeakers, microphones, function generators and an LDV. We record the effect of different gas compositions on the sound propagation velocity. Gas is added to the EC through the use of a customised delivery system (see Section 1 of Supplementary Materials for more details).

Experimental animals

This study used specimens of *Copiphora gorgonensis* that were 8th generation descendants of a colony collected in November 2015 from the National Natural Park Gorgona, Colombia (latitude 2°58’ 7.4208" N; longitude 78°11’ 10.4964" W). Insects were maintained in communal vivaria (temperature 22°C - 27°C). A total of 9 adult individuals (5 males and 4 females) were used in this study (n = 17 ears).

Experimental set-up

To observe the effects of the internal pathway only, we isolated the internal and external sound inputs. We did this by mounting the insect on a customised platform (Fig. 2). The platform consists of two Perspex panels that fit together, the dorsal of which encompasses a central notch for the insects’ head, along with two adjacent holes for the forelegs. These panels are held together within a metal frame (for additional details see Montealegre-Z et al., (2012) and Section 4 of Supplementary Materials).

A 23 kHz pure tone is produced by a function generator (SDG1000 Series Function/Arbitrary Waveform Generator, Siglent Technologies Co. Ltd., Shenzhen, P.R. China) and emitted via a MF1-S 1 Multi Field Speaker (Tucker Davis Technologies, Alachua, FL, US) with a modified probe attachment (see Section 5 of Supplementary Materials; Fig. S1).

Prior to each experiment, a standardised reference point was recorded. The probe-loudspeaker was mounted onto a micromanipulator (World Precision Instruments, Inc., Sarasota, FL, US). A calibrated 1/8" (3.2 mm) microphone (Brüel & Kjær, 4138, Nærum, Denmark) was held in a clamp and the loudspeaker probe positioned 2 mm away from the microphones protective cap. The time taken for sound to travel from the loudspeaker probe to the microphone was recorded as the reference time.

The mounted insect was positioned in front of the LDV, and the laser point focused on a tympanic membrane (Fig. 1; Fig. 2). A gas delivery system (enabling the manipulation of the gas composition between experiments) was introduced behind the prothoracic side keel, directed towards the acoustic spiracle (Fig. 1; see Section 1 of Supplementary Materials). The probe-loudspeaker was then placed 2 mm away from the spiracle (matching the distance of the microphone reference signal), allowing sound to travel through the acoustic trachea and vibrate the tympanum (Fig. 1). For each ear, the LDV was used to record the time for the signal vibrations to arrive at the tympanum, measured as tympanal displacement.

Recordings were first taken without changes to the gas composition within the ear canal (normal conditions). The time taken for sound to travel from the loudspeaker to the tympanic membrane was noted and used as a benchmark throughout the experiment, to indicate when the gas composition in the EC was normal. Then, over a period of five seconds, pure CO_2 (Genuine Innovations, CA, US) was introduced to the canal via the gas delivery system, and the time recorded again (see Section 1 of Supplementary Materials). The CO_2 was left to diffuse out of the trachea until the signal reaching the tympanum returned to normal. This was replicated three times, before being repeated on the opposite foreleg. Experiments were conducted at ambient temperatures of 19.8°C and 25.0°C, with the body temperatures of the insects ranging from 23.6°C to 28.1°C.

Anatomical measurements of the trachea

The anatomy of the acoustic trachea was examined using X-ray micro-CT and 3D reconstruction, using standard biomedical imaging software following the published protocols (Jonsson et al., 2016). All the specimens were scanned with a Bruker SkyScan 1272 (Bruker micro-CT, Kontich, Belgium) at 50 kV, 200 mA, with a voxel size ranging from 3.12 µm to 10.99 µm. Reconstruction and automated measurements of EC were carried out with AMIRA (v. 6.7, VSG, Berlin, Germany). The tracheal lengths of all individuals were measured from the 3D reconstructions using the Center Line Tree module in AMIRA.

Sound analysis and calculation of velocity

The first local minimum of the sine wave chirp was used to obtain time measurements (see Section 7 of Supplementary Materials for more details on the reference signal). The time delay between the reference signal and the amplitude signal of the tympanum was obtained using Matlab (R2014a, The Math-Works, Inc., Natick, MA, US). This delay was used to calculate the velocity of sound propagation through each acoustic trachea – dividing the tracheal lengths obtained from 3D segmentations by the respective mean time delay.

Mathematical model and numerical simulations

The numerical results are based on the following system of equations.

Let Ω denote the EC of *C. gorgonensis*, which is the domain of our mathematical model formed by the union of two parts: Ω_f is the inside of the EC (the fluid domain) and Ω_s is the EC wall (solid domain) that intersect at the interface $\gamma = \Omega_s \cap \Omega_f$. The boundary of Ω consists of γ_1 which denotes the acoustic spiracle; γ_2 denotes the TM and γ_3 is the outer surface of the wall.

In the fluid domain Ω_f, the propagation of the sound wave is modelled with the use of the scalar wave equation which also takes into account the viscosity of the quiescent fluid. This is represented with the following equation and initial conditions:

2650

$$\frac{\partial^2 p}{\partial t^2} + \frac{1}{\rho_f}\left(\frac{4\mu}{3} + \mu_B\right)\frac{\partial \nabla p}{\partial t} = c^2 \Delta p \text{ in } \Omega_f \times (0, t], \tag{2}$$

$$p(\mathbf{x}, 0) = 0, \qquad \frac{\partial p}{\partial p}(\mathbf{x}, 0) = 0 \; in \; \Omega_f, \tag{3}$$

2651

2652 where T > 0 is a fixed positive time, c = speed of sound, μ = dynamic viscosity, μ_B = bulk

2653 viscosity, ρ_f = fluid density, $\nabla = \frac{\partial}{\partial_x}, \frac{\partial}{\partial_y}, \frac{\partial}{\partial_z}$ and $\Delta = \nabla^2$. The dependent variable $p = p(\mathbf{x}, t)$ is the

2654 time-dependent sound pressure at the spatial point $\mathbf{x} = (x, y, z)$.

2655 A harmonic incident wave enters into the EC through the spiracle with a frequency of

2656 23 kHz and an amplitude of 1 Pa, travelling at 343 m/s, represented by boundary condition

2657

$$\mathbf{n} \cdot \left(\frac{1}{p_f}\nabla p\right) + \frac{1}{p_f}\left(\frac{1}{c}\frac{\partial p}{\partial t}\right) = \mathbf{n} \cdot \left(\frac{1}{p_f} p_i\right) + \frac{1}{p_f}\left(\frac{1}{c}\frac{\partial p_i}{\partial t}\right) \tag{4}$$

2658 on γ_1, where

$$p_i = \sin\left(2\pi \times 23000\left(t - \frac{(\mathbf{x} - \mathrm{e}_k)}{c|\mathrm{e}_k|}\right)\right),$$

2659

2660 and e_k is the wave direction. Taking into account the impedance of the TM, we request the

2661 boundary condition (5) given below is satisfied on γ_2.

2662

$$\mathbf{n} \cdot \left(\frac{1}{p_f}\nabla p\right) = \frac{1}{Z_i}\frac{\partial p}{\partial t} \tag{5}$$

2663

2664 where Z_i is the magnitude of the specific acoustic impedance of the TM.

2665 Next we consider the displacement in the elastic wall due to the sound propagating
2666 inside the EC. We make the simplifying assumption that the EC wall is built of an isotropic,
2667 incompressible and homogeneous material. This is represented by the elastic wave equation
2668 (6) given below which models the mechanical waves in the structure Ω_s assuming small
2669 deformations (Cummings and Feng, 1999). Equation (6) also accounts for the damping
2670 properties of the EC wall.
2671

$$\rho_s \frac{\partial^2 \mathbf{u}_s}{\partial t^2} + {\rho_s}^{\alpha} dM \frac{\partial \mathbf{u}_s}{\partial t} = \nabla \cdot \left(\sigma(\mathbf{u}_s) + \beta_{dK} \frac{\partial \sigma}{\partial t} \right) \text{ in } \Omega_s \times (0, T], \tag{6}$$

$$\mathbf{u}_s(\mathbf{x}, 0) = 0, \qquad \frac{\partial \mathbf{u}_s}{\partial t}(\mathbf{x}, 0) = 0 \text{ in } \Omega_s \tag{7}$$

2672
2673 where ρ_s is the density of the wall, the components of the stress tensor $\sigma(\mathbf{u}_s)$ are
2674

$$\sigma_{ij} = \frac{E}{1+v} \epsilon_{ij} + \frac{E_v}{(1+v)(1-2v)} \epsilon_{kk} \delta_{ij}, \qquad i, j = 1, 2, 3$$

2675
2676 with E = Young's modulus; v = Poisson's ratio, 0 < v < 1/2; $\epsilon_{ij} = \frac{1}{2}\left(\frac{\partial \mathbf{u}_{si}}{\partial x_j} + \frac{\partial \mathbf{u}_{sj}}{\partial x_i} \right)$ the strain
2677 tensor; δ_{ij} the Kronecker-delta function and the dependent variable $\mathbf{u}_s$ is the displacement
2678 vector in Ω_s. Furthermore, the Rayleigh damping parameters α_{dM} and β_{dM} satisfies the
2679 following relation between the damping ratio ξ_i and the natural frequencies ω_i of an
2680 undamped system:
2681

$$\xi_i = \frac{\alpha_{dM}}{2\omega_i} + \frac{\omega_i \beta_{dM}}{2},$$

2682

where α_{dM} and β_{dM} are the mass proportional and stiffness proportional Rayleigh damping coefficients, respectively.

On γ_3 we specify the boundary condition as

$$\sigma_{ij} \cdot n_j = 0, \qquad i,j = 1,2,3 \tag{8}$$

so that there is no external stress on the wall.

Finally, at the interface γ the defined fluid and solid systems are coupled. The coupling includes the fluid load on the structure and the structural acceleration as experienced by the fluid.

$$\mathbf{n} \cdot \frac{1}{\rho_f} \nabla p = -\mathbf{n} \cdot (\mathbf{u}_s)_{tt} \,, \tag{9}$$

$$\mathrm{F}_A = p\mathbf{n}, \tag{10}$$

where **n** is the surface normal and F_A is the force per unit area experienced by the structure.

As well as the pressure distribution in the EC for the time interval $(0, T]$, by solving system (2)-(10), we are also able to obtain the time taken for the sound stimulus to reach the TM, which is where the tracheal sound transmission takes place. Using this, we calculate the speed of sound during transmission by the elementary formula

$$speed = \frac{distance}{time}$$

Where $distance$ = length of EC.

For spatial discretization, the numerical solution of the variational form of the introduced equations, along with the defined boundary conditions are obtained with the finite element method using the commercial software Comsol Multiphysics® v.5.4 (COMSOL Multiphysics®). The finite element mesh constructed in the EC is demonstrated in Fig. 1. The tetrahedral elements forming the mesh in Ω_f have the restriction that the diameter of each element is less than the quantity

$$\frac{\text{wavelength of sound wave}}{30}.$$

The mesh in Ω_f is connected to the mesh on Ω_s, which is formed using shell elements of MITC (Mixed Interpolation of Tensorial Components) type (Bathe et al., 2000), a common mesh type used for capturing various shell behaviours. The solution of the system of finite element equations in space is based on Quadratic Lagrange elements for all the dependent variables.

For the discretization of the time derivatives in system (2)-(10), the Generalized alpha Method is employed, with a time step of $\tau = 2.174 \times 10^{-8}$ s. Taking into account that the frequency of the sound stimulus is 23 kHz, we took T = 5/(23 kHz) = 2.174 s, so that we assumed the sound stimulus has 5 cycles at 23 kHz.

Table S2 in the Supplementary Materials contains the values of the parameters used in the equations (2)-(10). The outlined equations are solved using the 3D Transient Acoustic-Shell interaction module of Comsol Multiphysics® (COMSOL Multiphysics®).

For the simulations that have been carried out on ECs with different radii, the conditions outlined above have been kept the same. The geometry of the EC, i.e. the stl file of the EC, has been changed by using the 'scale' feature of Comsol Multiphysics® v 5.5 (COMSOL Multiphysics®), which is available in the geometry node.

Data processing and statistical analysis

During each experiment, the time taken for sound to propagate through the EC, to the tympanic membrane was recorded using LDV. For each EC sample, the mean of a minimum of three replicates was calculated. Post experiment, recordings were standardized against a reference recording. For some recordings using CO_2 gas, the reference signal was invalidated due to too much gas dispensation, and therefore these recordings were removed from the analysis. The remaining values, along with length data obtained from μ-CT data, were then used to calculate the mean sound propagation velocity for each individual EC. The mean sound propagation velocity and standard deviation were taken and listed in Table 1.

Sound velocity in the acoustic tracheae was analysed using linear-mixed effects models. Velocity was the dependent variable, with tracheal length as a co-variate, and tympanum (ATM/PTM) and status (alive, dead, numerical model) as fixed factors. To account for repeated measures of the same individual and EC, EC (right/left) was nested within individual as a random factor. Linear mixed effects models were run using lmerTest (R Core Team, 2019) in R 3.6.1 (R Core Team, 2019). Post hoc testing was carried out using estimate marginal means from the emmeans package (Lenth, 2020).

References

Bailey, W.J. and Stephen, R.O., 1978. Directionality and auditory slit function: a theory of hearing in bushcrickets. *Science*, 201, 633-634.

Bailey, W.J., 1990. *The ear of the bushcricket. Tettigoniidae: Biology, Systematics and Evolution. Crawford House Press, Bathurst, Australia*, 217-247.

Bangert, M., Kalmring, K., Sickmann, T., Stephen, R., Jatho, M. and Lakes-Harlan, R., 1998. Stimulus transmission in the auditory receptor organs of the foreleg of bushcrickets (Tettigoniidae) I. The role of the tympana. *Hearing Research*, 115, 27-38.

Bathe, K.J., Iosilevich, A. and Chapelle, D., 2000. An evaluation of the MITC shell elements. *Computers & Structures*, 75, 1-30.

Benade, A.H., 1968. On the propagation of sound waves in a cylindrical conduit. *The Journal of the Acoustical Society of America*, 44, 616-623.

Calford, M.B. and Piddington, R.W., 1988. Avian interaural canal enhances interaural delay. *Journal of Comparative Physiology A*, 162, 503-510.

Carr, C.E., Soares, D., Smolders, J. and Simon, J.Z., 2009. Detection of interaural time differences in the alligator. *Journal of Neuroscience*, 29, 7978-7990.

Celiker, E., Jonsson, T. and Montealegre-Z, F., 2020. The Auditory Mechanics of the Outer Ear of the Bush Cricket: A Numerical Approach. *Biophysical Journal*, 118, 464-475.

Christensen-Dalsgaard, J. and Manley, G.A., 2005. Directionality of the lizard ear. *Journal of Experimental Biology*, 208, 1209-1217.

COMSOL Multiphysics® v. 5.4. www.comsol.com. COMSOL AB, Stockholm, Sweden.

Cummings, P. and Feng, X., 1999. Domain decomposition methods for a system of coupled acoustic and elastic Helmholtz equations. In Eleventh International Conference on Domain Decomposition Methods. *Domain Decomposition Press Bergen, Norway*, 205-213.

Gelfand, S. A. (2005) Hearing: An Introduction to Psychological and Physiological Acoustics. CRC Press.

Hartbauer, M. and Römer, H., 2014. From microseconds to seconds and minutes—time computation in insect hearing. *Frontiers in Physiology*, 5, 138.

Heffner, R.S. and Heffner, H.E., 1992. Evolution of sound localization in mammals. In *The evolutionary biology of hearing*, 691-715.

Hoffmann, E. and Jatho, M., 1995. The acoustic trachea of tettigoniids as an exponential horn: theoretical calculations and bioacoustical measurements. *The Journal of the Acoustical Society of America*, 98, 1845-1851.

Hubbard, A., Cohen, H., Karl, C., Freedman, D., Mountain, D., Ziph-Schatzberg, L., Karl, M.N., Kelsall, S., Gore, T., Pu, Y. and Yang, Z., 2009, May. Biologically inspired circuitry that mimics mammalian hearing. In *Bio-Inspired/Biomimetic Sensor Technologies and Applications International Society for Optics and Photonics*, 7321, p.732109.

Jonsson, T., Montealegre-Z, F., Soulsbury, C.D., Robson Brown, K.A. and Robert, D., 2016. Auditory mechanics in a bush-cricket: direct evidence of dual sound inputs in the pressure difference receiver. *Journal of the Royal Society Interface*, 13, p.20160560.

Kettler, L., Christensen-Dalsgaard, J., Larsen, O.N. and Wagner, H., 2016. Low frequency eardrum directionality in the barn owl induced by sound transmission through the interaural canal. *Biological Cybernetics*, 110, 333-343.

Larsen, O.N., 1981. Mechanical time resolution in some insect ears. *Journal of Comparative Physiology*, 143, 297-304.

Larsen, O.N., Christensen-Dalsgaard, J. and Jensen, K.K., 2016. Role of intracranial cavities in avian directional hearing. *Biological Cybernetics*, 110, 319-331.

Larsen, O.N., Dooling, R.J. and Michelsen, A., 2006. The role of pressure difference reception in the directional hearing of budgerigars (Melopsittacus undulatus). *Journal of Comparative Physiology A,* 192, 1063-1072.

Lenth, R. 2020. *emmeans: Estimated Marginal Means, aka Least-Squares Means*. R package version 1.4.5. https://CRAN.R-project.org/package=emmeans

Liu, H., Currano, L., Gee, D., Yang, B. and Yu, M., 2009, May. Fly-ear inspired acoustic sensors for gunshot localization. In *Bio-Inspired/Biomimetic Sensor Technologies and Applications International Society for Optics and Photonics*, 7321, p.73210A.

Lombard, R.E. and Bolt, J.R., 1979. Evolution of the tetrapod ear: an analysis and reinterpretation. *Biological Journal of the Linnean Society*, 11, 19-76.

Michelsen, A. and Larsen, O.N., 2008. Pressure difference receiving ears. *Bioinspiration & Biomimetics*, 3, p.011001.

Michelsen, A. and Rohrseitz, K., 1995. Directional sound processing and interaural sound transmission in a small and a large grasshopper. *Journal of Experimental Biology*, 198, 1817-1827.

Michelsen, A., Heller, K.G., Stumpner, A. and Rohrseitz, K., 1994. A new biophysical method to determine the gain of the acoustic trachea in bushcrickets. *Journal of Comparative Physiology A*, 175, 145-151.

Michelsen, A., Popov, A.V. and Lewis, B., 1994. Physics of directional hearing in the cricket Gryllus bimaculatus. *Journal of Comparative Physiology A*, 175,153-164.

Montealegre-Z, F., Jonsson, T., Robson-Brown, K.A., Postles, M. and Robert, D., 2012. Convergent evolution between insect and mammalian audition. *Science*, 338, 968-971.

R Core Team. 2019. *R: A language and environment for statistical computing*. R Foundation for Statistical Computing, Vienna, Austria. https://www.R-project.org/.

Rajaraman, K., Mhatre, N., Jain, M., Postles, M., Balakrishnan, R. and Robert, D., 2013. Low-pass filters and differential tympanal tuning in a paleotropical bushcricket with an unusually low frequency call. *Journal of Experimental Biology*, 216, 777-787.

Reeve, R., van Schaik, A., Jin, C., Hamilton, T., Torben-Nielsen, B. and Webb, B., 2007. Directional hearing in a silicon cricket. *Biosystems*, 87, 307-313.

2853 Reeve, R.E. and Webb, B.H., 2003. New neural circuits for robot phonotaxis. *Philosophical*
2854 *Transactions of the Royal Society of London. Series A: Mathematical, Physical and*
2855 *Engineering Sciences*, 361, 2245-2266.
2856
2857 Robert, D. 2005. Directional Hearing in Insects. *Springer Handbook of Auditory Research*,
2858 25, 6-35.
2859
2860 Rosowski, J.J. and Saunders, J.C., 1980. Sound transmission through the avian interaural
2861 pathways. *Journal of Comparative Physiology*, 136, 183-190.
2862
2863 Schmidt, A.K. and Römer, H., 2013. Diversity of acoustic tracheal system and its role for
2864 directional hearing in crickets. *Frontiers in Zoology*, 10, 1-9.
2865
2866 Schul, J., Holderied, M., Helversen, D.V. and Helversen, O.V., 1999. Directional hearing in
2867 grasshoppers: neurophysiological testing of a bioacoustic model. *Journal of Experimental*
2868 *Biology*, 202, 121-133.
2869
2870 Shen, J.X., 1993. A peripheral mechanism for auditory directionality in the bushcricket
2871 Gampsocleis gratiosa: acoustic tracheal system. *The Journal of the Acoustical Society of*
2872 *America*, 94, 1211-1217.
2873
2874 Tijdeman, H., 1975. On the propagation of sound waves in cylindrical tubes. *Journal of*
2875 *Sound and Vibration*, 39, 1-33.
2876
2877 Tucker, A.S., 2017. Major evolutionary transitions and innovations: the tympanic middle ear.
2878 *Philosophical Transactions of the Royal Society B: Biological Sciences*, 372, p.20150483.
2879 Webb, B., 1996. A cricket robot. *Scientific American*, 275, 94-99.
2880

2881 Volman, S.F. and Konishi, M., 1989. Spatial selectivity and binaural responses in the inferior
2882 colliculus of the great horned owl. *Journal of Neuroscience*, 9, 3083-3096.
2883
2884 Yack, J.E., 2004. The structure and function of auditory chordotonal organs in insects.
2885 *Microscopy Research and Technique*, 63, 315-337.

Figures

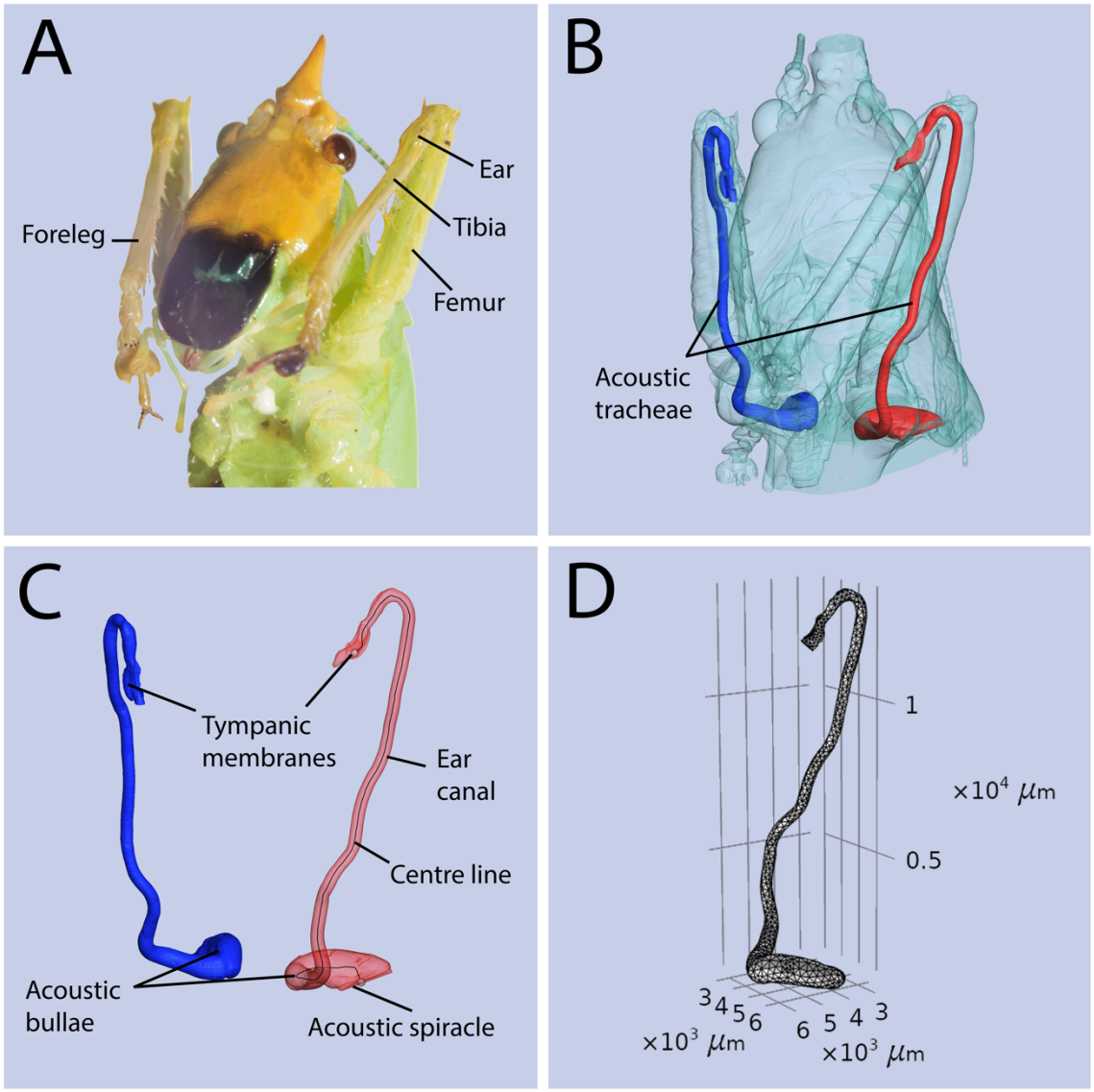

Figure 1. Anatomy and 3D reconstruction of the katydid ear canal. **A**) An image of the katydid *Copiphora gorgonensis*. **B**) The µ-CT image of the katydid highlighting the acoustic tracheae (which form the ear canal). **C**) The components of the acoustic trachea. **D**) The finite element mesh formed in the tracheal tube.

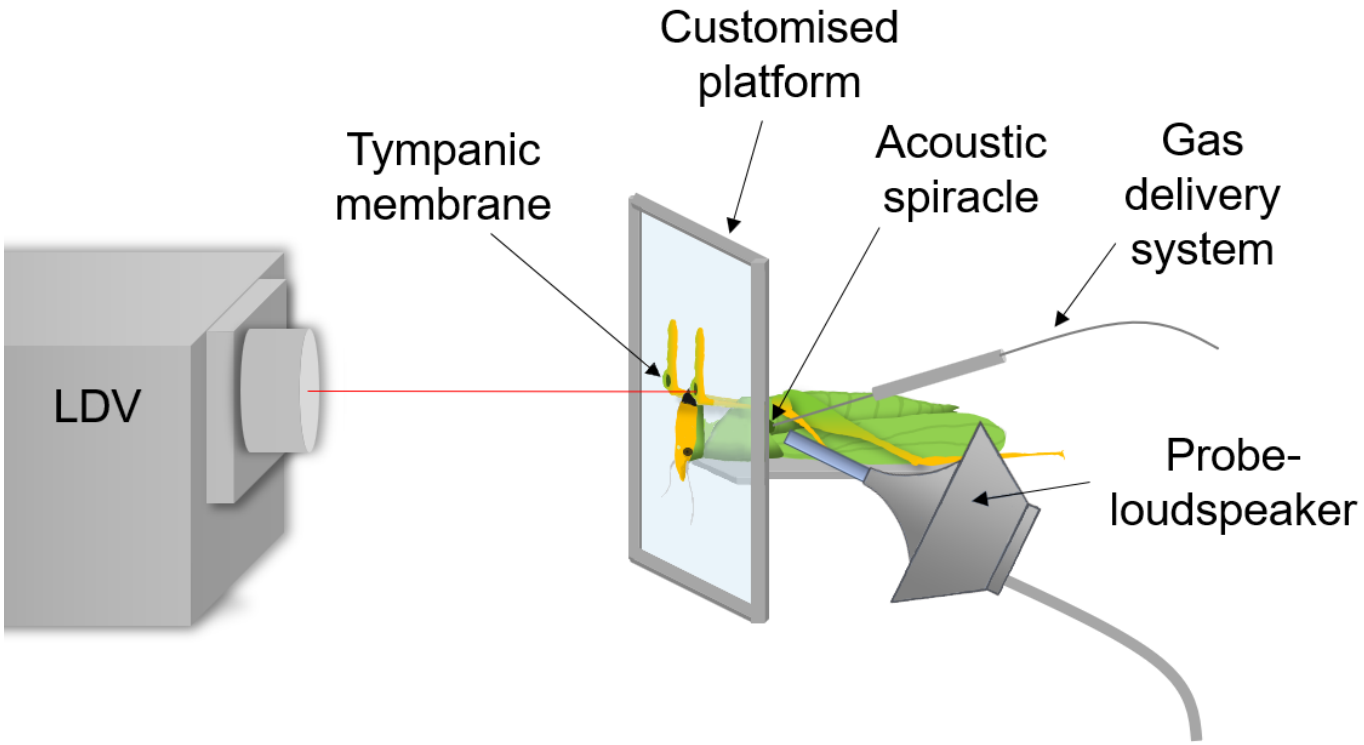

2893

2894 **Figure 2.** Experimental preparation. The illustration shows the platform used to acoustically separate the ears from the spiracle, along with the

2895 gas replacement dispenser, acoustic stimulation and laser recording system.

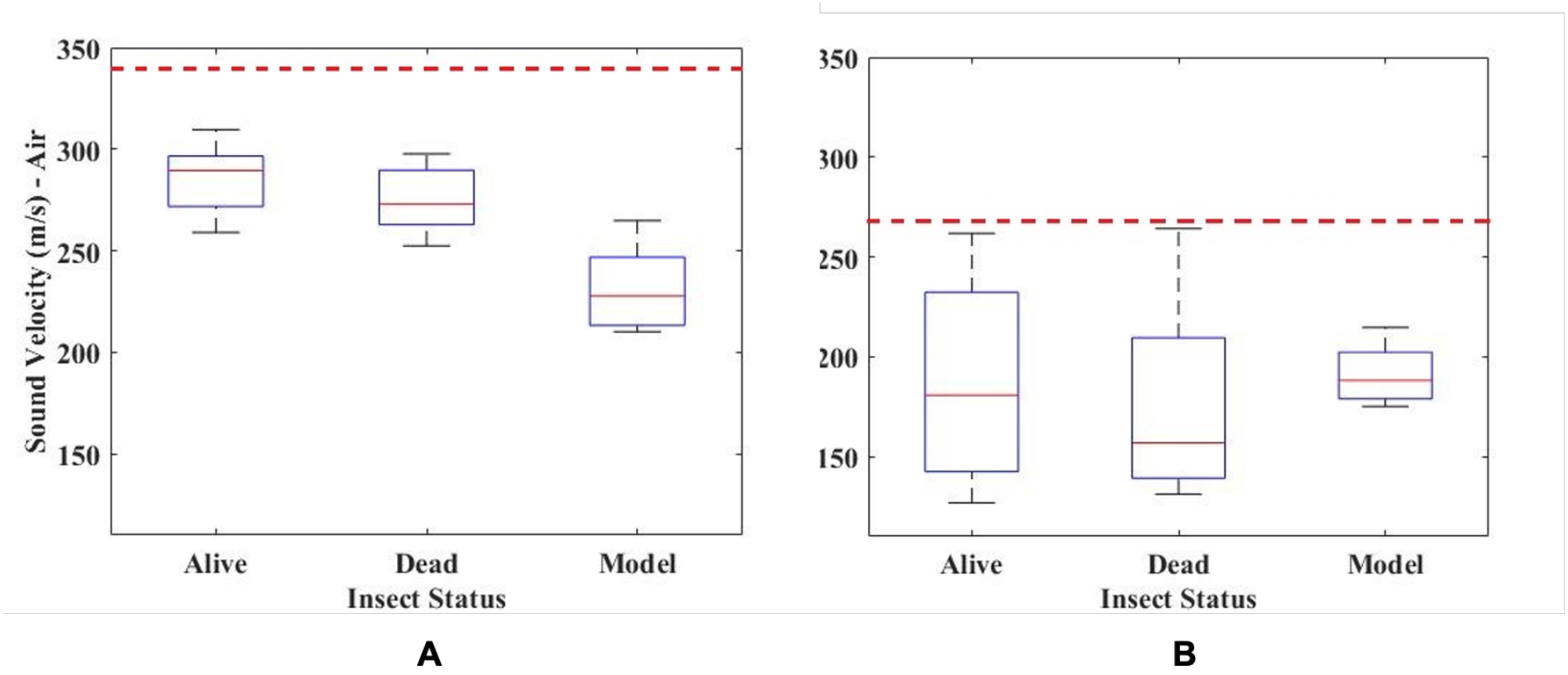

Figure 3. Sound propagation velocity measured experimentally and numerically. Experimental procedures were conducted in alive and dead specimens. **A**) EC filled with Air. The dashed line represents the free-field sound velocity in air, 343 m/s. **B**) EC filled with CO_2.The dashed line represents the free-field sound velocity in CO_2, 267 m/s.

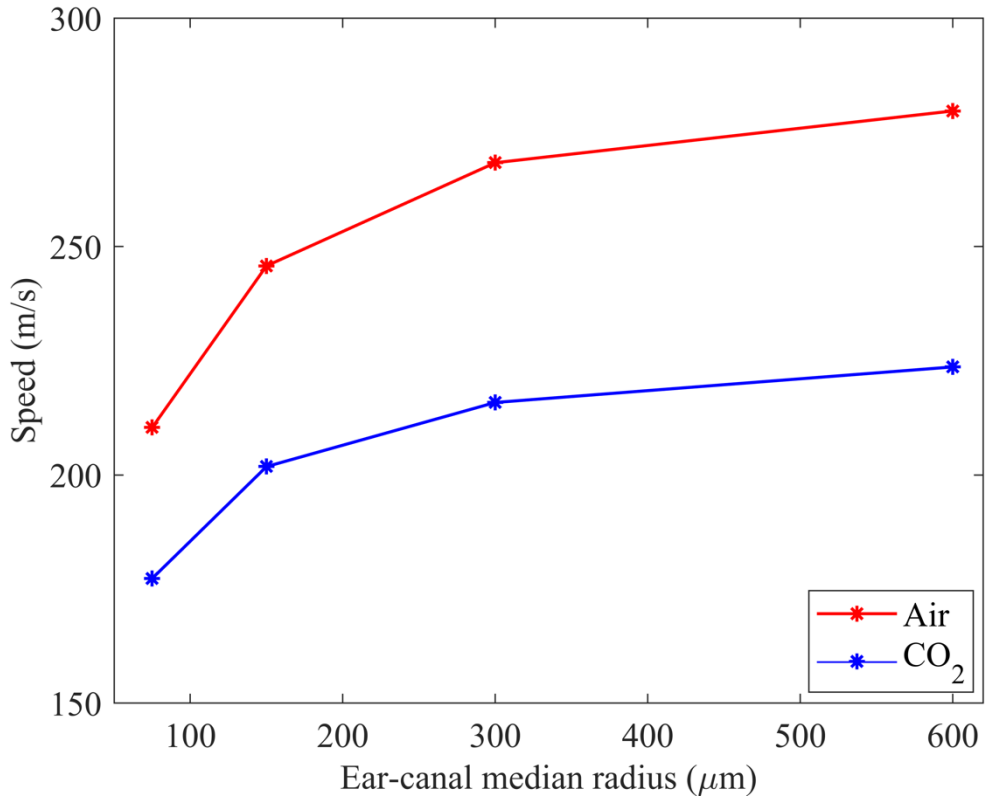

Figure 4. Artificial manipulation of the EC geometry and its effect on sound propagation velocity. The speed of sound measured at the end of the ear canals with different radii, while filled with air or CO_2, using Finite Element Analysis.

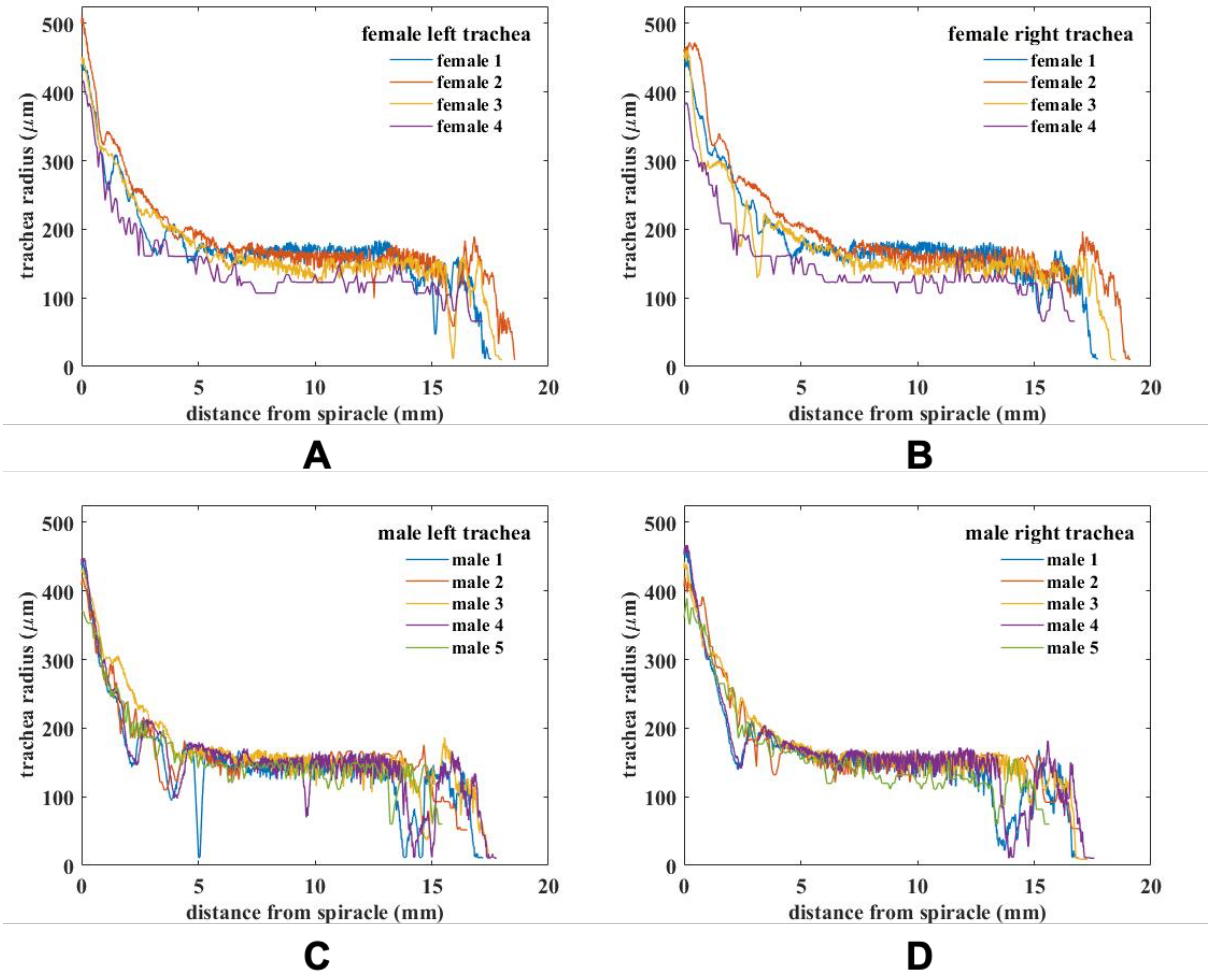

2905

2906 **Figure 5.** Quantitative relationship between EC (trachea) radius and length. Measured
2907 distance displayed from the acoustic spiracle to the tympanal organ area in males and
2908 females of *C. gorgonensis*. **A**) female left EC. **B**) female right EC. **C**) male left EC. **D**) male
2909 right EC.

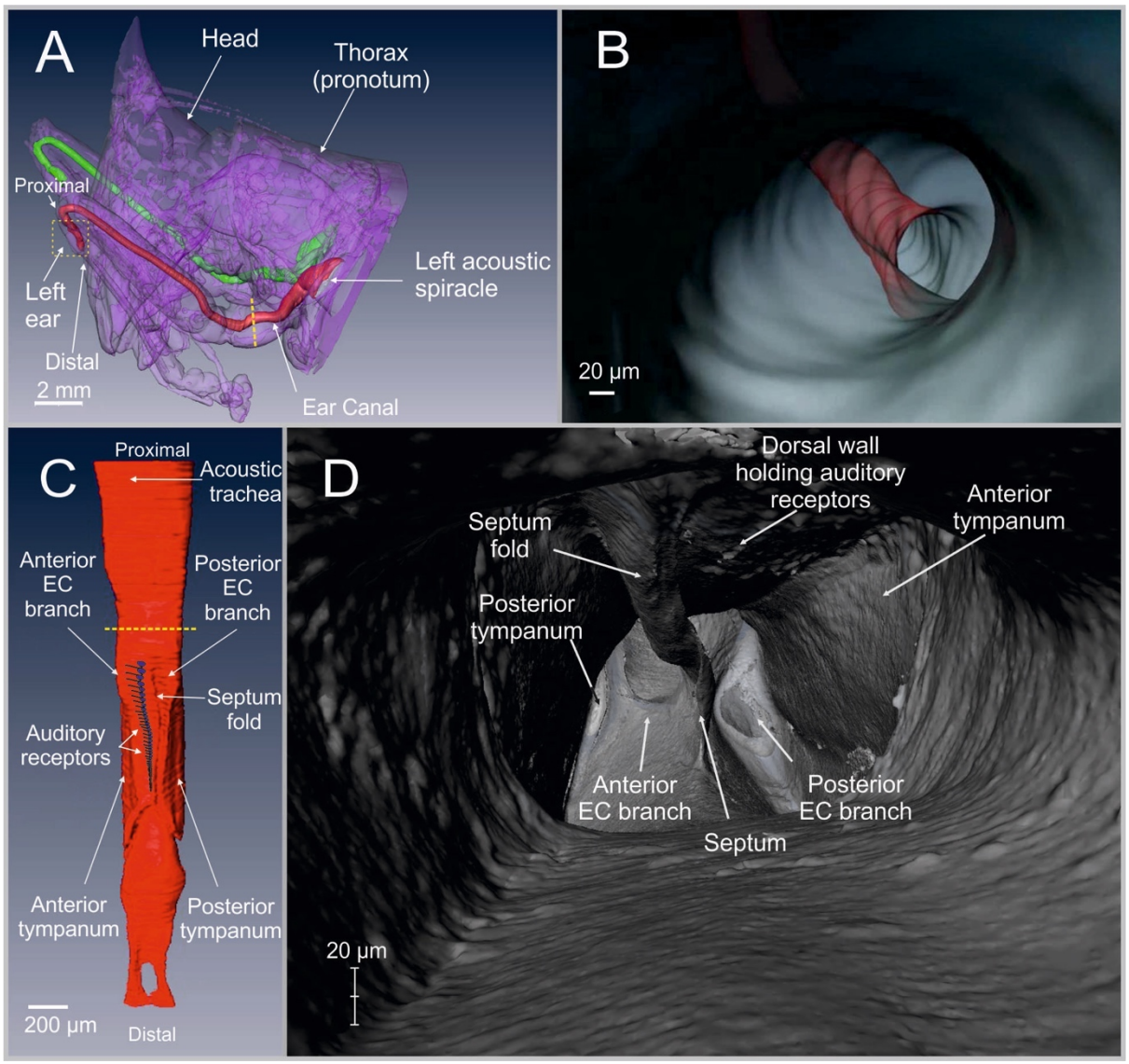

Figure 6. External and internal morphology of the EC showing the tracheal division at the tympanal organ location. **A**) Lateral view of the body in transparency showing left and right EC. **B**) Internal view inside the EC. **C**) Close up view of the ear section extracted from the dashed box in **A**. **D**) Internal view inside the EC showing the branch division of the trachea at the tympanal organ location. Camera placed inside the EC lumen approximately at the location of the yellow dashed line in **C**.

Tables

Table 1. A summary of data across all treatments. Sample size shows both the number of specimens (n_S) and number of ear canals (n_{EC}).

Air				
	Free-field	Alive	Dead	Numerical
Sample size	NA	$n_S = 8, n_{EC} = 14$	$n_S = 8, n_{EC} = 15$	$n_S = 7, n_{EC} = 13$
Mean sound velocity (m/s) ± SD	343	289.109 ± 16.245	280.172 ± 17.606	231.638 ± 16.763
% reduction from free-field sound velocity	NA	15.712	18.317	32.467
Mean EC length (mm) ± SD	NA	17.126 ± 0.998	17.067 ± 0.938	17.314 ± 0.935
Mean time (ms) ± SD	NA	0.0595 ± 0.00545	0.0611 ± 0.00445	0.0750 ± 0.00485
CO_2				
	Free-field	Alive	Dead	Numerical
Sample size	NA	$n_S = 8, n_{EC} = 14$	$n_S = 8, n_{EC} = 14$	$n_S = 7, n_{EC} = 13$
Mean sound velocity (m/s) ± SD	267	184.318 ± 42.546	181.13 ± 41.857	191.728 ± 12.046
% reduction from free-field sound velocity	NA	30.968	32.161	28.192
Mean EC length (mm) ± SD	NA	17.126 ± 0.998	17.095 ± 0.968	17.314 ± 0.935
Mean time (ms) ± SD	NA	0.0972 ± 0.00205	0.0987 ± 0.00209	0.0905 ± 0.00524

Supplementary Materials

Section 1: Design of the gas delivery system

In order for gas to be delivered from its container to the spiracular opening, a precise yet robust system was required. A micropipette puller (P30; Sutter Instruments, Novato, CA, USA) was used to produce a microcapillary from borosilicate glass tubing (external diameter: 1.2 mm, internal diameter: 0.9 mm; B120-69-8, Linton Instruments, Norfolk, England). The microcapillary was carefully shortened using tweezers. This increased the volume of air able to pass through the glass capillary, whist also maintaining the smaller size that wa required to insert the glass tube into the acoustic spiracle. The microcapillary was fixed into a PicoNozzle kit (5430-ALL, World Precision Instruments, Inc., Sarasota, FL, US), which was connected to PVC tubing (external diameter: 3 mm, internal diameter 1.5 mm). The tube allowed the gas to be dispensed far from the spiracle and minimised any disturbance to both the measurements and the experiment set up, and the gasket of the PicoNozzle Kit prevented gas from leaking the set-up. The carbon dioxide (CO_2) dispenser (Genuine Innovations, IN, US) required an extension for gas injection. This was made by sealing a pump needle adapter, with the threaded fixing removed, to the dispenser using Blu Tack (Bostik, WI, US). CO_2 was dispensed slowly, to allow the naturally occurring gas to escape the trachea. The gas delivery system assisted with this since the small microcapillary opening helped to regulate the gas pressure.

Section 2: Sound propagation through carbon dioxide

In order to provide a benchmark of sound velocity in the experimental carbon dioxide (CO_2), we measured sound propagation velocity through a linear tube A plastic tube (length: 101 mm, external diameter: 12 mm, internal diameter: 10 mm) was sealed by attaching two inflated balloons to each end, with Super Glue (Loctite, Düsseldorf, Germany). Using inflated

balloons provided a thin, taut membrane for efficiently capturing soundwaves. The excess material was cut away and the remainder was further secured to the tube. To allow the diffusion of gas in and out of the tube, two 3 mm airflow holes were drilled in the middle of the length; one dorsal, one ventral. A laser beam, one from the laser Doppler vibrometer (LDV) and another from a compact sensor head (OFV- 37 534, Polytec, Waldbronn, Germany), was placed onto each opposing balloon membrane, monitoring any vibrations. An MF1-S 1 Multi Field Speaker was placed facing a membrane, and a 20 kHz sound stimulus was produced. The laser beams recorded the arrival time of the stimulus at each membrane, allowing us to calculate the time difference between sound arrival. To ensure that no sound waves were passing the far membrane via an external route, a barrier of acoustic foam (Studiofoam Pyramids, Auralex Acoustics Inc., IN, US) was used to isolate this membrane from the microphone.

For the normal gas composition measurements, the airflow holes were covered with Parafilm (Sigma-Aldrich, Dorset, UK) ensuring the system was closed. These measurements occurred at 27°C and 55 % relative humidity. CO_2 was added via the gas delivery system; the syringe perforating the Parafilm and keeping the barrier airtight. The less dense gas composition of the room was allowed to escape through the dorsal airflow hole – which was then sealed with Blu Tack. LDV time measurements were taken and subsequently the time difference calculated. By combining the time data with the known length of the tube, the sound propagation velocity could be calculated. A total of ten measurements were taken in the natural air composition, and seven measurements in CO_2. The mean ± standard deviation sound velocity in air was 346.66 ± 0.00 m/s, and 262.08 ± 2.73 m/s in CO_2.

Section 3: Numerical simulation with helium

Whilst helium (He) would not naturally occur in the katydid ear canal (EC) at elevated levels, it was included in the study because the properties of the gas differ greatly to both air and CO_2. These simulations projected a 55.2 % decrease in sound velocity, relative to the

expected free-field sound velocity in He – a considerably larger reduction than compared to the results in air and CO_2 (Table S1). In an effort to provide a direct comparison with the models, experiments using helium were attempted. These recordings were invalidated, however, as the high rate of diffusion of He meant that it diffused out of the EC too quickly.

Section 4: Details of experimental set-up

All experiments were carried out inside an acoustic booth (IAC Acoustics, Series 120a, internal dimensions of 2.8 m x 2.7 m x 2 m), and at temperatures between 20.5°C and 25°C. All experiments were performed on a vibration isolation table (Pneumatic Vibration Isolation Table with a B120150B - Nexus Breadboard, 1200 mm x 1500 mm x 110 mm, M6 x 1.0 Mounting Holes; and a PFA52507 - 800 mm Active Isolation Frame 900 x 1200 mm, Thorlabs Inc., Newton, New Jersey, US).

Liquid latex (Magnacraft, Midhurst, UK) was applied between the two Perspex panels on the platform, and around the neck and fore-femora – this sealed any remaining gaps to form the continuous barrier necessary for preventing sound transmission. This design ensures acoustic isolation between the external, tympanal sound input and the internal sound input of EC. More details about this process are given in (Jonsson et al., 2016; Montealegre et al., 2012).

A sound level calibrator (Bruel & Kjaer, 4231; Nærum, Denmark) was used to calibrate the sensitivity of a 1/8” (3.2mm) microphone (Bruel & Kjaer, 4138). The LDV was combined with a close-up unit (PSV-A-410) and a 300 mm lens (PSV-A-CL-300). The live-camera feed of the laser system allowed the laser beam to be accurately aimed through the tympanal slits (avoiding obstruction by the tympanal flaps) and focused onto either the anterior or posterior tympanic membrane of the left leg. The gas delivery system was introduced behind the prothoracic side keel, directed towards the acoustic spiracle. To increase precision and accuracy, the katydid was illuminated using a dual arm fibre optic

illuminator (Meiji Techno UK Ltd, FL150, Somerset, UK). The probe loudspeaker was then introduced at a 2 mm distance to the acoustic spiracle.

Section 5: Design of the probe-loudspeaker

An MF1-S 1 Multi Field Speaker (Tucker Davis Technologies, Alachua, FL, US) was combined with its closed-field configuration attachment, which involves a CF adaptor and an exponential tip with a reduced tip of 3 mm. A probe was constructed out of a polypropylene tube (length: 35 mm, external diameter: 3 mm, internal diameter: 2 mm) which was then inserted into the speaker, functioning as an extension, to deliver sound stimuli directly to the acoustic spiracle (see Figure S1).

Section 6: Reference signal

To ensure we were measuring the same point in both the reference recording and the tympanal recording, we designed a wave that exhibited a marker on the first local maximum. The frequency of this theoretical wave was adjustable using the PSV 9.4 Acquisition Software (Polytec, Waldbronn, Germany). The wave was then played through the MF1-S 1 Multi Field Speaker, at 10 kHz, into the spiracle of the insect and a microphone, with both the tympanal and microphone response recorded (Fig. S2). The marker was clearly visible in both recordings, revealing the correct wave to extract the time signal from.

Section 7: Supplementary figures

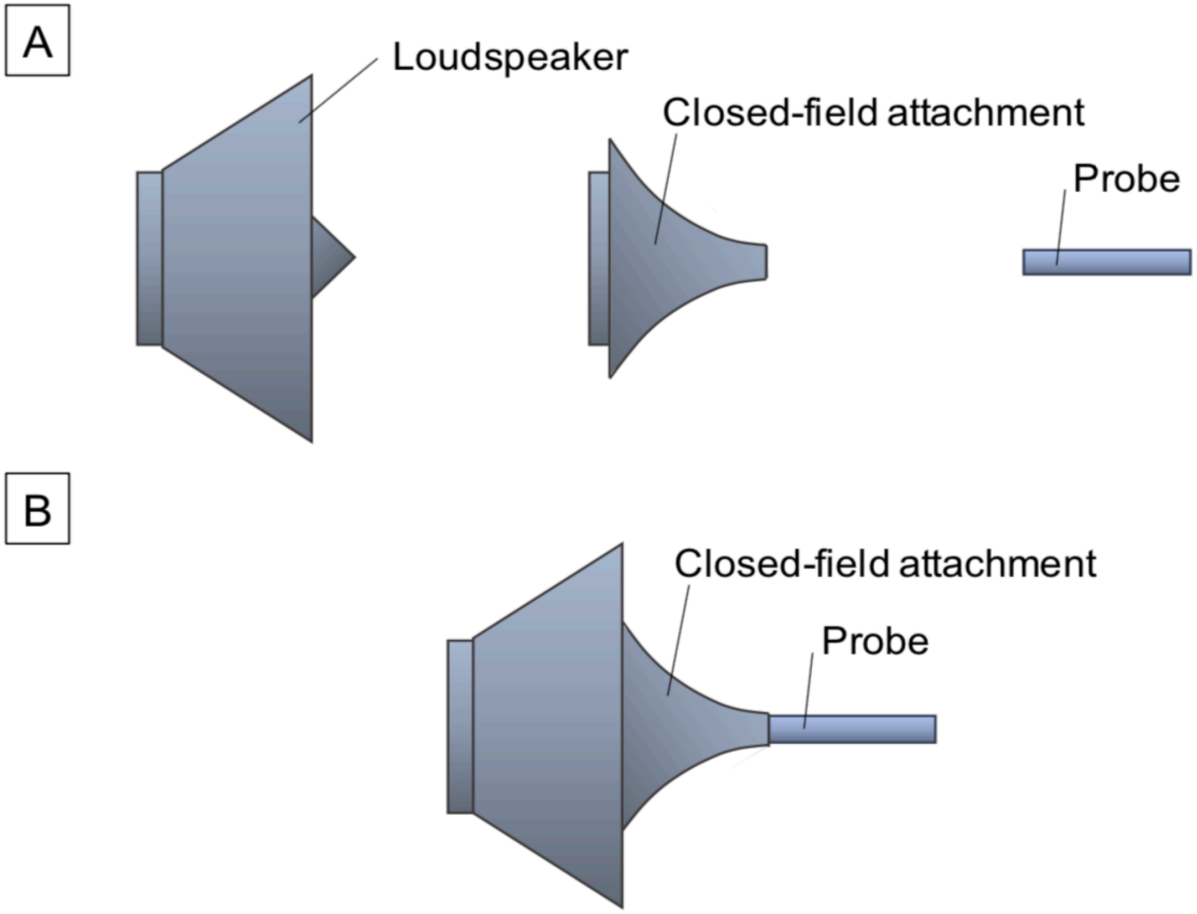

Figure S1. MF1-S 1 Multi Field Speaker (Tucker Davis Technologies, Alachua, FL, US). **A**) The separate components of the probe-loudspeaker. **B**) The probe-loudspeaker after construction.

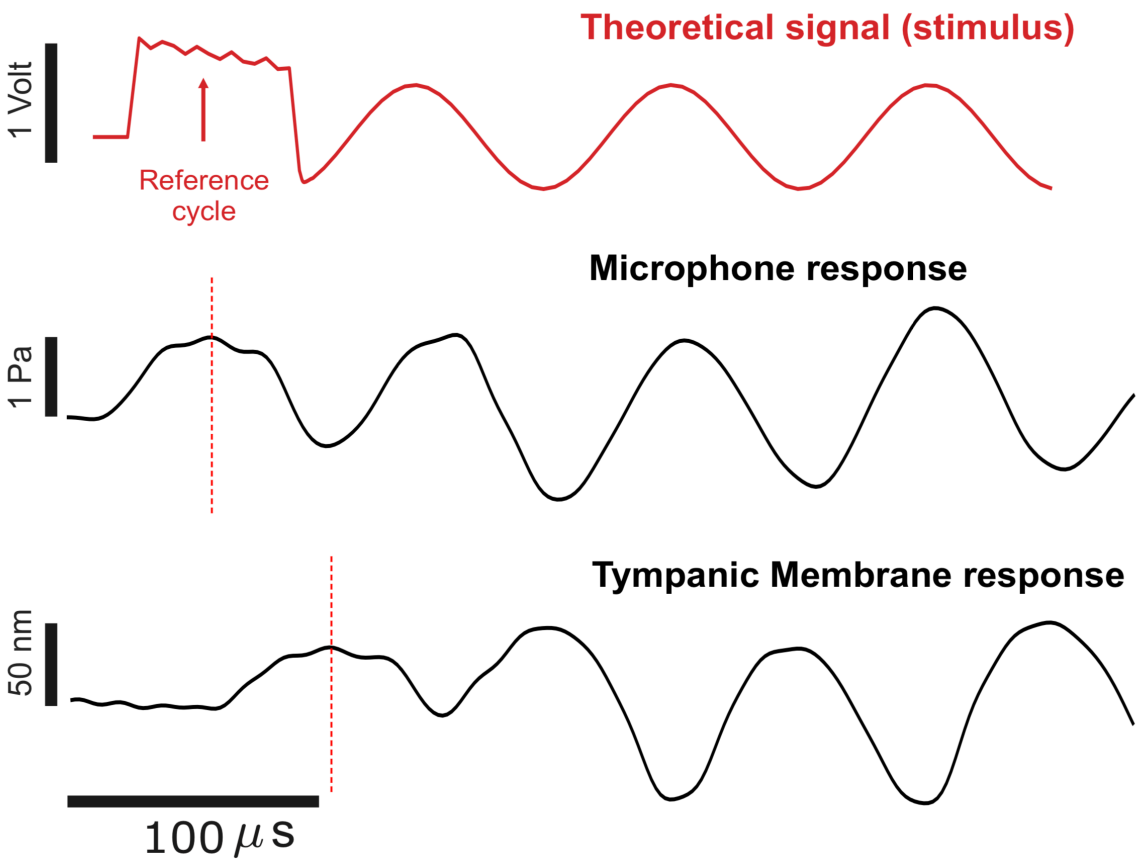

Figure S2. A specially designed wave with a unique marker on the first wave- length. The response of the microphone and tympanic membrane when the wave is played through a loudspeaker.

Section 8: Supplementary tables

Table S1: Parameters used in Benade's phase velocity equation for the gases Air, Helium and CO_2 at 293.15 K.

	Air	Helium	CO_2
Angular frequency, ω (kHz)	$2\pi\times23$	$2\pi\times23$	$2\pi\times23$
Density, ρ (kg/m^3)	1.204	0.1634	1.98
Median tube radius, a (μm)	150	150	150
Viscosity, η (Pa·s)	18.13e-6	1.96e-5	1.476e-5
Viscous boundary layer term, $r_v = (\omega\rho/\eta)^{1/2}a$	14.6947	5.20647	20.885
Specific heat at constant pressure, C_p (J/Kg·k)	1006.1	5192.6	846
Thermal conductivity, κ (W/m·k)	0.02514	0.1567	0.0162
Thermal boundary layer term, $r_t = (\omega\rho C_p/\kappa)^{1/2}a$	12.5169	4.19594	18.336
Ratio of specific heats, γ	1.4	1.66	1.28
Free-space sound velocity, c (m/s)	343	1007	267
Phase velocity inside tube, v (m/s)	318.7442	758.233	255.077
Reduction percentage from c	7.3%	24.73%	4.5%

Table S2: Parametric values incorporated into the mathematical model.

Parameter	Value
Pressure at γ_1, p_{bnd}	1 Pa
Normal Impedance of TM, Z_0	8000 Pa·s/m
AT Wall - Young's Modulus, E	1.7 GPa
AT Wall - Poisson's Ratio, ν	0.3
AT Wall - Density, ρ_s	1300 kg/m^3
Rayleigh Damping	$\alpha_{dM} = 260$ s^{-1}; $\beta_{dK} = 37 \times 10^{-6}$s
AT Wall Thickness	13 μm
Equilibrium Temperature, T_0	293.15 K
Equilibrium Pressure, p_0	1 atm

References

Jonsson, T., Montealegre-Z, F., Soulsbury, C.D., Robson Brown, K.A. and Robert, D., 2016. Auditory mechanics in a bush-cricket: direct evidence of dual sound inputs in the pressure difference receiver. *Journal of the Royal Society Interface*, 13, p.20160560.

Montealegre-Z, F., Jonsson, T., Robson-Brown, K.A., Postles, M. and Robert, D., 2012. Convergent evolution between insect and mammalian audition. *Science*, 338, 968-971.